References

1. Feldman, D. (2008). Polymer history. *Designed monomers and polymers*, *11*(1), 1-15.

2. Schubert, U.S., & Zechel S. (2020). The year of polymers–100 years of macromolecular chemistry. *Macromolecular chemistry and physics*, *221*(1), 1900530.

3. Meneghetti, P., & Qutubuddin, S. (2004). Synthesis of poly (methyl methacrylate) nanocomposites via emulsion polymerization using a zwitterionic surfactant. *Langmuir*, *20*(8), 3424-3430.

4. Mi, F. L., Shyu, S. S., Lin, Y. M., Wu, Y. B., Peng, C. K., & Tsai, Y. H. (2003). Chitin/PLGA blend microspheres as a biodegradable drug delivery system: a new delivery system for protein. *Biomaterials*, *24*(27), 5023-5036.

5. Mosthaf, H. (1990). An erster Stelle steht die Ökobilanz. *Plastverarbeiter*, *41*(8), 50-52.

6. Webb, H. K., Arnott, J., Crawford, R. J., & Ivanova, E. P. (2012). Plastic degradation and its environmental implications with special reference to poly (ethylene terephthalate). *Polymers*, *5*(1), 1-18.

7. Song, R. (2018). Current development of biodegradable polymeric materials for biomedical applications. *Drug Design, Development and Therapy, 12,* 3117-3145.

8. Chandra, R. U. S. T. G. I., & Rustgi, R. (1998). Biodegradable polymers. *Progress in polymer science*, *23*(7), 1273-1335.

9. Correlo, V. M., Boesel, L. F., Bhattacharya, M., Mano, J. F., Neves, N. M., & Reis, R. L. (2005). Properties of melt processed chitosan and aliphatic polyester blends. *Materials Science and Engineering: A*, *403*(1-2), 57-68.

10. Dutta, P. K., Dutta, J., & Tripathi, V. S. (2004). Chitin and chitosan: Chemistry, properties and applications. *Journal of Scientific & Industrial Research, 63,* 20-31.

11. Möller, H., Grelier, S., Pardon, P., & Coma, V. (2004). Antimicrobial and physicochemical properties of chitosan− HPMC-based films. *Journal of agricultural and food chemistry*, *52*(21), 6585-6591.

12. Hamed, I., Özogul, F., & Regenstein, J. M. (2016). Industrial applications of crustacean by-products (chitin, chitosan, and chitooligosaccharides): A review. *Trends in food science & technology*, *48*, 40-50.

13. Mourya, V. K., & Inamdar, N. N. (2008). Chitosan-modifications and applications: Opportunities galore. *Reactive and Functional polymers*, *68*(6), 1013-1051.

14. Alabaraoye, E., Achilonu, M., & Hester, R. (2018). Biopolymer (Chitin) from various marine seashell wastes: isolation and characterization. *Journal of Polymers and the Environment*, *26*, 2207-2218.

15. Sayari, N., Sila, A., Abdelmalek, B. E., Abdallah, R. B., Ellouz-Chaabouni, S., Bougatef, A., & Balti, R. (2016). Chitin and chitosan from the Norway lobster by-products: Antimicrobial and anti-proliferative activities. *International journal of biological macromolecules*, *87*, 163-171.

16. Felt, O., Buri, P., & Gurny, R. (1998). Chitosan: a unique polysaccharide for drug delivery. *Drug development and industrial pharmacy*, *24*(11), 979-993.

17. Chandy, T., & Sharma, C. P. (1990). Chitosan-as a biomaterial. *Biomaterials, artificial cells and artificial organs*, *18*(1), 1-24.

18. Balamurugan, M. A. N. I. C. K. A. M. (2012). Chitosan: A perfect polymer used in fabricating gene delivery and novel drug delivery systems. *Int J Pharm Pharm Sci*, *4*(3), 54-56.

19. Hejazi, R., & Amiji, M. (2003). Chitosan-based gastrointestinal delivery systems. *Journal of controlled release*, *89*(2), 151-165.

20. Global Industry Analysts, Inc. (2012). Chitin & Chitosan: A Global Strategic Business Report. San Jose, CA: Global Industry Analysts, Inc.

21. Badawy, M. E. (2012). A new rapid and sensitive spectrophotometric method for determination of a biopolymer chitosan. *International Journal of Carbohydrate Chemistry, 2012(1*), 139328.

22. Kafetzopoulos, D., Martinou, A., & Bouriotis, V. (1993). Bioconversion of chitin to chitosan: purification and characterization of chitin deacetylase from Mucor rouxii. *Proceedings of the National Academy of Sciences*, *90*(7), 2564-2568.

23. Younes, I., & Rinaudo, M. (2015). Chitin and chitosan preparation from marine sources. Structure, properties and applications. *Marine drugs*, *13*(3), 1133-1174.

24. Ji, J., Wang, L., Yu, H., Chen, Y., Zhao, Y., Zhang, H., Amer, W. A., Sun, Y., Huang, L., & Saleem, M. (2014). Chemical modifications of chitosan and its applications. *Polymer-Plastics Technology and Engineering*, *53*(14), 1494-1505.

25. Zhao, T., & Feng, T. (2016). Application of modified chitosan microspheres for nitrate and phosphate adsorption from aqueous solution. *RSC advances*, *6*(93), 90878-90886.

26. El Fray, M., Niemczyk, A., & Pabin-Szafko, B. (2012). Chemical modification of chitosan with fatty acids. *Progress on Chemistry and Application of Chitin and its Derivatives*, *17*, 29-36.

27. Sobahi, T. R., Abdelaal, M. Y., & Makki, M. S. (2014). Chemical modification of chitosan for metal ion removal. *Arabian Journal of Chemistry*, *7*(5), 741-746.

28. Rinaudo, M. (2006). Chitin and chitosan: Properties and applications. *Progress in polymer science*, *31*(7), 603-632.

29. Hua, D., Tang, J., Cheng, J., Deng, W., & Zhu, X. (2008). A novel method of controlled grafting modification of chitosan via RAFT polymerization using chitosan-RAFT agent. *Carbohydrate polymers*, *73*(1), 98-104.

30. Elieh-Ali-Komi, D., & Hamblin, M. R. (2016). Chitin and chitosan: production and application of versatile biomedical nanomaterials. *International journal of advanced research*, *4*(3), 411.

31. Amaral, I. F., Granja, P. L., & Barbosa, M. A. (2005). Chemical modification of chitosan by phosphorylation: an XPS, FT-IR and SEM study. *Journal of Biomaterials Science, Polymer Edition*, *16*(12), 1575-1593.

32. Guo, M., & Hsieh, Y. L. (2022). One-pot synthesis of 2-bromopropionyl esterified cellulose nanofibrils as hydrophobic coating and film. *RSC advances*, *12*(24), 15070-15082.

33. Guo, M., & Hsieh, Y. L. (2022). 2-Bromopropionyl Esterified Cellulose Nanofibrils as Chain Extenders or Polyols in Stoichiometrically Optimized Syntheses of High-Strength Polyurethanes. *Biomacromolecules*, *23*(11), 4574-4585.

34. Dey, S. C., Al-Amin, M., Rashid, T. U., Ashaduzzaman, M., & Shamsuddin, S. M. (2016). pH induced fabrication of kaolinite-chitosan biocomposite. *Int. Lett. Chem. Phys. Astron*, *68*, 1-9.

35. Kumar, M. N. R. (2000). A review of chitin and chitosan applications. *Reactive and functional polymers*, *46*(1), 1-27.

36. Popuri, S. R., Vijaya, Y., Boddu, V. M., & Abburi, K. (2009). Adsorptive removal of copper and nickel ions from water using chitosan coated PVC beads. *Bioresource technology*, *100*(1), 194-199.

37. Ngah, W. W., Teong, L. C., & Hanafiah, M. M. (2011). Adsorption of dyes and heavy metal ions by chitosan composites: A review. *Carbohydrate polymers*, *83*(4), 1446-1456.

38. Okamoto, M. (2004). Biodegradable polymer/layered silicate nanocomposites: a review. *Journal of Industrial and Engineering Chemistry*, *10*(7), 1156-1181.

39. Hristodor, C. M., Vrinceanu, N., Pui, A., Novac, O., Copcia, V. E., & Popovici, E. (2012). Textural and morphological characterization of chitosan/bentonite nanocomposite. *Environmental Engineering & Management Journal (EEMJ)*, *11*(3), 573-578.

40. Abou Alsoaud, M. M., Taher, M. A., Hamed, A. M., Elnouby, M. S., & Omer, A. M. (2022). Reusable kaolin impregnated aminated chitosan composite beads for efficient removal of Congo red dye: Isotherms, kinetics and thermodynamics studies. *Scientific Reports*, *12*(1), 12972.

41. Sun, X., Tang, Z., Pan, M., Wang, Z., Yang, H., & Liu, H. (2017). Chitosan/kaolin composite porous microspheres with high hemostatic efficacy. *Carbohydrate polymers*, *177*, 135-143.

42. Şimşek, S., Şenol, Z. M., & Ulusoy, H. I. (2017). Synthesis and characterization of a composite polymeric material including chelating agent for adsorption of uranyl ions. *Journal of hazardous materials*, *338*, 437-446.

43. Şenol, Z. M., Keskin, Z. S., Özer, A., & Şimşek, S. (2022). Application of kaolinite-based composite as an adsorbent for removal of uranyl ions from aqueous solution: kinetics and equilibrium study. *Journal of Radioanalytical and Nuclear Chemistry, 331(1)*, 403-414.

44. Zhu, H. Y., Jiang, R., & Xiao, L. (2010). Adsorption of an anionic azo dye by chitosan/kaolin/γ-Fe2O3 composites. *Applied clay science*, *48*(3), 522-526.

45. Darder, M., Colilla, M., & Ruiz-Hitzky, E. (2003). Biopolymer− clay nanocomposites based on chitosan intercalated in montmorillonite. *Chemistry of Materials*, *15*(20), 3774-3780.

46. Bensalem, S., Hamdi, B., Del Confetto, S., & Calvet, R. (2021). Characterization of surface properties of chitosan/bentonite composites beads by inverse gas chromatography. *International Journal of Biological Macromolecules*, *166*, 1448-1459.

47. Jia, J., Liu, Y., & Sun, S. (2021). Preparation and characterization of chitosan/bentonite composites for Cr (VI) removal from aqueous solutions. *Adsorption Science & Technology*, *2021*, 1-15.

48. Guo, X., Wu, Z., Wang, Z., Lin, F., Li, P., & Liu, J. (2023). Preparation of Chitosan-Modified Bentonite and Its Adsorption Performance on Tetracycline. *ACS omega*, *8*(22), 19455-19463.

49. Abukhadra, M. R., Refay, N. M., El-Sherbeeny, A. M., Mostafa, A. M., & Elmeligy, M. A. (2019). Facile synthesis of bentonite/biopolymer composites as low-cost carriers for 5-fluorouracil drug; equilibrium studies and pharmacokinetic behavior. *International journal of biological macromolecules*, *141*, 721-731.

50. Shen, Q., Xu, M. H., Wu, T., Pan, G. X., & Tang, P. S. (2022). Adsorption behavior of tetracycline on carboxymethyl starch grafted magnetic bentonite. *Chemical Papers*, *76*(1), 123-135.

51. Budnyak, T. M., Pylypchuk, I. V., Tertykh, V. A., Yanovska, E. S., & Kolodynska, D. (2015). Synthesis and adsorption properties of chitosan-silica nanocomposite prepared by sol-gel method. *Nanoscale research letters*, *10*, 1-10.

52. Arruebo, M. (2012). Drug delivery from structured porous inorganic materials. *Wiley Interdisciplinary Reviews: Nanomedicine and Nanobiotechnology*, *4*(1), 16-30.

53. Zhong, T., Xia, M., Yao, Z., & Han, C. (2022). Chitosan/Silica Nanocomposite Preparation from Shrimp Shell and Its Adsorption Performance for Methylene Blue. *Sustainability*, *15*(1), 47.

54. Dongre, R., Thakur, M., Ghugal, D., & Meshram, J. (2012). Bromine pretreated chitosan for adsorption of lead (II) from water. *Bulletin of Materials Science*, *35*, 875-884.

55. Domard, A., Rinaudo, M., & Terrassin, C. (1986). New method for the quaternization of chitosan. *International Journal of Biological Macromolecules*, *8*(2), 105-107.

56. Kurita, Y., & Isogai, A. (2010). Reductive N-alkylation of chitosan with acetone and levulinic acid in aqueous media. *International journal of biological macromolecules*, *47*(2), 184-189.

57. Sashiwa, H., Kawasaki, N., Nakayama, A., Muraki, E., Yamamoto, N., & Aiba, S. I. (2002). Chemical modification of chitosan. 14: Synthesis of water-soluble chitosan derivatives by simple acetylation. *Biomacromolecules*, *3*(5), 1126-1128.

58. Jayakumar, R., Prabaharan, M., Reis, R. L., & Mano, J. (2005). Graft copolymerized chitosan—present status and applications. *Carbohydrate Polymers*, *62*(2), 142-158.

59. Bao, H., Hu, J., Gan, L. H., & Li, L. (2009). Stepped association of comb-like and stimuli-responsive graft chitosan copolymer synthesized using ATRP and active ester conjugation methods. *Journal of Polymer Science Part A: Polymer Chemistry*, *47*(23), 6682-6692.

60. Liu, L., & Sun, G. (2017). Promoting the OH-ion conductivity of chitosan membrane using quaternary phosphonium polymer brush functionalized graphene oxide. *International Journal of Electrochemical Science*, *12*(10), 9262-9278.

61. El Tahlawy, K., & Hudson, S. M. (2003). Synthesis of a well-defined chitosan graft poly (methoxy polyethyleneglycol methacrylate) by atom transfer radical polymerization. *Journal of applied polymer science*, *89*(4), 901-912.

62. Chen, C., Liu, M., Gao, C., Lü, S., Chen, J., Yu, X., Ding, E., Yu, C., Guo, J., & Cui, G. (2013). A convenient way to synthesize comb-shaped chitosan-graft-poly (N-isopropylacrylamide) copolymer. *Carbohydrate polymers*, *92*(1), 621-628.

63. Li, N., Bai, R., & Liu, C. (2005). Enhanced and selective adsorption of mercury ions on chitosan beads grafted with polyacrylamide via surface-initiated atom transfer radical polymerization. *Langmuir*, *21*(25), 11780-11787.

64. Dryabina, S. S., Fotina, K. M., Shulevich, Y. V., Klimov, V. V., Bryuzgin, E. V., Navrotskii, A. V., & Novakov, I. A. (2020). Synthesis of water-soluble grafted chitosan copolymers by atom transfer radical polymerization. *Polymer Bulletin*, *77*, 1541-1554.

65. Huang, L., Yuan, S., Lv, L., Tan, G., Liang, B., & Pehkonen, S. O. (2013). Poly (methacrylic acid)-grafted chitosan microspheres via surface-initiated ATRP for enhanced removal of Cd (II) ions from aqueous solution. *Journal of colloid and interface science*, *405*, 171-182.

66. Tang, F., Zhang, L., Zhu, J., Cheng, Z., & Zhu, X. (2009). Surface functionalization of chitosan nanospheres via surface-initiated AGET ATRP mediated by iron catalyst in the presence of limited amounts of air. Industrial & engineering chemistry research, 48(13), 6216-6223.

67. Madni, A., Kousar, R., Naeem, N., & Wahid, F. (2021). Recent advancements in applications of chitosan-based biomaterials for skin tissue engineering. *Journal of Bioresources and Bioproducts*, *6*(1), 11-25.

68. Ngah, W. W., Teong, L. C., & Hanafiah, M. M. (2011). Adsorption of dyes and heavy metal ions by chitosan composites: A review. *Carbohydrate polymers*, *83*(4), 1446-1456.

69. Tan, W., Zhang, Y., Szeto, Y. S., & Liao, L. (2008). A novel method to prepare chitosan/montmorillonite nanocomposites in the presence of hydroxy-aluminum oligomeric cations. *Composites Science and Technology*, *68*(14), 2917-2921.

70. Ma, W., Dai, J., Dai, X., & Yan, Y. (2014). Preparation and characterization of chitosan/kaolin/Fe3O4 magnetic microspheres and their application for the removal of ciprofloxacin. *Adsorption Science & Technology*, *32*(10), 775-790.

71. Biswas, S., Rashid, T. U., Mallik, A. K., Islam, M. M., Khan, M. N., Haque, P., Khan, M., & Rahman, M. M. (2017). Facile preparation of biocomposite from prawn shell derived chitosan and kaolinite-rich locally available clay. *International Journal of Polymer Science*, *2017(1),* 6472131.

72. Chen, I. P., Kan, C. C., Futalan, C. M., Calagui, M. J. C., Lin, S. S., Tsai, W. C., & Wan, M. W. (2015). Batch and fixed bed studies: removal of copper (II) using chitosan-coated kaolinite beads from aqueous solution. *Sustainable Environment Research, 25(2)*, 73-81.

73. Abou Alsoaud, M. M., Taher, M. A., Hamed, A. M., Elnouby, M. S., & Omer, A. M. (2022). Reusable kaolin impregnated aminated chitosan composite beads for efficient removal of Congo red dye: Isotherms, kinetics and thermodynamics studies. *Scientific Reports*, *12*(1), 12972.

74. Lefatle, M. C., Matong, J. M., Mpupa, A., Munonde, T. S., Waleng, N. J., Madikizela, L. M., Pakade, V. E., & Nomngongo, P. N. (2023). Preparation, characterization, and application of chitosan–kaolin-based nanocomposite in magnetic solid-phase extraction of tetracycline in aqueous samples. *Chemical Papers*, *77*(3), 1601-1618.

75. Yarangsee, C., Wattanaarsakit, P., Sirithunyalug, J., & Leesawat, P. (2021). Particle Engineering of Chitosan and Kaolin Composite as a Novel Tablet Excipient by Nanoparticles Formation and Co-Processing. *Pharmaceutics*, *13*(11), 1844.

76. Rekik, S. B., Gassara, S., Bouaziz, J., Deratani, A., & Baklouti, S. (2017). Development and characterization of porous membranes based on kaolin/chitosan composite. *Applied Clay Science*, *143*, 1-9.

77. Lin, K. F., Hsu, C. Y., Huang, T. S., Chiu, W. Y., Lee, Y. H., & Young, T. H. (2005). A novel method to prepare chitosan/montmorillonite nanocomposites. *Journal of Applied Polymer Science*, *98*(5), 2042-2047.

78. Laaraibi, A., Moughaoui, F., Damiri, F., Ouakit, A., Charhouf, I., Hamdouch, S., Jaafari, A., Abourriche, A., Knouzi, N., Bennamara, A., & Berrada, M. (2018). Chitosan-clay based (CS-NaBNT) biodegradable nanocomposite films for potential utility in food and environment. *Chitin-Chitosan-Myriad Functionalities in Science and Technology*, 45-69.

79. Cankaya, N., & Sahin, R. (2019). Chitosan/clay bionanocomposites: Structural, antibacterial, thermal and swelling properties. *Cellulose Chemistry and Technology*, *53*(5-6), 537-549.

80. Cacciotti, I., Lombardelli, C., Benucci, I., & Esti, M. (2019). Clay/chitosan biocomposite systems as novel green carriers for covalent immobilization of food enzymes. *Journal of Materials Research and Technology*, *8*(4), 3644-3652.

81. Benucci, I., Liburdi, K., Cacciotti, I., Lombardelli, C., Zappino, M., Nanni, F., & Esti, M. (2018). Chitosan/clay nanocomposite films as supports for enzyme immobilization:

An innovative green approach for winemaking applications. *Food Hydrocolloids*, *74*, 124-131.

82. Benucci, I., Lombardelli, C., Cacciotti, I., & Esti, M. (2020). Papain covalently immobilized on chitosan–clay nanocomposite films: Application in synthetic and real white wine. *Nanomaterials*, *10*(9), 162

83. Huang, R., Liu, Q., Zhang, L., & Yang, B. (2015). Utilization of cross-linked chitosan/bentonite composite in the removal of methyl orange from aqueous solution. *Water Science and Technology*, *71*(2), 174-182.

84. Devi, N., & Dutta, J. (2017). Preparation and characterization of chitosan-bentonite nanocomposite films for wound healing application. *International journal of biological macromolecules*, *104*, 1897-1904.

85. Savitri, E., & Budhyantoro, A. (2017, July). The effect of ratio chitosan-bentonite and processing time on the characterization of chitosan-bentonite composite. In *IOP Conference Series: Materials Science and Engineering* (Vol. 223, No. 1, p. 012034). IOP Publishing.

86. Teofilović, V., Pavličević, J., Bera, O., Jovičić, M., Budinski-Simendić, J., Mészáros-Szécsényi, K., & Aroguz, A. (2014). Preparation and thermal properties of chitosan/bentonite composite beads. *Hemijska industrija*, *68*(6), 653-659.

87. Marey, A. (2019). Composite of chitosan and Bentonite as coagulant agents in removing turbidity from Ismailia canal as water treatment plant. *RB*, *4*, 897-900.

88. Jatrana, A., Chauhan, S., Maan, S., & Kumar, V. (2022). Inexpensive and Environment Friendly Chitosan-Bentonite Composite as A Potential Adsorbent for Thiomethoxam Removal. *Chemical Science Review and Letters*, *11*(44), 430-437.

89. Nie, J., Feng, D., Shang, J., Nasen, B., Jiang, T., Liu, Y., & Hou, S. (2023). Green composite aerogel based on citrus peel/chitosan/bentonite for sustainable removal Cu (II) from water matrices. *Scientific Reports*, *13*(1), 15443.

90. Lin, Z., Yang, Y., Liang, Z., Zeng, L., & Zhang, A. (2021). Preparation of chitosan/calcium alginate/bentonite composite hydrogel and its heavy metal ions adsorption properties. *Polymers*, *13*(11), 1891.

91. Salama, A., & Abou-Zeid, R. E. (2021). Ionic chitosan/silica nanocomposite as efficient adsorbent for organic dyes. *International Journal of Biological Macromolecules*, *188*, 404-410.

92. Mohammed, M. I., Ismael, M. K., & Gönen, M. (2020, February). Synthesis of chitosan-silica nanocomposite for removal of methyl orange from water: composite

characterization and adsorption performance. In *IOP Conference Series: Materials Science and Engineering* (Vol. 745, No. 1, p. 012084). IOP Publishing.

93. Al-Sagheer, F., & Muslim, S. (2010). Thermal and mechanical properties of chitosan/SiO2 hybrid composites. *Journal of Nanomaterials*, *2010*, 1-7.

94. Blachnio, M., Budnyak, T. M., Derylo-Marczewska, A., Marczewski, A. W., & Tertykh, V. A. (2018). Chitosan–silica hybrid composites for removal of sulfonated azo dyes from aqueous solutions. *Langmuir*, *34*(6), 2258-2273.

95. Ma, I. W., Sh, A., Bashir, S., Kumar, S. S., Ramesh, K., & Ramesh, S. (2021). Development of active barrier effect of hybrid chitosan/silica composite epoxy-based coating on mild steel surface. *Surfaces and Interfaces*, *25*, 101250.

96. Sumarni, W., Iswari, R. S., Marwoto, P., & Rahayu, E. F. (2016). Physical characteristics of chitosan-silica composite of rice husk ash. In *IOP Conference Series: Materials Science and Engineering* (Vol. 107, No. 1, p. 012039). IOP Publishing.

97. Wang, J., Zhou, Q., Song, D., Qi, B., Zhang, Y., Shao, Y., & Shao, Z. (2015). Chitosan–silica composite aerogels: preparation, characterization and Congo red adsorption. *Journal of Sol-Gel Science and Technology*, *76*, 501-509.

98. Valgas, C., Souza, S. M. D., Smânia, E. F., & Smânia Jr, A. (2007). Screening methods to determine antibacterial activity of natural products. *Brazilian journal of microbiology*, *38*, 369-380.

99. Magaldi, S., Mata-Essayag, S., De Capriles, C. H., Pérez, C., Colella, M. T., Olaizola, C., & Ontiveros, Y. (2004). Well diffusion for antifungal susceptibility testing. *International journal of infectious diseases*, *8*(1), 39-45.

100. Lee, C., Yang, W., & Parr, R. G. (1988). Development of the Colle-Salvetti correlation-energy formula into a functional of the electron density. *Physical review B*, *37*(2), 785.

101. Ditchfield, R. H. W. J., Hehre, W. J., & Pople, J. A. (1971). Self-consistent molecular-orbital methods. IX. An extended Gaussian-type basis for molecular-orbital studies of organic molecules. *The Journal of Chemical Physics*, *54*(2), 724-728.

102. Gaussian 16, Revision C.01, M. J. Frisch, G. W. Trucks, H. B. Schlegel, G. E. Scuseria, M. A. Robb, J. R. Cheeseman, G. Scalmani, V. Barone, G. A. Petersson, H. Nakatsuji, X. Li, M. Caricato, A. V. Marenich, J. Bloino, B. G. Janesko, R. Gomperts, B. Mennucci, H. P. Hratchian, J. V. Ortiz, A. F. Izmaylov, J. L. Sonnenberg, D. Williams-Young, F. Ding, F. Lipparini, F. Egidi, J. Goings, B. Peng, A. Petrone, T. Henderson, D. Ranasinghe, V. G. Zakrzewski, J. Gao, N. Rega, G. Zheng, W. Liang, M. Hada, M. Ehara,

K. Toyota, R. Fukuda, J. Hasegawa, M. Ishida, T. Nakajima, Y. Honda, O. Kitao, H. Nakai, T. Vreven, K. Throssell, J. A. Montgomery, Jr., J. E. Peralta, F. Ogliaro, M. J. Bearpark, J. J. Heyd, E. N. Brothers, K. N. Kudin, V. N. Staroverov, T. A. Keith, R. Kobayashi, J. Normand, K. Raghavachari, A. P. Rendell, J. C. Burant, S. S. Iyengar, J. Tomasi, M. Cossi, J. M. Millam, M. Klene, C. Adamo, R. Cammi, J. W. Ochterski, R. L. Martin, K. Morokuma, O. Farkas, J. B. Foresman, D. J. Fox, Gaussian, Inc., Wallingford CT, 2016.

103. GaussView, Version 6, R. Dennington, T. A. Keith, J. M. Millam, Semichem Inc., Shawnee Mission, KS, 2019.

104. Politzer, P., Laurence, P. R., & Jayasuriya, K. (1985). Molecular electrostatic potentials: an effective tool for the elucidation of biochemical phenomena. *Environmental health perspectives*, *61*, 191-202.

105. Lu, T., & Chen, F. (2012). Multiwfn: A multifunctional wavefunction analyzer. *Journal of computational chemistry*, *33*(5), 580-592.

106. Humphrey, W., Dalke, A., & Schulten, K. (1996). VMD: visual molecular dynamics. *Journal of molecular graphics*, *14*(1), 33-38.

107. Riplinger, C., & Neese, F. (2013). An efficient and near linear scaling pair natural orbital based local coupled cluster method. *The Journal of chemical physics*, *138*(3).

108. Neese, F. (2022). Software update: The ORCA program system—Version 5.0. *Wiley Interdisciplinary Reviews: Computational Molecular Science*, *12*(5), e1606.

109. Muzzarelli, R. A., Boudrant, J., Meyer, D., Manno, N., DeMarchis, M., & Paoletti, M. G. (2012). Current views on fungal chitin/chitosan, human chitinases, food preservation, glucans, pectins and inulin: A tribute to Henri Braconnot, precursor of the carbohydrate polymers science, on the chitin bicentennial. *Carbohydrate polymers*, *87*(2), 995-1012.

110. El Hamdaoui, L., El Marouani, M., Kifani-Sahban, F., & El Moussaouiti, M. (2021). Synthesis, characterization and pyrolysis kinetics of chitosan-N-phenylacetamide in an ionic liquid 1-butyl-3-methylimidazolium chloride. *Biointerface Res Appl Chem*, *11*(3), 10287-10292.

111. Je, J. Y., & Kim, S. K. (2006). Chitosan derivatives killed bacteria by disrupting the outer and inner membrane. *Journal of agricultural and food chemistry*, *54*(18), 6629-6633.

112. Aranaz, I., Mengíbar, M., Harris, R., Paños, I., Miralles, B., Acosta, N., Galed G, & Heras, Á. (2009). Functional characterization of chitin and chitosan. *Current chemical biology*, *3*(2), 203-230.

113. Kenawy, E. R., Abdel-Hay, F. I., Tamer, T. M., Abo-Elghit Ibrahim, E. M., & Mohy Eldin, M. S. (2020). Antimicrobial activity of novel modified aminated chitosan with aromatic esters. *Polymer Bulletin*, *77*, 1631-1647.

114. Heras, A., Rodriguez, N. M., Ramos, V. M., & Agullo, E. (2001). N-methylene phosphonic chitosan: a novel soluble derivative. *Carbohydrate Polymers*, *44*(1), 1-8.

115. Ramos, V. M., Rodrıguez, N. M., Dıaz, M. F., Rodrıguez, M. S., Heras, A., & Agullo, E. (2003). N-methylene phosphonic chitosan. Effect of preparation methods on its properties. *Carbohydrate Polymers*, *52*(1), 39-46.

116. Matevosyan, G. L., Yukha, Y. S., & Zavlin, P. M. (2003). Phosphorylation of chitosan. *Russian journal of general chemistry*, *73*(11), 1725-1728.

117. Queiroz, M. F., Teodosio Melo, K. R., Sabry, D. A., Sassaki, G. L., & Rocha, H. A. O. (2014). Does the use of chitosan contribute to oxalate kidney stone formation? *Marine drugs*, *13*(1), 141-158.

118. Guarnieri, A., Triunfo, M., Scieuzo, C., Ianniciello, D., Tafi, E., Hahn, T., Zibek, S., Salvia, R., Bonis A. D. & Falabella, P. (2022). Antimicrobial properties of chitosan from different developmental stages of the bioconverter insect Hermetia illucens. *Scientific Reports*, *12*(1), 8084.

119. Wanjun, T., Cunxin, W., & Donghua, C. (2005). Kinetic studies on the pyrolysis of chitin and chitosan. *Polymer Degradation and Stability*, *87*(3), 389-394.

120. Sirvio, J. A., Kantola, A. M., Komulainen, S., & Filonenko, S. (2021). Aqueous modification of chitosan with itaconic acid to produce strong oxygen barrier film. *Biomacromolecules*, *22*(5), 2119-2128.

121. Li, C., Cui, J., Wang, F., Peng, W., & He, Y. (2016). Adsorption removal of Congo red by epichlorohydrin-modified cross-linked chitosan adsorbent. *Desalination and Water Treatment*, *57*(30), 14060-14066.

122. Saber-Samandari, S., Yilmaz, O., & Yilmaz, E. (2012). Photoinduced graft copolymerization onto chitosan under heterogeneous conditions. *Journal of Macromolecular Science, Part A*, *49*(7), 591-598.

123. Goy, R. C., Britto, D. D., & Assis, O. B. (2009). A review of the antimicrobial activity of chitosan. *Polímeros*, *19*, 241-247.

124.   Hahn, T., Zibek, S. (2018). Sewage polluted water treatment via chitosan: A review. In: Dongre, R. S. (Eds.), Chitin-Chitosan—Myriad functionalities in science and technology. InTech. London, UK.

125.   Casariego, A. B. W. S., Souza, B. W. S., Cerqueira, M. A., Teixeira, J. A., Cruz, L., Díaz, R., & Vicente, A. A. (2009). Chitosan/clay films' properties as affected by biopolymer and clay micro/nanoparticles' concentrations. *Food Hydrocolloids*, *23*(7), 1895-1902.

126.   Hule, R. A., & Pochan, D. J. (2007). Polymer nanocomposites for biomedical applications. *MRS bulletin*, *32*(4), 354-358.

127.   Bharath, K. N., & Basavarajappa, S. (2016). Applications of biocomposite materials based on natural fibers from renewable resources: a review. *Science and Engineering of Composite Materials*, *23*(2), 123-133.

128.   Tang, R., Du, Y., & Fan, L. (2003). Dialdehyde starch-crosslinked chitosan films and their antimicrobial effects. *Journal of Polymer Science Part B: Polymer Physics*, *41*(9), 993-997.

129.   Trujillo, S., Pérez-Román, E., Kyritsis, A., Gomez Ribelles, J. L., & Pandis, C. (2015). Organic–inorganic bonding in chitosan–silica hybrid networks: Physical properties. *Journal of Polymer Science Part B: Polymer Physics*, *53*(19), 1391-1400.

130.   Hench, L. L. (1998). Biomaterials: a forecast for the future. *Biomaterials*, *19*(16), 1419-1423.

131.   Desbrières, J., & Guibal, E. (2018). Chitosan for wastewater treatment. *Polymer International*, *67*(1), 7-14.

132.   Qasim, S. B., Zafar, M. S., Najeeb, S., Khurshid, Z., Shah, A. H., Husain, S., & Rehman, I. U. (2018). Electrospinning of chitosan-based solutions for tissue engineering and regenerative medicine. *International journal of molecular sciences*, *19*(2), 407.

133.   Horue, M., Silva, J. M., Berti, I. R., Brandão, L. R., Barud, H. D. S., & Castro, G. R. (2023). Bacterial cellulose-based materials as dressings for wound healing. *Pharmaceutics*, *15*(2), 424.

134.   Islam, M. S., Haque, P., Rashid, T. U., Khan, M. N., Mallik, A. K., Khan, M. N. I., Khan, M., & Rahman, M. M. (2017). Core–shell drug carrier from folate conjugated chitosan obtained from prawn shell for targeted doxorubicin delivery. *Journal of Materials Science: Materials in Medicine*, *28*, 1-10.

135. Gontard, N., Thibault, R., Cuq, B., & Guilbert, S. (1996). Influence of relative humidity and film composition on oxygen and carbon dioxide permeabilities of edible films. *Journal of Agricultural and Food Chemistry*, *44*(4), 1064-1069.

136. Rhim, J. W., Hong, S. I., Park, H. M., & Ng, P. K. (2006). Preparation and characterization of chitosan-based nanocomposite films with antimicrobial activity. *Journal of agricultural and food chemistry*, *54*(16), 5814-5822.

137. Gu, S., Kang, X., Wang, L., Lichtfouse, E., & Wang, C. (2019). Clay mineral adsorbents for heavy metal removal from wastewater: a review. *Environmental Chemistry Letters*, *17*, 629-654.

138. Karathanasis, A. D. (2006). Clay minerals: weathering and alteration of. Encyclopedia of Soil Science, *2*, 281-6.

139. Oun, A., Tahri, N., Mahouche-Chergui, S., Carbonnier, B., Majumdar, S., Sarkar, S., Sahoo, G. C., & Amar, R. B. (2017). Tubular ultrafiltration ceramic membrane based on titania nanoparticles immobilized on macroporous clay-alumina support: elaboration, characterization and application to dye removal. *Separation and Purification Technology*, *188*, 126-133.

140. Ebrahimi, H., Abedi, B., Bodaghi, H., Davarynejad, G., Haratizadeh, H., & Conte, A. (2018). Investigation of developed clay-nanocomposite packaging film on quality of peach fruit (Prunus persica Cv. Alberta) during cold storage. *Journal of Food Processing and Preservation*, *42*(2), e13466.

141. Martino, L., Guigo, N., van Berkel, J. G., & Sbirrazzuoli, N. (2017). Influence of organically modified montmorillonite and sepiolite clays on the physical properties of bio-based poly (ethylene 2, 5-furandicarboxylate). *Composites Part B: Engineering*, *110*, 96-105.

142. Mohanasrinivasan, V., Mishra, M., Paliwal, J. S., Singh, S. K., Selvarajan, E., Suganthi, V., & Subathra Devi, C. (2014). Studies on heavy metal removal efficiency and antibacterial activity of chitosan prepared from shrimp shell waste. *3 Biotech*, *4*, 167-175.

143. Barman, J., Sarma, K. C., Sarma, M., & Sarma, K. (2008). Structural and optical studies of chemically prepared CdS nanocrystalline thin films. *Indian Journal of Pure & Applied Physics*, *46*, 339-343.

144. Kumar, S., & Koh, J. (2012). Physiochemical, optical and biological activity of chitosan-chromone derivative for biomedical applications. *International journal of molecular sciences*, *13*(5), 6102-6116.

145. Sudarshan, N. R., Hoover, D. G., & Knorr, D. (1992). Antibacterial action of chitosan. *Food biotechnology*, *6*(3), 257-272.

146. Tiwari, K., Singh, M., Kumar, P., & Mukhopadhyay, K. (2022). Binding of cationic analogues of α-MSH to lipopolysaccharide and disruption of the cytoplasmic membranes caused bactericidal action against Escherichia coli. *Scientific Reports*, *12*(1), 1987.

147. Ahari, H., Golestan, L., Anvar, S. A. A., Cacciotti, I., Garavand, F., Rezaei, A., Sani, M. A., & Jafari, S. M. (2022). Bio-nanocomposites as food packaging materials; the main production techniques and analytical parameters. *Advances in Colloid and Interface Science*, *310*, 102806.

148. Garavand, Y., Taheri-Garavand, A., Garavand, F., Shahbazi, F., Khodaei, D., & Cacciotti, I. (2022). Starch-polyvinyl alcohol-based films reinforced with chitosan nanoparticles: physical, mechanical, structural, thermal and antimicrobial properties. *Applied Sciences*, *12*(3), 1111.

149. GRIM, R. (1978). Bentonites-geology, mineralogy, properties, and uses. The history of the development of clay mineralogy. *Clays Clay Minerals, 36*, 97-101.

150. Blachnio, M., Budnyak, T. M., Derylo-Marczewska, A., Marczewski, A. W., & Tertykh, V. A. (2018). Chitosan–silica hybrid composites for removal of sulfonated azo dyes from aqueous solutions. *Langmuir*, *34*(6), 2258-2273.

151. Vijayalekshmi, V. (2015). UV-Visible, mechanical and anti-microbial studies of chitosan-montmorillonite clay/TiO_2 nanocomposites. *Research Journal of Recent Sciences,* 131-135.

152. Abdelkrim, S., Mokhtar, A., Djelad, A., Bennabi, F., Souna, A., Bengueddach, A., & Sassi, M. (2020). Chitosan/Ag-bentonite nanocomposites: preparation, characterization, swelling and biological properties. *Journal of Inorganic and Organometallic Polymers and Materials*, *30*, 831-840.

International e-Poster Conference on Current Outlook in Material Science and Engineering
(COMSE-2k20)

from 15-16th May 2020

Organized by
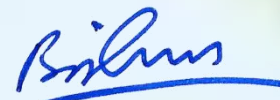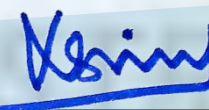### Bodoland University
in Association with
Tripura University, ADP College, Nagaon & MIT Aurangabad
On Facebook

Certificate of Achievement

This is to certify that Dr./Mr./Ms. **Madhabi Bhattacharjee** *of Department of Chemistry, Bodoland University has presented his/her paper entitled as* **"RDRP Modified Chitosan and Their Application"** *in "International e-Poster Conference on Current Outlook in Material Science and Engineering (COMSE-2k20)" on 15-16th May 2020.*

Dr. Dhruba J. Haloi
(Convener)

Dr. Bishnu Prasad Koiry
(Convener)

Dr. Subhendu Bhandari
(Co-Convener)

Dr. Lakshmi K. Singh
(Co-Convener)

National Conference on
Advances in Sustainable Chemistry and Material Science
(ASCMS-2022)

Paper Presentation Certificate

This is to certify that

Prof./Dr./Mr./Ms................ *Madhabi Bhattacharjee* .... of

.... *Bodoland University, Kokrajhar* .... has made oral

presentation on the topic entitled " .... *Preparation and Characterization of* ....

Chitosan/Kaolin Biocomposite Film ...." in the National

Conference on Advances in Sustainable Chemistry and Material Science-2022 held on 29th & 30th

April 2022 in the Department of Chemistry, Bodoland University, Kokrajhar, Assam, India.

Prof. Laishram Ladu Singh
(Vice Chancellor)

Dr. Manjil Basumatary
(Chairperson)

Dr. Sanjay Basumatary
(Convenor)

Dr. Dhrubajyoti Haloi
(Convenor)

Dr. Hemaprabha Saikia
(Convenor)

REVIEW

Recent advances in RDRP-modified chitosan: a review of its synthesis, properties and applications

Madhabi Bhattacharjee,[a] Nabendu B. Pramanik, [ID] [b] Nikhil K. Singha [ID] [c] and Dhruba J. Haloi [ID] *[a]

Modified chitosan (CS) has kindled considerable research interest in the last few decades due to its outstanding biological, chemical and physical properties. Generally, CS can be re-formed with different structural modifications by using various functional groups. Due to the addition of these functional groups, the physico-chemical properties of CS can be enhanced without hampering the degree of polymerization inherent in the CS. Different techniques were employed for the modification of CS. Among these, modifications *via* reversible-deactivation radical polymerization (RDRP) are found to be the most efficient. RDRP techniques mostly include atom transfer radical polymerization (ATRP), reversible addition–fragmentation chain transfer polymerization (RAFT) and nitroxide-mediated polymerization (NMP). These methods provide tailored modifications of CS with controlled molecular weight and dispersity ($Đ$) leading to better mechanical properties compared to the modifications performed *via* conventional methods. Various analytical techniques such as FT-IR, UV-Vis, ^{1}H-NMR, ^{13}C-NMR, XRD, SEM, TEM, TGA, DSC, GPC, *etc*. are employed to characterize and elucidate the physico-chemical properties of these modified polymers. These modifications make CS a strong candidate for different applications in diverse fields of pharmaceuticals, biomedicine, water treatment, *etc*. This review covers the recent advances in the syntheses, properties and applications of modified CS *via* RDRP techniques.

[a]*Bodoland University, Kokrajhar-783370, Assam, India.*
E-mail: dhruba2k3@gmail.com; Tel: +91-78967-77085
[b]*Lehigh University, Department of Chemistry, Bethlehem, PA 18015, USA*
[c]*Rubber Technology Centre, Indian Institute of Technology Kharagpur, West Bengal 721302, India*

Madhabi Bhattacharjee

Madhabi Bhattacharjee completed her Master of Science in Chemistry from Bodoland University, Assam, India in 2017. Later the same year, she joined the Ph.D. program of Bodoland University. She is now pursuing her Ph.D. on Chemical Modification of Chitosan via RDRP under the supervision of Dr Dhrubajyoti Haloi, Assistant Professor in the Department of Chemistry, Bodoland University.

Nabendu B. Pramanik

Nabendu B. Pramanik earned his M.Sc. in Organic Chemistry in 2010 from Vidyasagar University, West Bengal. He received his Ph.D. from the Indian Institute of Technology Kharagpur, India in 2016 on self-healing polymers via controlled radical polymerization under the guidance of Prof. Nikhil K. Singha. After that he worked as a post-doctoral researcher in The City College of New York, USA for one year. From December 2017 he is working as a post-doctoral research associate at Lehigh University, USA. His current research interest lies in the preparation of hyper-thin polymeric membranes for the separation of CO_2 from flue gas using a layer-by-layer assembly technique.

1. Introduction

1.1 Biodegradable polymers (chitin and chitosan)

In the present scenario, the use of synthetic polymers is a serious threat to the environment. Most of the synthetic polymers are non-biodegradable in nature and cause different kinds of environmental pollution. Therefore, the materials communities are exploring different biodegradable polymers as their substitutes. Various environment-friendly biodegradable polymers have already been developed as substitutes of synthetic polymers because they undergo bacterial decomposition to form different gases and smaller molecules such as water, organic molecules and various inorganic salts. Cellulose, collagen, chitin, silk, starch, *etc*. are the most commonly discussed examples of biodegradable polymers.[1] Among these, chitin is the second-most abundant biodegradable biopolymer after cellulose.[2] In general, chitin is obtained from the exoskeletons of different arthropods and the cell walls of some fungi.[3] It is a linear homopolymer of *N*-acetylglucosamine having β(1,4) linkages and shows cationic behavior (Fig. 1).[4] Chitin has a poor solubility profile and therefore needs more attention for its further improvement.[5]

Chitosan (CS) is considered as the most improved version of chitin. This white to light red powdery substance has a better solubility profile than chitin. Although chitosan is insoluble in water, it is soluble in many organic acids such as formic acid, acetic acid, tartaric acid, *etc*. It is also one of the most versatile, unique and multi-functional biopolymers with inherent biological properties. CS is a linear polysaccharide designed with randomly distributed β-1,4-linkages of D-glucosamine and *N*-acetyl-D-glucosamine residues (Fig. 2).[4]

CS can be obtained from chitin *via* enzymatic or chemical modification.[6] Kafetzopoulos *et al.* reported a procedure for
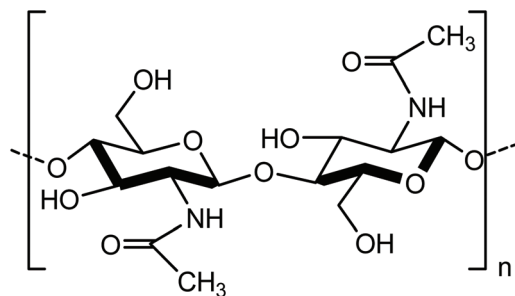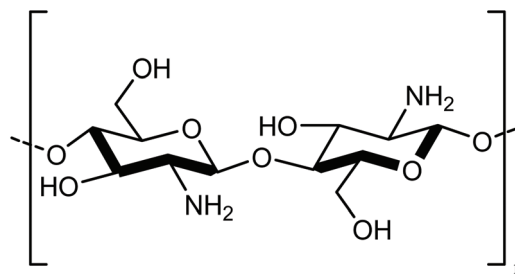

Fig. 1   Structure of chitin.

Fig. 2   Structure of chitosan (CS).

the biosynthesis of chitosan from chitin using the enzyme chitin deacetylase. The enzyme used in the conversion was obtained from the mycelial extracts of the fungus *Mucor rouxiia* that catalyzes the hydrolysis of the acetamido groups of *N*-acetyl-glucosamine in chitin.[7] The same conversion however is performed chemically by the process of deacetylation in the presence of sodium hydroxide (NaOH) at a temperature above 80 °C (Fig. 3).[8] The degree of deacetylation of CS can be

Nikhil K. Singha obtained his Ph.D. from IIT Bombay in 1996 while carrying out research work at the National Chemical Laboratory (NCL), Pune, India. He spent about seven years doing research in DSM Research, The Netherlands, in the Dutch Polymer Institute, Eindhoven University of Technology and in TNO Industries, The Netherlands. He joined IIT Kharagpur in 2003. Presently he is a Full Professor there. His research interests include the synthesis of functional polymers; block, graft and star copolymers based on polyacrylates; polyzwitterions; glycopolymers; polyurethanes; and fluoropolymers via *RDRP and "click" chemistry and their applications in self-healing, superhydrophobic, shape-memory, thermoplastic elastomers, antifouling materials, and their bio-applications.*

Nikhil K. Singha

Dhruba J. Haloi received his MTech degree in Rubber Technology (in 2008) and Ph.D. in Polymer Chemistry (in 2012) both from the Indian Institute of Technology Kharagpur, India. He worked for Zydex Industries, Vadodara, India as a Senior Researcher for a little more than one year. Later he joined Bodoland University in 2014. Currently he is working as an Assistant Professor of Chemistry in Bodoland University. His research interest is focussed mainly on the preparation of tailor-made synthetic polymers with the advantage of biodegradability.
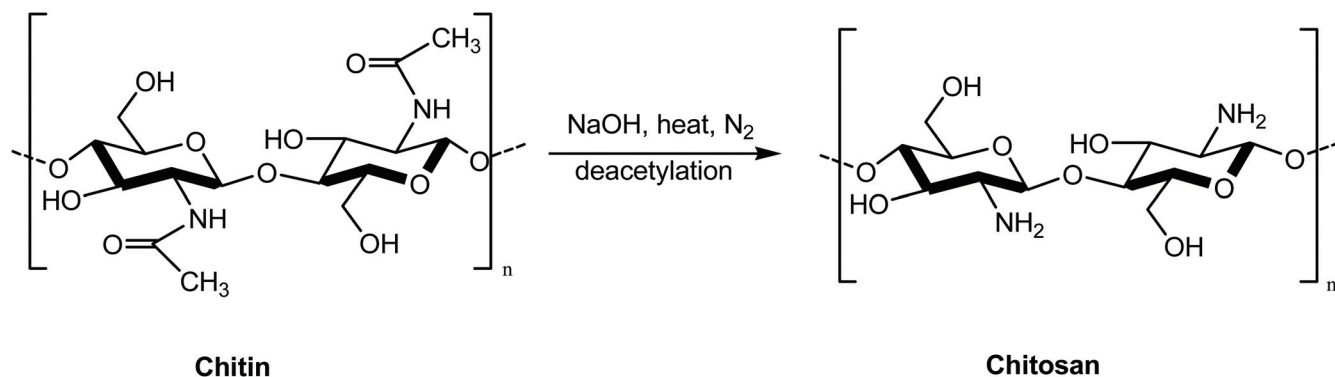
Dhruba J. Haloi

Fig. 3 Conversion of chitin to chitosan (CS).

between 40% to 98% and the molecular weights of CS are in the range of 5×10^4 Da to 2×10^6 Da.[9]

CS possesses a special chemical structure, due to which it shows some interesting and exceptional properties and applications. It is biocompatible, biodegradable,[6] non-toxic, antimicrobial,[10,11] and environmentally friendly, besides having good adsorption property, and so on.[12,13] Basically, CS comprises three functional entities, namely a primary amine and primary and secondary hydroxyl groups in its monomer skeleton (Fig. 4).[14,15] Although CS has poor solubility in water and is insoluble in many common organic solvents, its multifunctional nature makes it a peculiar compound. The primary amino group has the tendency to donate the free lone pair of electrons which makes it soluble in various aqueous organo-acidic solvents and capable of forming coordination bonds.[16]

Copious modifications were performed on CS to increase its solubility[17] and applicability, such as quaternization,[18] alkylation,[19] acetylation,[20] graft copolymerization,[21] phosphorylation,[22] reversible-deactivation radical polymerization (RDRP),[17] etc. These modifications make it a strong candidate for different applications in diverse fields of pharmaceuticals, biomedicine,[10] water treatment,[23] cosmetics,[3] agriculture,[24] etc. The average degree of acetylation determines the dissolution property of CS.[23]

1.2   Reversible-deactivation radical polymerization (RDRP)

As mentioned earlier, CS can be readily derivatized by various processes for diverse applications, and RDRP has been found to be one of the outstanding methods for controlling radical polymerization via controlling the molecular weight of polymers and dispersity ($Đ$).[25] Polymers obtained via RDRP methods have well-defined architectures and possess very good mechanical strength. RDRP can be broadly classified into three main subcategories, viz. ATRP, RAFT and NMP.[26–29] RDRP processes have great potential in different industries.[30]

Among these processes, the ATRP technique is involved in the formation of a carbon–carbon bond with a transition metal as a catalyst, and it is primarily used for the preparation of polymers with predetermined molecular weights. Numerous transition metal complexes are employed as catalysts for ATRP,
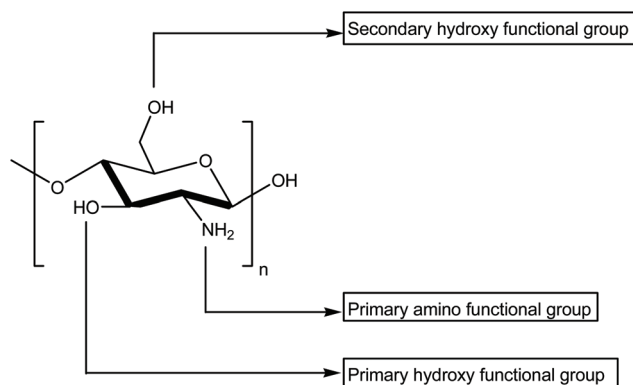

Fig. 4 Functional groups present in CS.[15]

including those of Cu, Fe, Ru, Ni and Pd. Among them CuBr is the most commonly used catalyst for this technique.[28,29] In ATRP, the transition metal (Cu) can exist in two different oxidation states. Of the two, the lower oxidation metal complexes (Cu^I/L) react with the alkyl halide (R_n–X, where X = Cl, Br, I) initiator to reversibly produce propagating radicals ($R^\bullet$) and transition metal complexes coordinated with halide ligands (X–Cu^{II}/L) with a rate constant of activation, say, k_{act}. The complex then transfers the halogen atom to the radical, and the alkyl halide and the lower-oxidation-state metal complex is regenerated. The radicals that arise thus can react with the monomer unit M and propagate the polymerization with some rate constant, say, k_p. In the termination step, the radicals can react with each other to form the required polymer with the rate constant, say, k_t. In the further step, the radicals react with X–Cu^{II}/L and deactivate the process with the rate constant, say, k_{deact} (Scheme 1).[31–33]

RAFT is another RDRP technique that involves the preparation of living polymers via a conventional radical polymerization mediated by a reagent called the RAFT agent. It basically makes use of a chain transfer agent in the form of a thiocarbonylthio compound to achieve control over the generated molecular weight and polydispersity during the free radical polymerization. RAFT polymerization uses thiocarbonyl com-
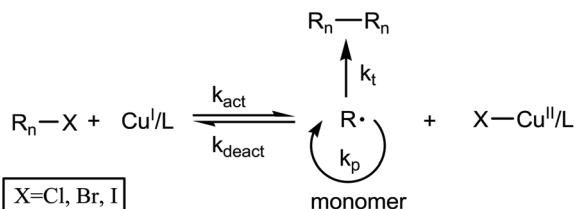
Scheme 1 Illustration of the ATRP process.

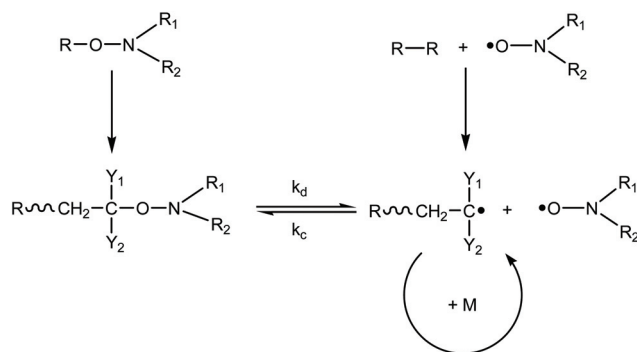**Scheme 3** Illustration of the NMP process.

pounds such as dithioesters, thiocarbamates and xanthates to mediate and enhance the polymerization process *via* a reversible chain transfer process. In this process, the RAFT agent acts as a transfer agent to form the desired polymer and the termination cannot be stopped (Scheme 2).[34–39]

The NMP process is carried out between the growing propagating radical and the nitroxide *via* radical polymerization. In this technique, the nitroxide is used as an initiator which has the ability to generate some well-controlled polymers with very low dispersity (*Đ*). Depending on the nature of the R, R_1 and R_2 groups present on the nitrogen atom, nitroxides can be prepared using various synthetic routes. The nitroxide radicals thus formed are organic compounds which contain an aminoxyl group. The polymerization kinetics for this process is controlled by both the activation and deactivation equilibria (Scheme 3).[40–43]

These techniques have made RDRP one of the most promising processes over the last few decades. Moreover, these techniques provide new ways to polymerize and utilize CS in various aspects.[44] This review mostly delineates the modification of CS *via* RDRP techniques which have been carried out by various research groups around the globe. The modified CS shows some fascinating and unique properties that eventually lead to diverse applications in various fields. The obtained bioactive macromolecular CS and its derivatives were characterized and well explained by different physico-chemical techniques such as FT-IR, UV-Vis, ^{1}H-NMR, ^{13}C-NMR, XRD, SEM, TEM, TGA, DSC, and GPC analyses. These analyses provided the details of the polymers formed for the desired purpose.

2.   Modification of chitosan *via* RDRP

As stated in previous discussions, although CS is a biodegradable polymer, it has very limited applications due to its

poor solubility in water and various organic solvents. To overcome these problems, various modifications were carried out by different research groups. This section of the review mostly emphasizes on different modifications of CS performed *via* RDRP, *viz*. ATRP, RAFT and NMP techniques.

## 2.1   Modification of chitosan *via* ATRP

CS has been modified using the ATRP technique by many research groups. Bao *et al.* used a *grafting onto* method to prepare a well-defined graft copolymer, poly[(2-dimethylamino) ethyl methacrylate]-*graft*-chitosan (PDMAEMA-*g*-CS), under mild conditions by combining ATRP with active ester conjugation (Scheme 4).[45] Furthermore, the same group synthesized a comb-like graft CS terpolymer, *i.e.* chitosan-*graft*-poly[(2-di-methylamino)ethyl methacrylate]-*graft*-poly(*N*-isopropyl-acrylamide) or CS(-*g*-PDMAEMA)-*g*-PNIPAM, by combining ATRP and "click" chemistry. First, PDMAEMA and PNIPAM were prepared *via* ATRP and the halide end groups were substituted by azido groups. Then alkynyl-CS was prepared from CS *via* amidation. Finally, PDMAEMA-N_3 and PNIPAM-N_3 were grafted onto alkynyl-CS to prepare the novel stimuli-responsive graft terpolymer (Scheme 5).[46] In a similar manner, Yuan *et al.* synthesized an amphiphilic chitosan-*graft*-poly(ε-caprolac-tone)-(*graft*-poly(2–2(methoxyethoxy)ethyl methacrylate-*co*-oligo-(ethylene glycol) methacrylate)) (CS-*g*-PCL(-*g*-P(MEO$_2$MA-*co*-OEGMA))) graft copolymer by combining ring-opening polymerization (ROP), ATRP and click chemistry (Scheme 6).[47] In another work, novel alkaline anion exchange membranes (AEMs) were prepared by Liu *et al. via* inserting quaternary phosphonium polymer brush graphene oxide (QPGO) into the
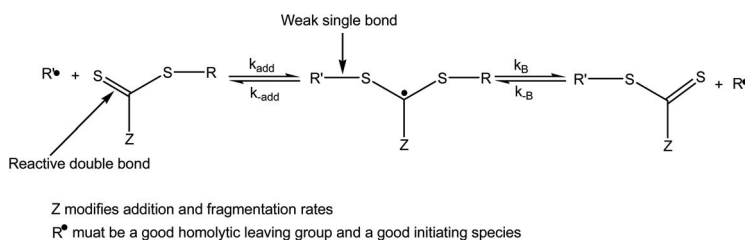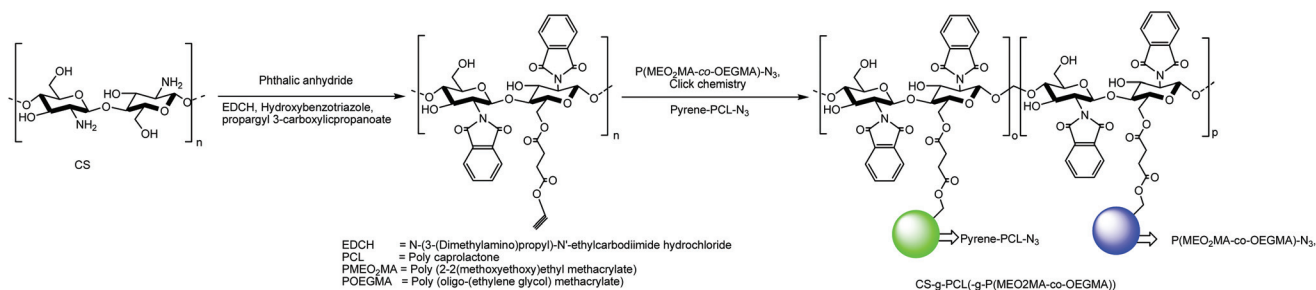

Scheme 2 Illustration of the RAFT process.
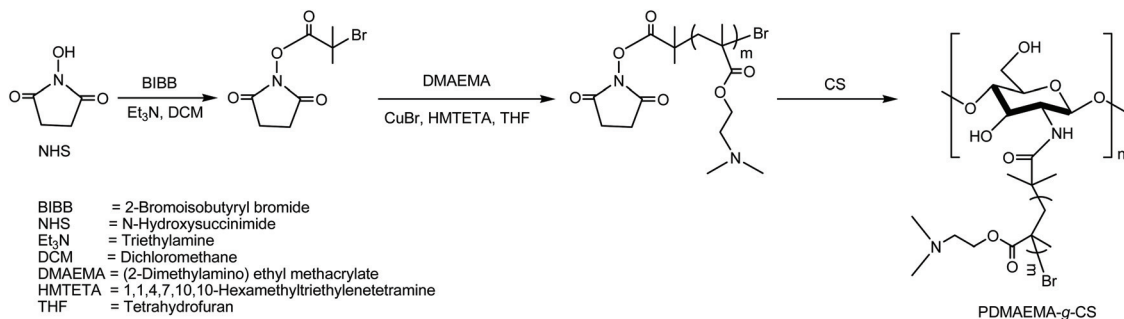
Scheme 4 Synthesis of PDMAEMA-*g*-CS *via* ATRP.[45]
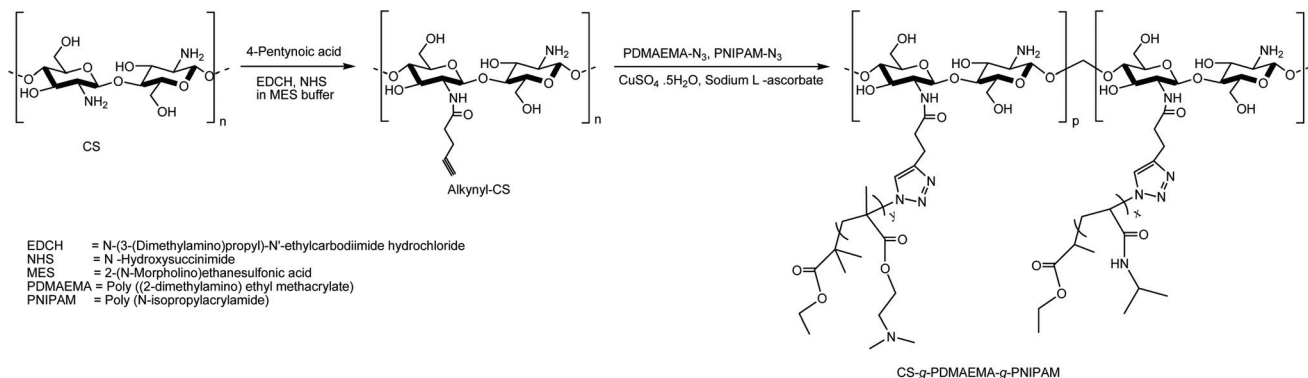
Scheme 5 Synthesis of the CS-*g*-PDMAEMA-*g*-PNIPAM graft terpolymer *via* ATRP and alkyne-azide click chemistry.[46]


Scheme 6 Synthesis of CS-*g*-PCL(-*g*-P(MEO$_2$MA-*co*-OEGMA)) *via* ROP, ATRP and alkyne-azide click chemistry.[47]

CS matrix (Scheme 7). Firs, QPGO was prepared *via* ATRP and then grafted into the CS matrix to form AEMs.[48]

Another investigation was carried out by Tahlawy *et al.* using the *grafting from* approach. First, CS was modified to serve as a co-initiator. The CS macro-initiator was prepared by the reaction of CS with 2-bromo-isobutyryl bromide (BIBB) in the presence of pyridine. The macroinitiator helped to polymerize methoxy-poly(ethylene glycol) methacrylate [MeO (PEG350)MA] *via* ATRP (Scheme 8).[49] Applying a similar approach, Chen *et al.* developed another comb-shaped CS-*g*-PNIPAM copolymer from bromoisobutyryl-terminated CS *via* ATRP, in which PNIPAM was used as a side chain (Scheme 9).[50]

Li *et al.* synthesized chitosan-*g*-polyacrylamide (CS-*g*-PAM) *via* surface-initiated (SI) ATRP and investigated to attain better and selective removal of mercury ions from aqueous solution (Scheme 10a). The modified CS beads thus obtained were very efficient in adsorbing mercury ions when compared to pristine CS beads. The adsorbed mercury ions on the modified CS beads were desorbed in a perchloric acid solution and the regenerated beads had almost the same adsorption capacity.[51]

In a similar approach, Liu *et al.* developed a polystyrene (PSty)-grafted chitosan particle (CS-*g*-PS) in the presence of 1,10-phenanthroline and Cu(ɪ)Br as a catalyst in toluene where CS bromo-acetamide was applied as a macro-initiator (Scheme 10b).[52] Another investigation of CS as a macroinitia-
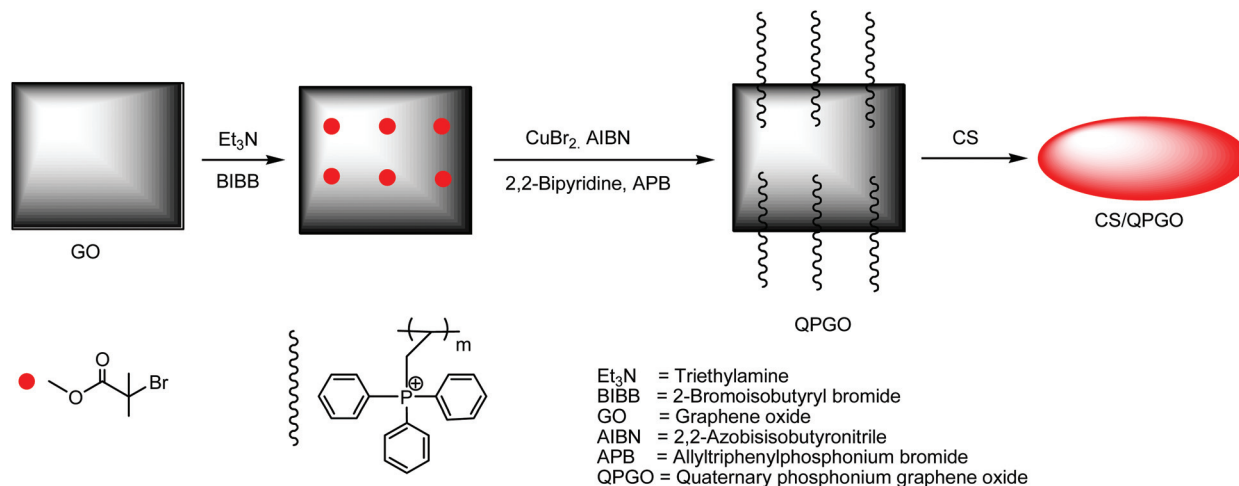
Scheme 7 Synthesis of AEMs *via* ATRP.[48]
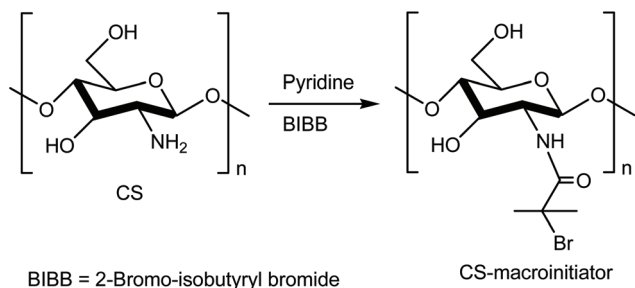
Scheme 8 Synthesis of the CS macroinitiator.[49]

tor was carried out by Dryabina *et al.* in which CS reacted with 2-bromoisobutyl bromide (BIBB) in the presence of DMF (Scheme 11). Then the pre-prepared macroinitiator was used to polymerize trimethyloxyethylmethacryloyl ammonium ethyl sulfate (MEMA MS) to form the CS-*g*-MEMA MS graft copolymer *via* ATRP.[53] Moreover, Huang *et al.* reported functionalized cross-linked chitosan (CCS) microspheres with pH-sensitive poly(methacrylic acid) (PMAA) to eliminate Cd^{2+} ions from aqueous solution *via* SI-ATRP of sodium methacrylate (MAAS) (Scheme 12).[54]

A new approach for the modification of CS was developed by Tang *et al.* in which poly(methylmethacrylate) (PMMA) and poly(methylmethacrylate)-*block*-poly(poly(ethylene glycol) methyl ether methacrylate) (PMMA-*b*-P(PEGMA)) were grafted onto chitosan nanospheres (CSNSs) by using FeCl$_3$·6H$_2$O as the catalyst, triphenylphosphine (PPh$_3$) as the ligand and ascorbic acid as the reducing agent *via* an iron(III)-mediated surface-initiated activator generated by the electron transfer (AGET) ATRP technique (Scheme 13).[55]

Another series of new degradable cationic polymers known as PDCS was developed by Ping *et al. via* ATRP to functionalize CS (Scheme 14). PDCS is composed of CS and PDMAEMA, and it is flexible enough to condense plasmid DNA (pDNA).[56]

2.2 Modification of chitosan *via* RAFT

RAFT is another advantageous RDRP technique used by various research groups for the modification of CS. Hua *et al.* first successfully modified CS using phthalic anhydride, and *S*-1-dodecyl-*S′*-(α,α′-dimethyl-α″-acetic acid) trithiocarbonate (DDACT) acted as a RAFT reagent.

The polymer thus formed undergoes a graft copolymerization with acrylic acid (AA) at 80 °C to form chitosan-*graft*-poly (acrylic acid) (CS-*g*-PAA) (Scheme 15a).[23] By applying a similar
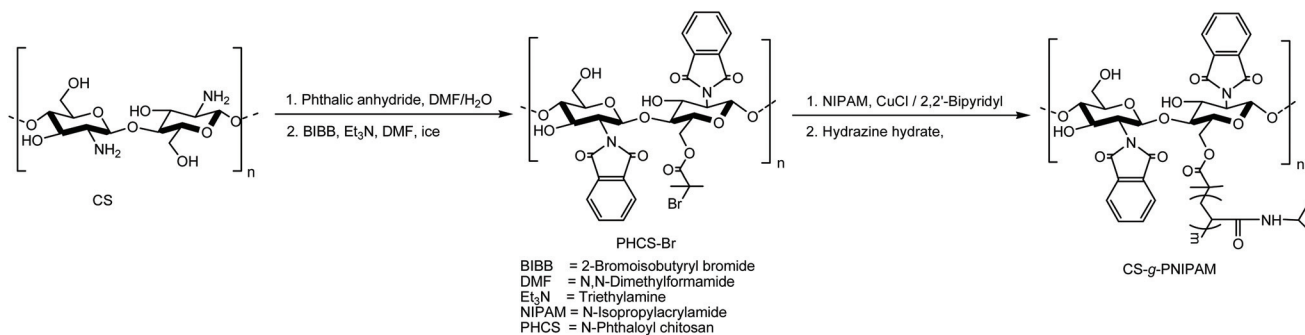
Scheme 9 Synthesis of CS-*g*-PNIPAM *via* ATRP.[50]
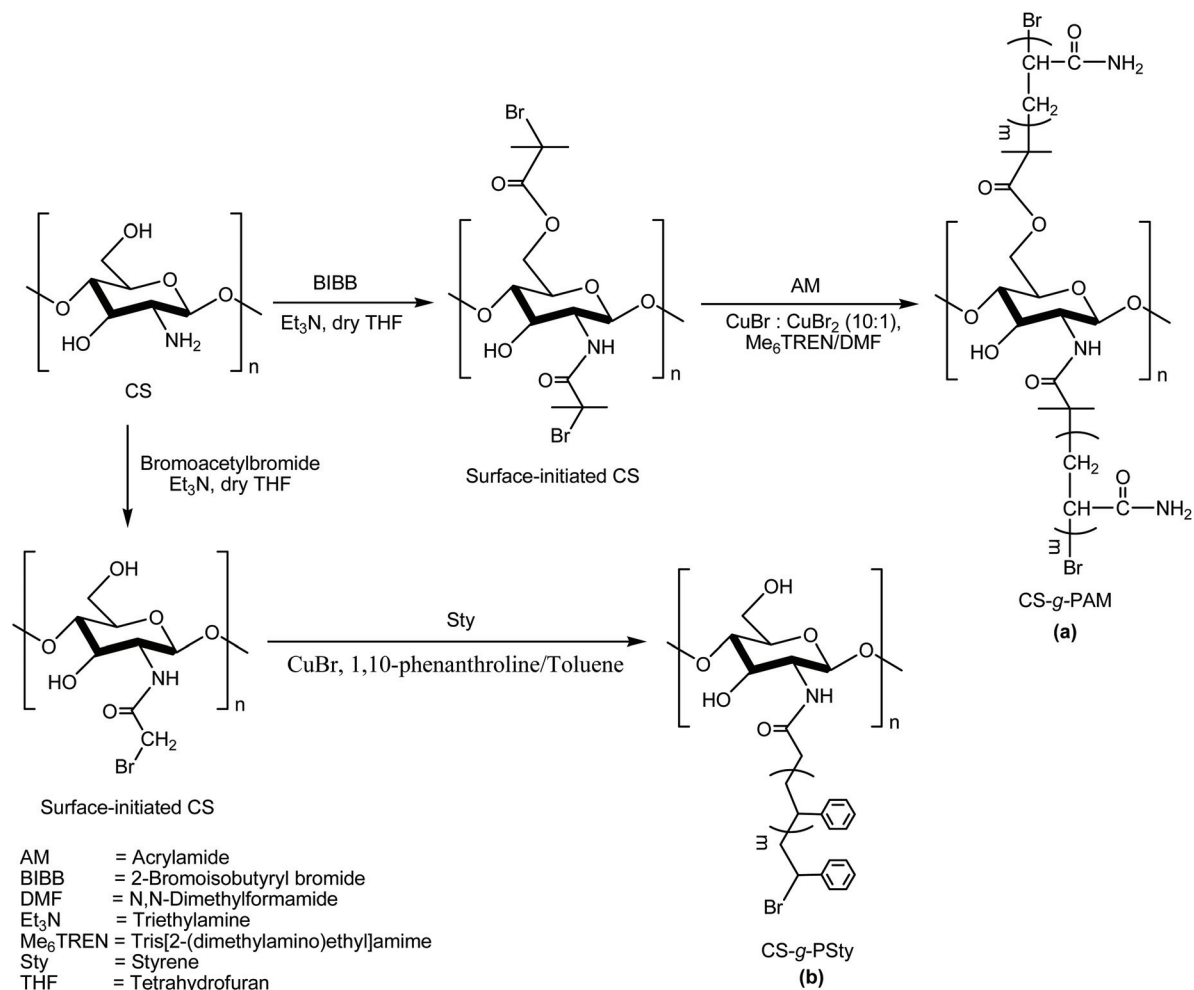
Scheme 10 Synthesis of (a) CS-*g*-PAM and (b) CS-*g*-PSty from the CS macroinitiator *via* SI-ATRP.[51,52]
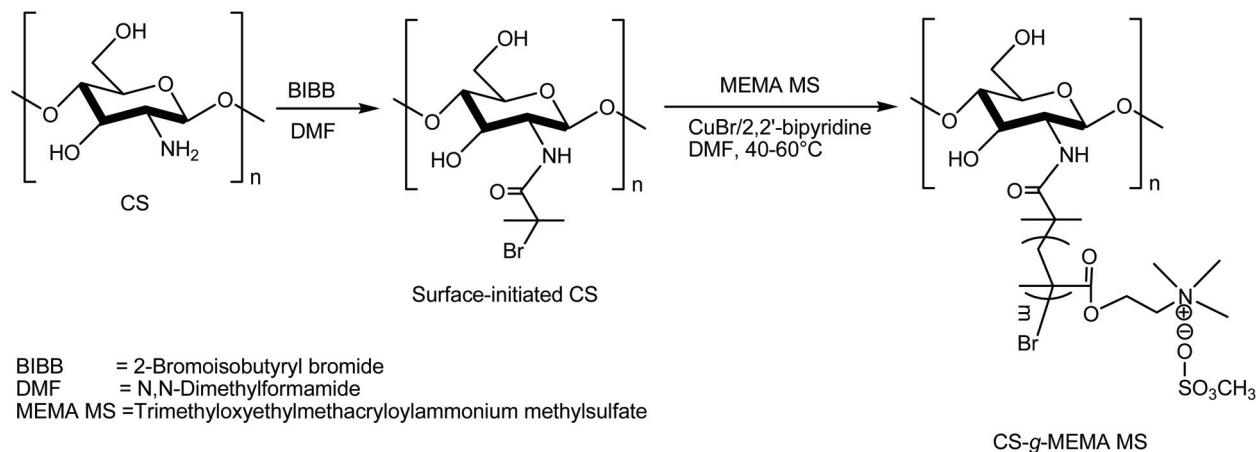
Scheme 11 Synthesis of CS-*g*-MEMA MS from the CS macroinitiator *via* ATRP.[53]

procedure, Abbasian *et al.* also synthesized CS-*g*-PAA using 4-cyano-4-[(phenylcarbithiol)sulfanyl] pentanoic (RA) acid as a RAFT reagent at 75 °C (Scheme 15b).[57] In another attempt,

Hua *et al.* also outstandingly synthesized chitosan-*graft*-poly(*N*-isopropylacrylamide) (CS-*g*-PNIPAM) using DDACT as a RAFT reagent (Scheme 15c).[58] In another work, *N*-phthaloychitosan-
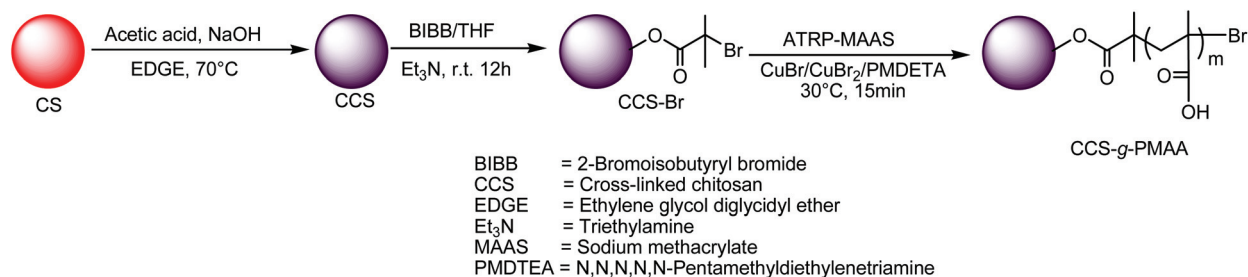
Scheme 12 Synthesis of CCS-*g*-PMAA *via* SI-ATRP of MAAS.[54]

BIBB = 2-Bromoisobutyryl bromide
CCS = Cross-linked chitosan
EDGE = Ethylene glycol diglycidyl ether
Et₃N = Triethylamine
MAAS = Sodium methacrylate
PMDTEA = N,N,N,N,N-Pentamethyldiethylenetriamine
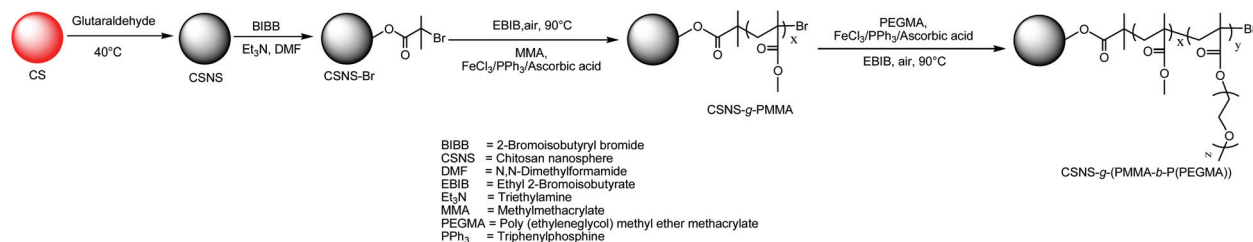
Scheme 13 Synthesis of CSNS-*g*-PMMA and CSNS-*g*-(PMMA-*b*-P(PEGMA)) *via* SI-AGET-ATRP.[56]

BIBB = 2-Bromoisobutyryl bromide
CSNS = Chitosan nanosphere
DMF = N,N-Dimethylformamide
EBIB = Ethyl 2-Bromoisobutyrate
Et₃N = Triethylamine
MMA = Methylmethacrylate
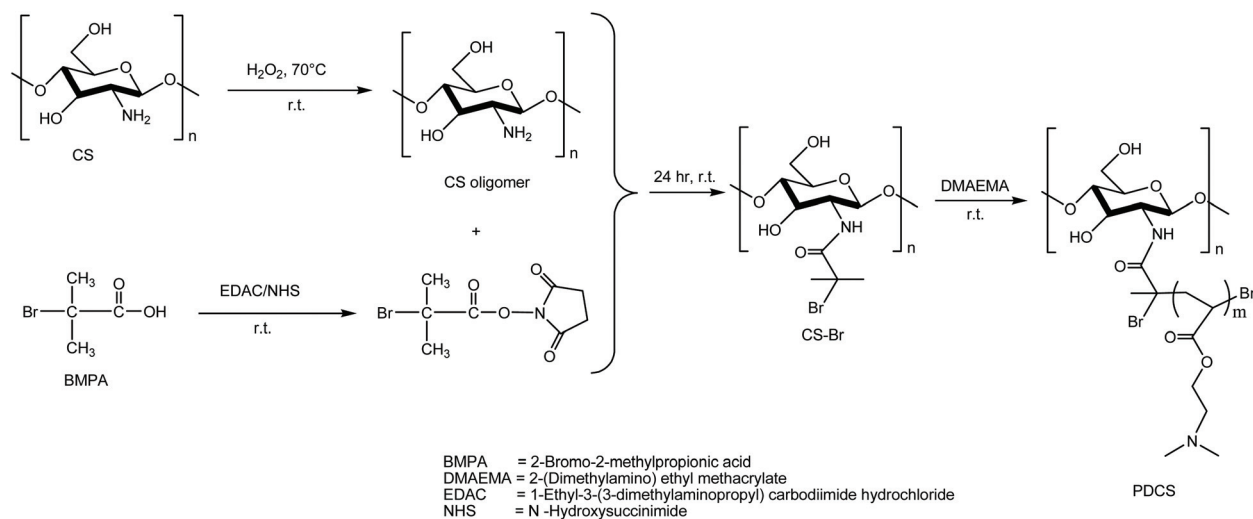PEGMA = Poly (ethyleneglycol) methyl ether methacrylate
PPh₃ = Triphenylphosphine

BMPA = 2-Bromo-2-methylpropionic acid
DMAEMA = 2-(Dimethylamino) ethyl methacrylate
EDAC = 1-Ethyl-3-(3-dimethylaminopropyl) carbodiimide hydrochloride
NHS = N-Hydroxysuccinimide

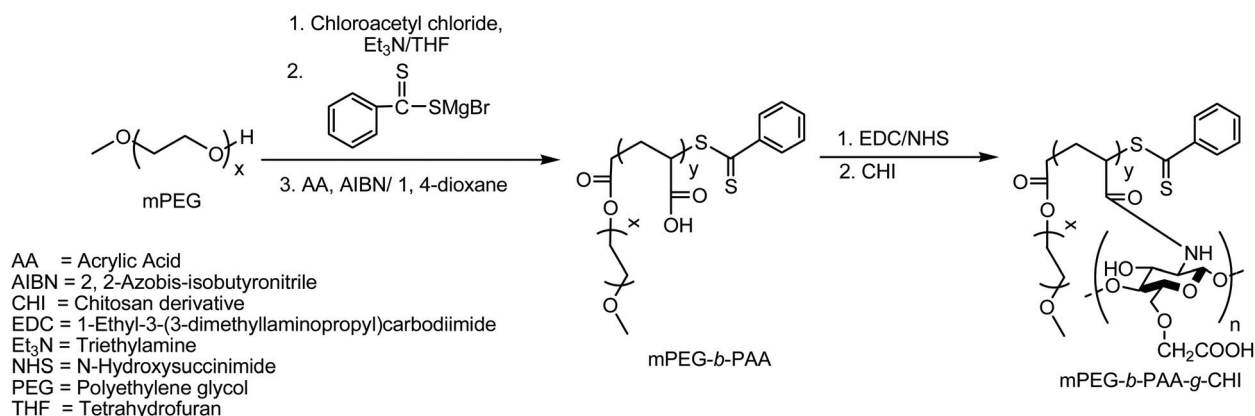**Scheme 14** Synthesis of PDCS vectors.[56]

graft-(poly(*N*-isopropylacrylamide)-*block*-poly(acrylic acid)(*N*-phthaloychitosan-*g*-PNIPAM-*b*-PAA) was notably prepared by Zhang *et al.* *via* RAFT polymerization. In this synthetic procedure, *N*-phthaloychitosan was initially modified using 3-benzylsulfanyl thiocarbonyl sulfanyl propionic acid (BPATT) as a macro RAFT agent. Then graft copolymerization of AA and NIPAM was carried out in the presence of DMF to obtain the desired modified polymer (Scheme 15d).[59]

In a different approach, a multifunctional graft copolymer polyethylene glycol-*block*-polyacrylic acid-*graft*-chitosan derivative (mPEG-*b*-PAA-*g*-CHI) was successfully prepared by Cheng-

bin *et al.* First, the block copolymer mPEG-*b*-PAA was synthesized by using mPEG as a chain transfer agent (mPEG-CTA) *via* RAFT polymerization. Afterwards, the pre-prepared block copolymer was grafted on the desired chitosan derivative (CHI) to form the new multifunctional graft copolymer (Scheme 16).[60] In another attempt at applying the *grafting onto* approach, the chitosan-*graft*-poly[poly(ethyleneglycol)methacrylate]-*graft*-L-glutathione (CS-*g*-PMPEG-*g*-GSH) conjugate was prepared by Li *et al.* *via* RAFT polymerization. Initially, PMPEG polymers along with dithioester residues were synthesized *via* RAFT polymerization and then grafted onto allyl-CS *via* the radical coupling method (Scheme 17).[61]
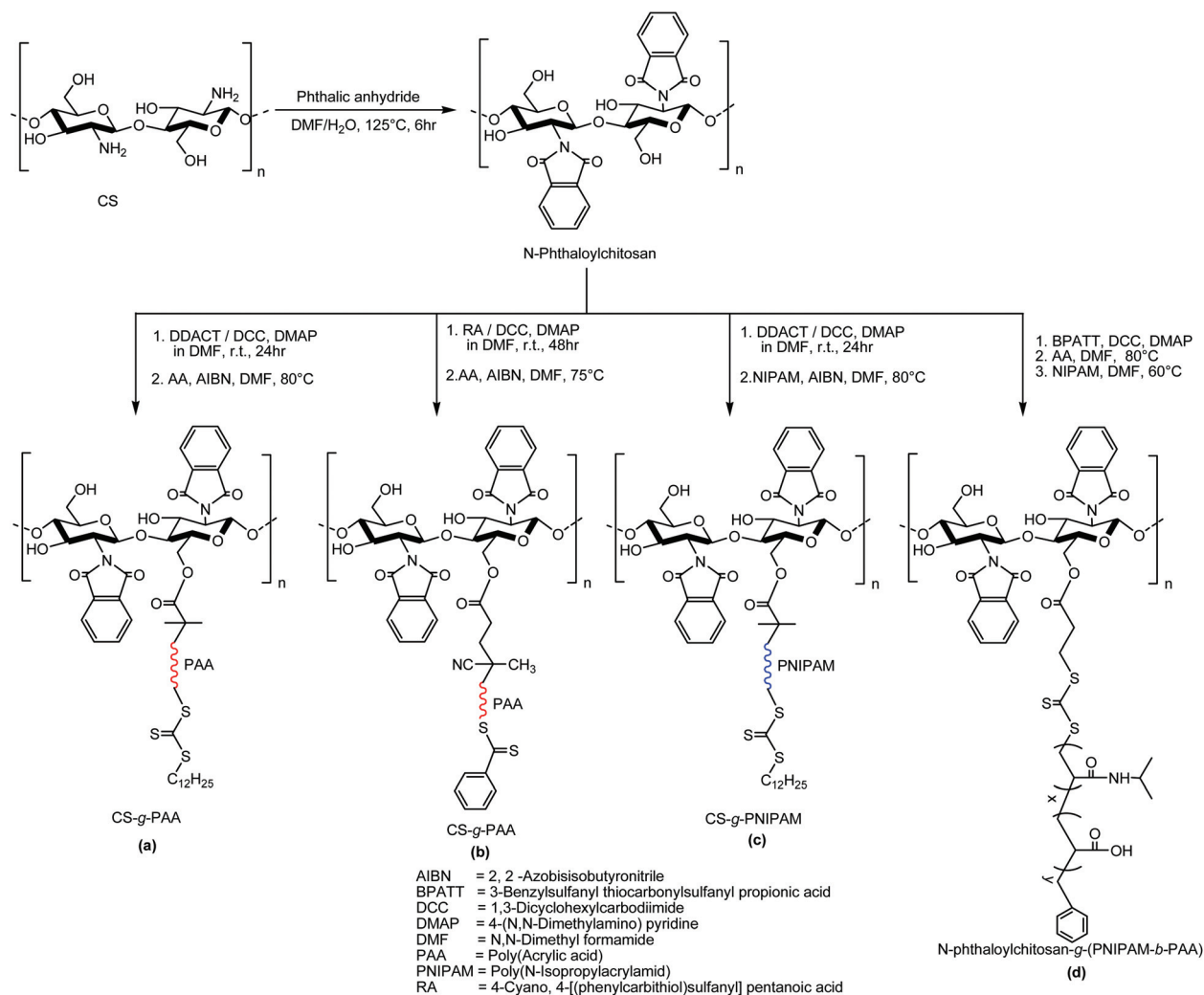
Scheme 15 Synthesis of (a) CS-*g*-PAA, (b) CS-*g*-PAA, (c) CS-*g*-PNIPAM and (d) CS-*g*-(PNIPAM-*b*-PAA) *via* RAFT polymerization.[23,57–59]

Within Scheme 15:

AIBN = 2, 2 -Azobisisobutyronitrile
BPATT = 3-Benzylsulfanyl thiocarbonylsulfanyl propionic acid
DCC = 1,3-Dicyclohexylcarbodiimide
DMAP = 4-(N,N-Dimethylamino) pyridine
DMF = N,N-Dimethyl formamide
PAA = Poly(Acrylic acid)
PNIPAM = Poly(N-Isopropylacrylamid)
RA = 4-Cyano, 4-[(phenylcarbithiol)sulfanyl] pentanoic acid

Scheme 16 Synthesis of mPEG-*b*-PAA-*g*-CHI *via* RAFT polymerization.[60]

Within Scheme 16:

AA = Acrylic Acid
AIBN = 2, 2-Azobis-isobutyronitrile
CHI = Chitosan derivative
EDC = 1-Ethyl-3-(3-dimethyllaminopropyl)carbodiimide
Et₃N = Triethylamine
NHS = N-Hydroxysuccinimide
PEG = Polyethylene glycol
THF = Tetrahydrofuran

In a novel approach, Huang *et al.* developed a simple method for the controlled modification of CS *via* the RAFT technique using the *grafting to* approach under exposure to γ-radiation. In this method, poly[*N*-(2-hydroxyethyl) prop-2-enamide] (PHEPE) was grafted onto CS using *S,S′*-bis(*R,R′*-dimethyl-*R″*-acetic acid) trithiocarbonate (BDACT) at room
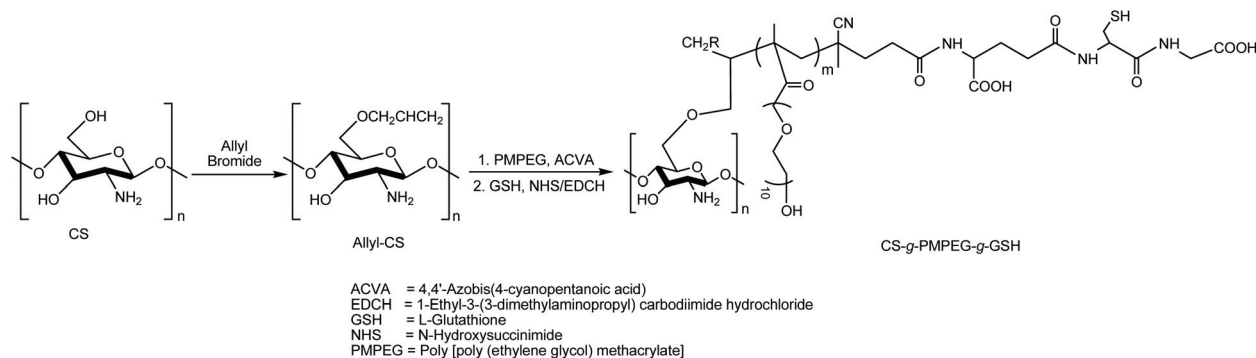
**Scheme 17** Synthesis of the CS-g-PMPEG-g-GSH conjugate *via* RAFT polymerization and the radical coupling method.[61]

temperature under γ-ray irradiation. The unprotected amino groups present in CS were used for the conjugation with an anticancer agent, namely chromone-3-carboxaldehyde (Scheme 18).[44] In another work using the same RAFT agent (BDACT), Hosseinzadeh *et al.* modified the surface of CS by using an esterification reaction through encapsulation of Fe_3O_4 nanoparticles and were able to synthesize magnetic CS

hydrogel nanocomposites *via* the RAFT polymerization technique (Scheme 19).[62]

2.3 Modification of chitosan *via* NMP

In addition to other techniques, NMP is another important technique through which CS can be modified. Various groups have made efforts to modify CS using NMP. The first initiative
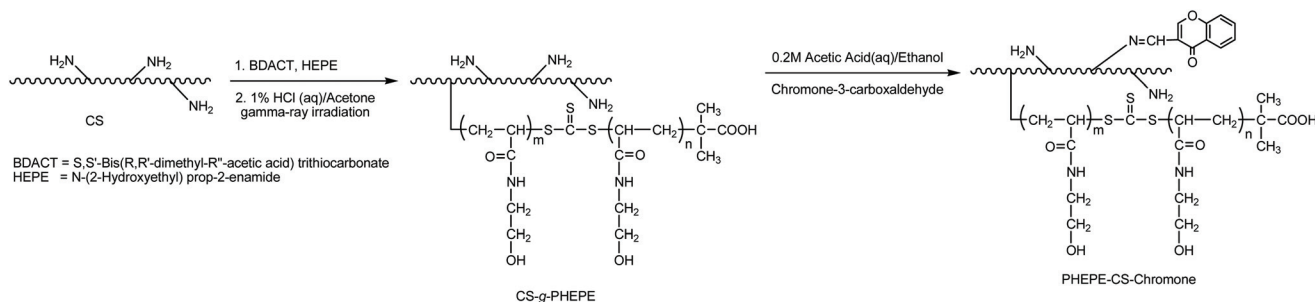
Scheme 18 Synthesis of PHEPE-CS-chromone *via* RAFT under γ-ray irradiation.[44]
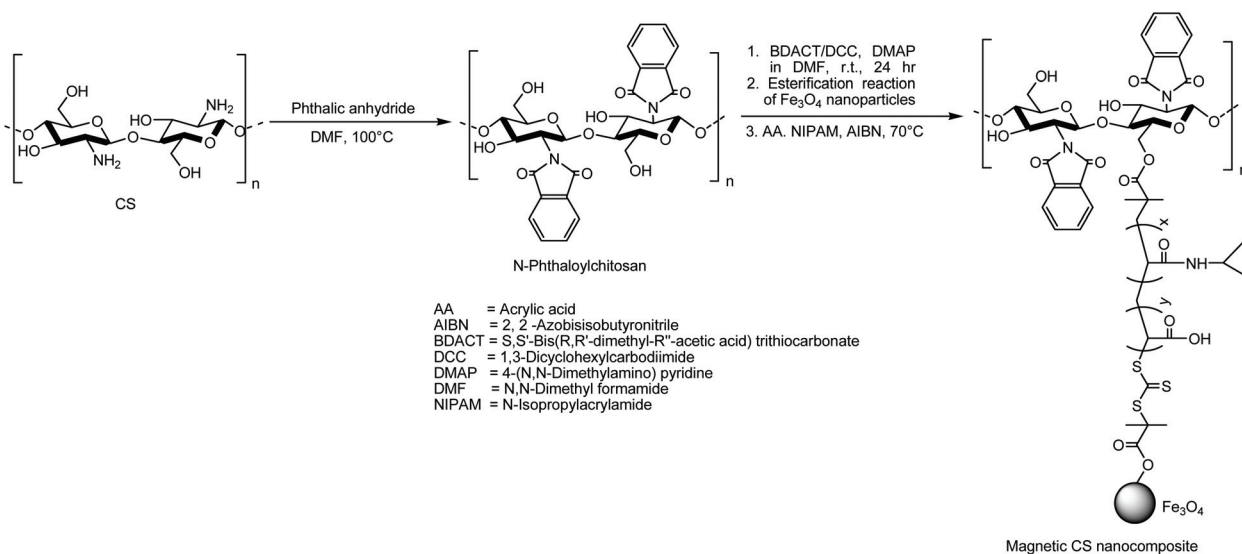
Scheme 19 Synthesis of a magnetic chitosan nanocomposite *via* RAFT polymerization.[62]

was put forward by Hua *et al.* They modified CS with phthalic anhydride. Thereafter, [60]Co γ-ray irradiation of *N*-phthaloyl chitosan and 4-hydroxy-2,2,6,6-tetramethyl piperidine-1-oxyl (4-OHTEMPO) in DMF yielded the CS-TEMPO macroinitiator

under an argon atmosphere. The macroinitiator thus formed was then used to graft PSty onto the CS matrix at 110 °C *via* the NMP technique (Scheme 20a).[63] Subsequently, by using the same macroinitiator, the same group was able to syn-
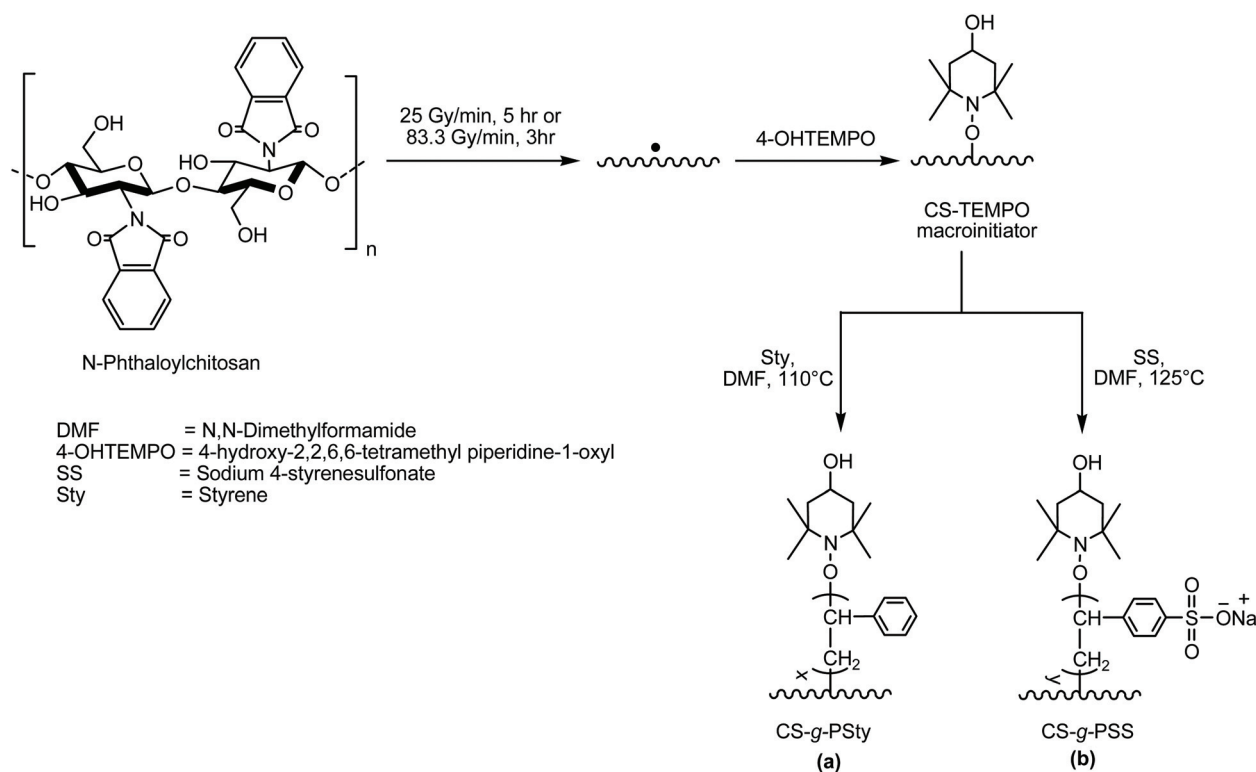

DMF = N,N-Dimethylformamide
4-OHTEMPO = 4-hydroxy-2,2,6,6-tetramethyl piperidine-1-oxyl
SS = Sodium 4-styrenesulfonate
Sty = Styrene

Scheme 20 Synthesis of (a) CS-*g*-PSty and (b) CS-*g*-PSS *via* NMP.[63,64]

Et₃N = Triethylamine
PSMA = Poly(styrene-maleic anhydride)
scCO₂ = Supercritical carbon dioxide
Sty = Styrene
TEMPO = 2,2,6,6-Tetramethylpiperidin1-oxy
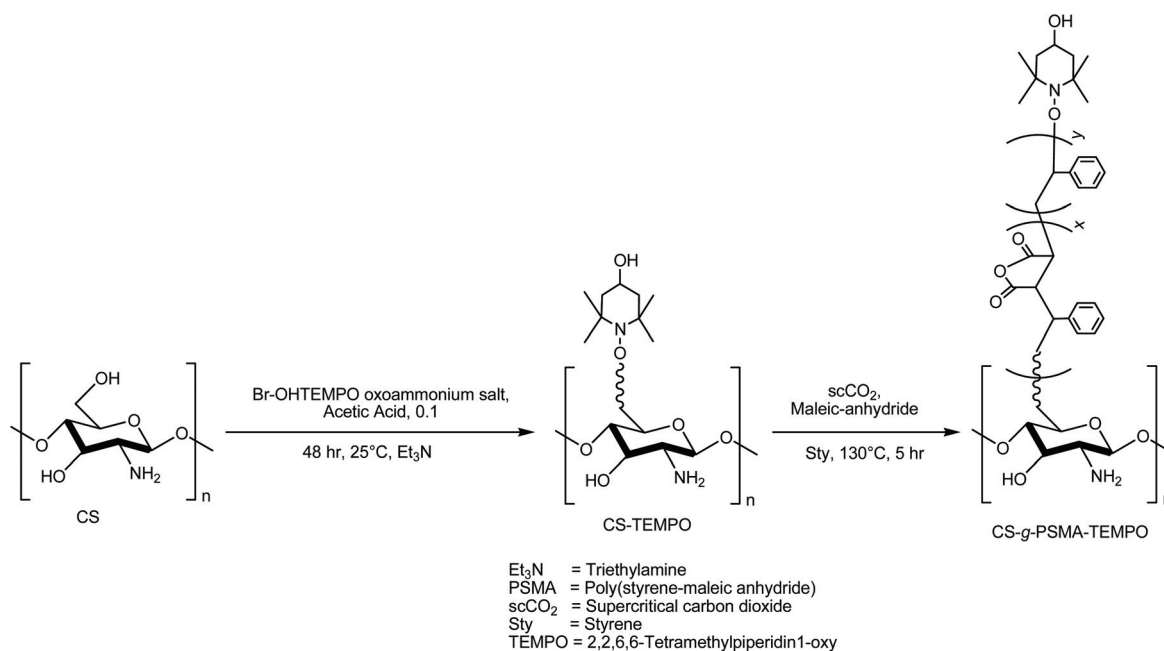
Scheme 21 Synthesis of CS-*g*-PSMA-TEMPO *via* NMRP.[65]

thesize chitosan-*graft*-poly(sodium 4-styrenesulfonate) (CS-*g*-PSS) *via* NMP (Scheme 20b).[64] In another work, García-Valdez *et al.* have successfully prepared macroalkoxyamine TEMPO-functionalized CS which later served as a macroinitiator for the graft co-polymerization of styrene-maleic anhydride (SMA) on CS *via* nitroxide-mediated radical polymerization (NMRP). The polymerization was carried out in the presence of super-critical carbon dioxide (scCO$_2$) along with camphorsulfonic acid (Scheme 21).[65]
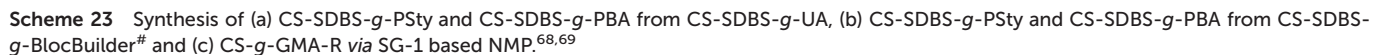
In a novel approach, Lefay *et al.* prepared chitosan-*graft*-poly(methyl methacrylate-*co*-acrylonitrile) [CS-*g*-P(MMA-*co*-AN)] (Scheme 22a) and chitosan-*graft*-poly(sodium 4-styrenesulfonate) (CS-*g*-PSS) (Scheme 22b) graft copolymers by using the *grafting from* approach. Initially the process was carried out by modifying CS with acrylamide and/or acrylate *via* SG-1-based NMP under heterogeneous conditions. Then the polymerization was accompanied by intermolecular 1,2 radical addition of the BlocBuilder® [2-methyl-2-(*N*-tert-butyl-*N*-(1-diethoxyphosphoryl-2,2-dimethylpropyl)aminoxy)-propionic acid] alkoxyamine and methyl methacrylate (MMA) in the presence of a small amount of acrylonitrile (AN) or sodium 4-styrenesulfonate (SS) to produce SS and MMA-*co*-AN, which was confirmed

by ESR and free-solution capillary electrophoresis. Finally, the synthesized copolymers were corroborated by TGA and solid-state NMR spectroscopy.[66] Following a similar approach, Kwan *et al.* grafted a series of oligo-(ethylene glycol) methacrylate (OEGMA)/diethylene glycol methacrylate (MEO$_2$MA)/acrylonitrile (AN) terpolymers from a CS backbone (Scheme 22c).[67]

Besides the heterogeneous approach, various modifications of CS were also carried out under homogeneous conditions. García-Valdez *et al.* initially reported the modification of CS with PSty and poly(butyl acrylate) (PBA) *via* NMP and the *grafting from* approach. First, CS was modified with glycidyl methacrylate (GMA) to form CS-*g*-GMA and then it was functionalized with sodium dodecylbenzenesulfonate (SDBS) to produce CS-SDBS-*g*-GMA. After the formation of CS-SDBS-*g*-GMA, it was converted to a macroalkoxyamine by intermolecular 1,2 radical addition by either of two ways: 2,2,5-trimethyl-3-(1-phenylethoxy)-4-phenyl-3-azahexane (TIPNO)-based alkoxyamine, also known as universal alkoxyamine (UA), to form CS-SDBS-*g*-GMA-TIPNO (Scheme 23a) or the BlocBuilder# [*N*-(2-methyl-propyl)-*N*-(1-diethylphosphono-2,2-dimethylpropyl)-*O*-(2-carboxylprop-2-yl)hydroxylamine] to yield CS-SDBS-*g*-GMA-BB (Scheme 23b). These macroalkoxyamines were then used to
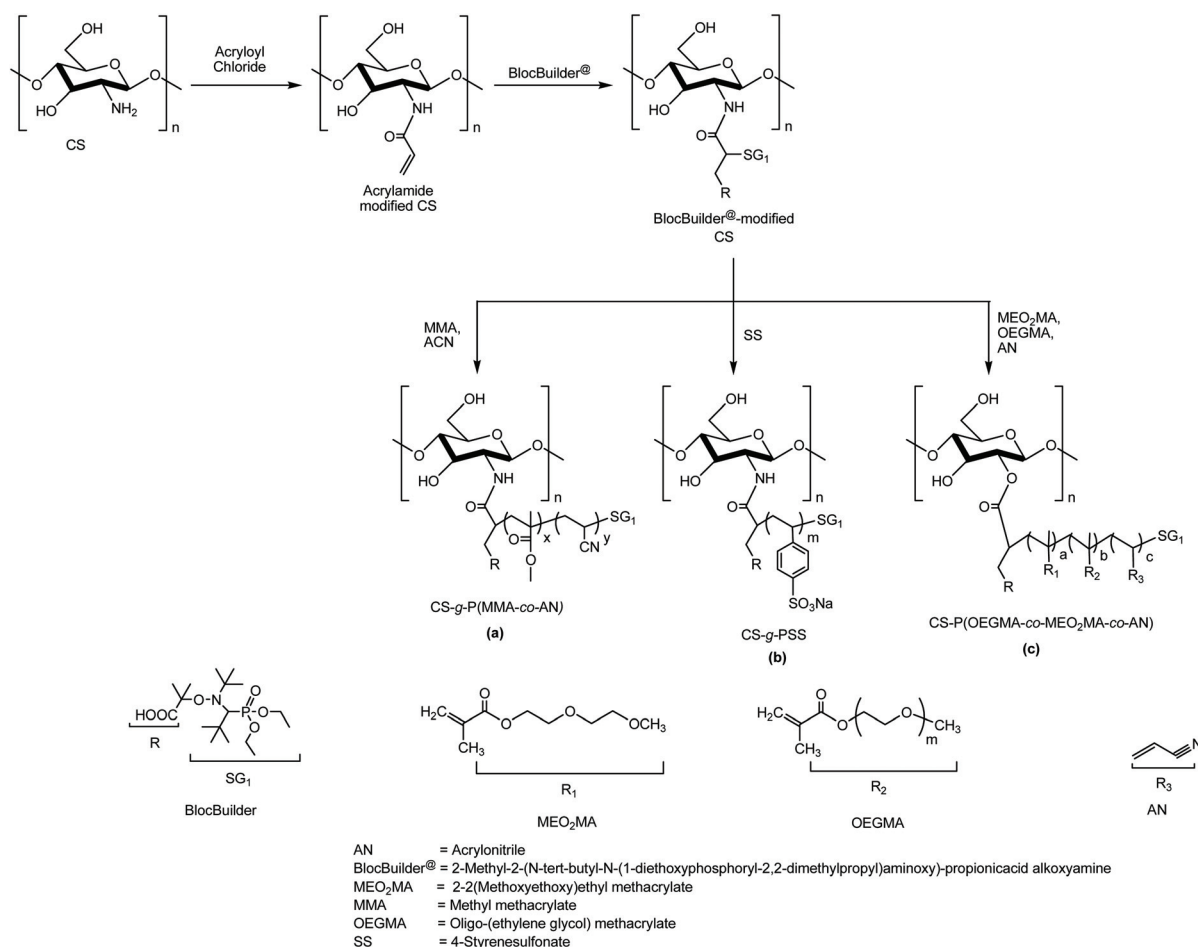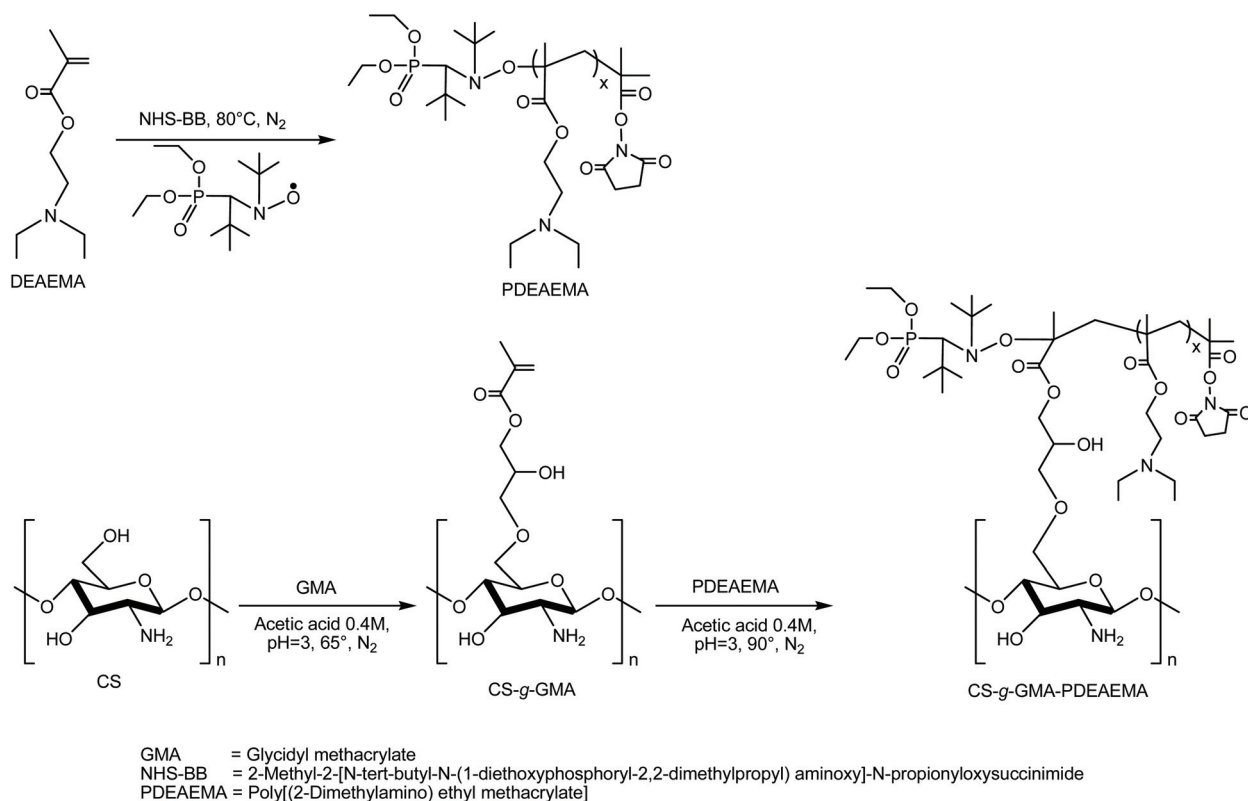

Scheme 22 Synthesis of (a) CS-*g*-P(MMA-*co*-AN), (b) CS-*g*-PSS and (c) CS-P(OEGMA-*co*-MEO$_2$MA-*co*-AN) *via* SG-1 based NMP.[66,67]

Scheme 23 Synthesis of (a) CS-SDBS-*g*-PSty and CS-SDBS-*g*-PBA from CS-SDBS-*g*-UA, (b) CS-SDBS-*g*-PSty and CS-SDBS-*g*-PBA from CS-SDBS-*g*-BlocBuilder# and (c) CS-*g*-GMA-R *via* SG-1 based NMP.[68,69]

perform the graft polymerization of Sty and BA under homogeneous media. They reported that homogeneous graft polymerization had higher graft efficiency as well as more uniform grafting tendency than the heterogeneous reactions.[68] In a different work, another graft polymer CTS-SDBS-*g*-GMA was synthesized by the same group. Using the *grafting to* approach, it was then polymerized to form various functionalized copolymers with PSty, PBA, PAA, PSty-*b*-PAA and PSty-*r*-

PAA (*r* = random) which were prepared *via* the SG-1-based NMP polymerization technique. Finally, SDBS was removed by tris(hydroxymethyl)aminomethane to form CTS-*g*-GMA-R (where R = PSty, PBA, PAA, PSty-*b*-PAA, PSty-*r*-PAA) (Scheme 23c).[69]

In another attempt, Madill *et al.* modified CS with PDEAEMA to produce CS-*g*-GMA-PDEAEMA *via* NMP by applying the *grafting to* approach. The efficacy of the synthesized

GMA   = Glycidyl methacrylate
NHS-BB   = 2-Methyl-2-[N-tert-butyl-N-(1-diethoxyphosphoryl-2,2-dimethylpropyl) aminoxy]-N-propionyloxysuccinimide
PDEAEMA = Poly[(2-Dimethylamino) ethyl methacrylate]

Scheme 24 Synthesis of CS-*g*-GMA–PDEAEMA *via* NMP.[70]

GMA   = Glycidyl methacrylate
NHS-BB   = 2-Methyl-2-[N-tert-butyl-N-(1-diethoxyphosphoryl-2,2-dimethylpropyl) aminoxy]-N-propionyloxysuccinimide
PEGMA   = Poly (ethyleneglycol) methyl ether methacrylate
Sty   = Styrene
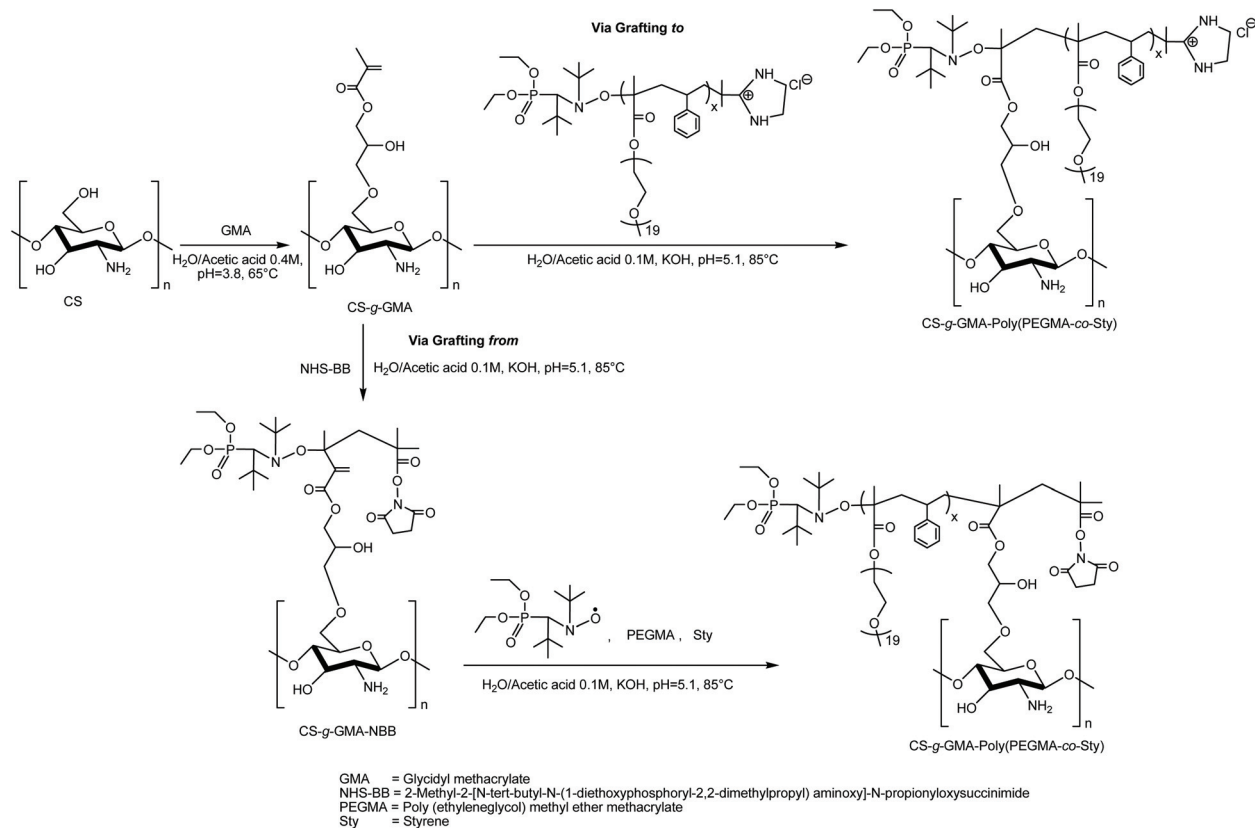
Scheme 25 Synthesis of CS-*g*-poly(PEGMA-*co*-Sty) *via* NMP and *grafting to* and *from* approaches.[71]
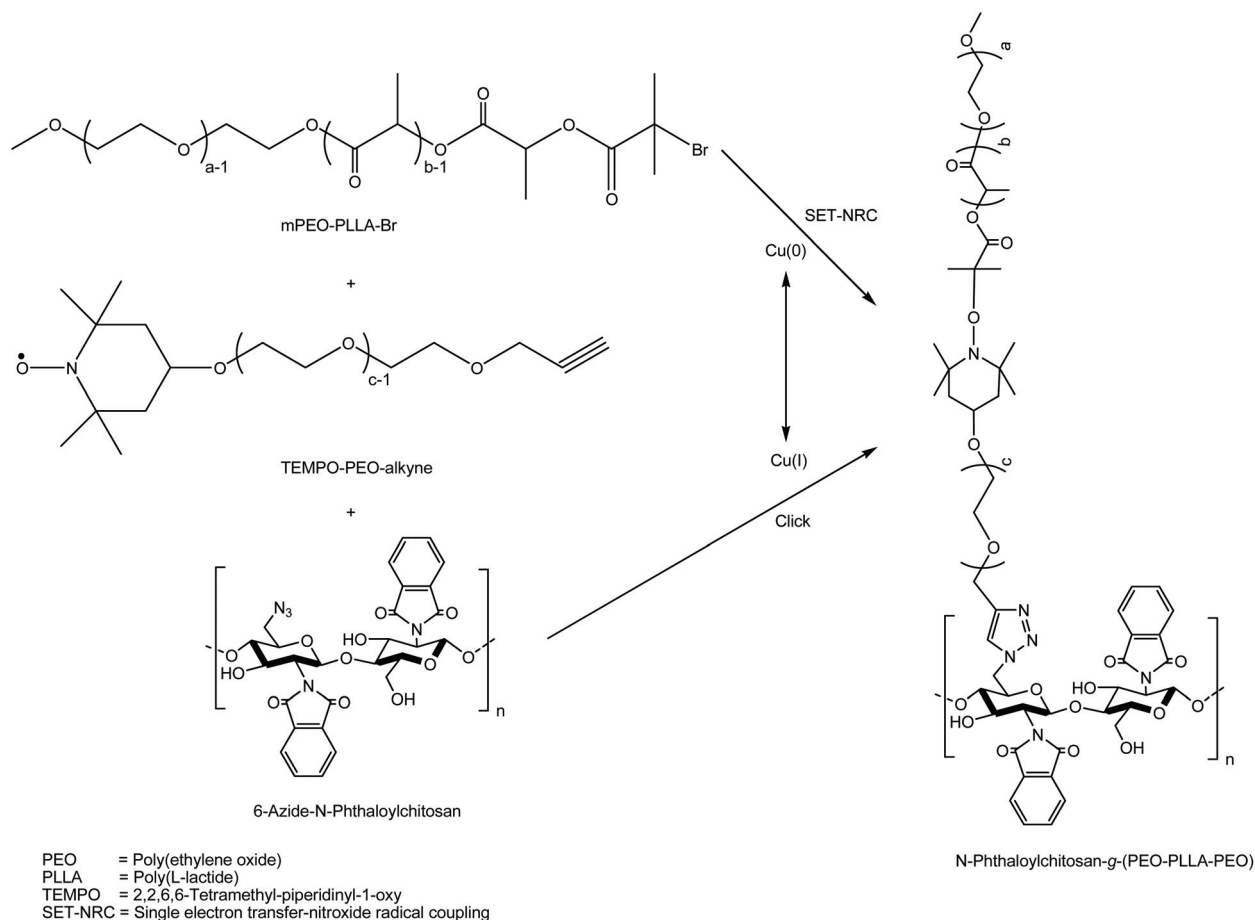
Scheme 26 Synthesis of *N*-phthaloylchitosan-*g*-(PEO-PLLA-PEO) *via* click chemistry and SET-NRC reaction.[72]

polymer was enhanced by grafting CO_2-responsive tertiary amine-containing polymers onto the backbone of CS. The main purpose of preparation of this type of polymer using the novel CO_2-switchable adsorbent concept was to enhance the performance of CS (Scheme 24).[70]

Darabi *et al.* reported the PEGlytation of CS using poly (PEGMA-*co*-Sty) by applying both the *grafting to* and *from* approaches in an aqueous medium. The whole synthesis was performed *via* the NMP technique. The report revealed that CS was initially functionalized using GMA to produce the CS-*g*-GMA macromer by the *grafting to* approach, and this step was followed by *grafting to* poly(PEGMA-*co*-Sty) to form a new polymer. Again, by using the *grafting from* approach, CS-*g*-GMA was first converted into a macroalkoxyamine using an SG1-based alkoxyamine, and afterwards graft copolymerization of PEGMA-*co*-Sty was achieved in aqueous media (Scheme 25).[71]

In another pioneering investigation in the advancement of biocompatible and degradable biomaterials, Zhang *et al.* synthesized an interesting copolymer comprising a CS backbone and amphiphilic poly(ethylene oxide)-poly(L-lactide)-poly(ethylene oxide) (PEO-PLLA-PEO) branch chains by a Cu(0)-catalyzed

one-pot procedure consolidating "click" chemistry and single electron transfer-nitroxide radical coupling (SET-NRC) reaction. Initially, the precursors of 6-azide-*N*-phthaloyl-CS, TEMPO-PEO-alkyne and mPEO-PLLA-Br were designed and implemented in the further reaction process. Afterwards, in the presence of nanosized Cu and PMDETA, the one-pot coupling reactions between these precursors were carried out to obtain the desired products (Scheme 26).[72]

3. Properties and applications of various modified chitosans

Being a natural polymer, modified CS has tremendous scope for research. Moreover, it has several interesting properties such as biocompatibility, multifunctionality and controlled biodegradability. It is mentioned in section 2 that modified CS has numerous applications in diverse fields. For the convenience of the readers and the research community, an exhaustive review of the publications referred to in section 2 along with the various properties and applications of various modified CS are discussed in Table 1.

Table 1 Modified chitosans, different RDRP techniques, reagents used and properties/applications

Modified form of chitosan	CRP techniques applied	Reagent used	Properties/applications	Ref.
PDMAEMA-*g*-CS	ATRP and active ester conjugation method (*grafting to*)	NHS, BIBB, Et$_3$N, DCM, DMAEMA, CuBr, HMTETA, THF	• Shows pH-responsive association behaviour	45
			• Used for gene/drug delivery and controlled release	
CS(-*g*-PDMAEMA)-*g*-PNIPAM	ATRP and click chemistry (*grafting to*)	4-Pentynoic acid, EDCH, NHS, MES buffer, PDMAEMA-N$_3$, PNIPAM-N$_3$, CuSO$_4$·5H$_2$O, sodium L-ascorbate	• Shows thermosensitive and pH-responsive association behaviour	46
			• Used in biomedical science and engineering	
			• Used for gene/drug delivery and controlled release	
CS-*g*-PCL(-*g*-P(MEO$_2$MA-*co*-OEGMA))	ATRP, ROP and click chemistry (*grafting to*)	Phthalic anhydride, EDCH, hydroxybenzotriazole, propargyl-3-carboxylicpropanoate, P(MEO$_2$MA-*co*-OEGMA)-N$_3$, pyrene-PCL-N$_3$	• Shows thermosensitive properties	47
			• Used in drug delivery and controlled release	
AEMs	ATRP (*grafting to*)	GO, Et$_3$N, BIBB, 2,2-bipyridine, AIBN, APB	• High mobility and activity	48
			• Promotes hydroxide conductivity	
			• Higher fuel cell performance	
CS-macroinitiator	—	BIBB, pyridine	• Helps in the formation of CS-*g*-MeO (PEG350)MA *via* ATRP	49
CS-*g*-PNIPAM	ATRP (*grafting from*)	Phthalic anhydride, DMF, BIBB, Et$_3$N, NIPAM, CuCl, 2,2′-bipyridyl, hydrazine hydrate	• Suitable for delivery of hydrophobic drug molecules	50
CS-*g*-PAM	SI-ATRP (*grafting from*)	BIBB, Et$_3$N, dry THF, PA, CuBr, CuBr$_2$, Me$_6$TREN, DMF	• Greater absorption capacity and faster absorption kinetics for mercury ions	51
			• Helps in the removal of mercury ions from aqueous solution	
CS-macroinitiator	—	Bromo-acetamide, Et$_3$N, THF, Sty, 1,10-phenanthroline, CuBr, toluene	• Helps in the formation of CS-*g*-PSty *via* SI-ATRP	52
CS-macroinitiator	——	BIBB, DMF, CuBr, 2,2′-bipyridine	• Helps in the formation of CS-*g*-MEMA MS *via* ATRP	53
CCS-*g*-PMAA	SI ATRP	CH$_3$COOH, NaOH, EDGE, BIBB, THF, MAAS, CuBr, CuBr$_2$, PMDETA	• Helps in the removal of Cd(II) ions from aqueous solution	54
CSNS-*g*-PMMA & CS-*g*-(PNIPAM-*b*-PAA)	SI AGET ATRP (*grafting from*)	Glutaraldehyde, Et$_3$N, BIBB, DMF, MMA, PEGMA, FeCl$_3$/PPh$_3$/ascorbic acid, EBIB	• Good biocompatibility	55
			• Low toxicity	
			• Used for the synthesis of materials for *in vivo* biomedical applications as well as polymerization for industrial-scale production	
PDCS vectors	ATRP (*grafting from*)	H$_2$O$_2$, BMPA, EDAC, NHS	• Exhibits good ability to condense pDNA into nanoparticles with a positive charge at a nitrogen/phosphorus ratio of 4 or higher	56
			• Lower cytotoxicity	
			• Have great potential as efficient gene vectors in future gene therapy	
CS-*g*-PAA	RAFT (*grafting from*)	Phthalic anhydride, DMF, DDACT, DCC, DMAP, AA, AIBN	• pH-Sensitivity and stimulating response	23
			• Used as a degradable matrix for drug delivery applications	
		Phthalic anhydride, DMF, RA, DCC, DMAP, AA, AIBN, DMF	• Used as a stabilizing agent for the preparation of colloidal silver nanoparticles in the range of 2–10 nm	57
			• Thermally stable	
			• Good antibacterial activity	
			• Used as a degradable matrix for drug delivery applications	
CS-*g*-PNIPAM	RAFT (*grafting from*)	Phthalic anhydride, DMF, DDACT, DCC, DMAP, NIPAM, AIBN	• Thermosensitive degradable matrix for drug delivery applications	58
N-Phthaloylchitosan-*g*-(PNIPAM-*b*-PAA)	RAFT (*grafting from*)	Phthalic anhydride, DMF, BPATT, DCC, DMAP, AA, NIPAM	• Used as a macro RAFT agent	59
mPEG-*b*-PAA-*g*-CHI	RAFT (*grafting from*)	mPEG, chloroacetyl chloride, Et$_3$N, THF, bromobenzene, Mg turnings, CS$_2$, AA, AIBN, 1,4-dioxane, EDC, NHS	• Used in gene/drug delivery applications	60

Table 1 *(Contd.)*

Modified form of chitosan	CRP techniques applied	Reagent used	Properties/applications	Ref.
CS-g-PMPEG-g-GSH	RAFT (*grafting to*) and radical coupling method	Allyl bromide, PMPEG, ACVA, GSH, NHS, EDCH	• Exhibits good ability to condense pDNA • Increases the binding ability to cell membrane efficiently • Improves decondensing ability of pDNA from nanoparticles in the cytoplasm, which results in higher transfection efficiency in mouse embryonic fibroblast cells • Used for gene therapy in clinical applications • Shows great potential as an efficient and safe nonviral gene vector	61
PHEPE-CS-chromone	RAFT (*grafting to*) and γ-ray irradiation	BDACT, HEPE, 1% HCl/acetone, CH$_3$COOH/ethanol, chromone-3-carboxaldehyde	• Used as a pH- and thermo-responsive carrier for drug delivery	44
CS hydrogel nano-composites	RAFT	Phthalic anhydride, DMF, BDACT, DCC, DMAP, Fe$_3$O$_4$, AA, NIPAM, AIBN	• Used as promising anticancer-targeted drug delivery carriers for cancer therapy	62
CS-g-PSty	NMP (*grafting from*)	4-OHTEMPO, Sty, DMF	• Good compatibility	63
CS-g-PSS	NMP (*grafting from*)	4-OHTEMPO, SS, DMF	• Shows ion-exchange property which may promote the graft copolymers to be used in ion exchange processes for environmental protection	64
CS-g-PSMA-TEMPO	NMP	Acryloyl chloride, BlocBuilder®, SS Br-OHTEMPO, oxoammonium salt, CH$_3$COOH, Et$_3$N, scCO$_2$, maleic-anhydride, Sty	• Used as a bio-compatibilizer • Useful for therapeutic applications • Thermally stable	66 65
CS-g-P(MMA-co-AN)	NMP (*grafting from*)	Acryloyl chloride, BlocBuilder®, MMA, ACN	• Used as a bio-compatibilizer	66
CS-P(OEGMA-co-MEO2MA-co-AN)	NMP (*grafting from*)	Acryloyl chloride, BlocBuilder®, MEO$_2$MA, OEGMA, AN	• Thermally responsive • Shows antimicrobial properties	67
CS-SDBS-g-PS	NMP (*grafting from*)	GMA, CH$_3$COOH, SDBS, DMSO, DMF, Sty, UA, BlocBuilder$^{\#}$	• Considered as potential precursors of new bio-hybrid materials • Used in the recovery of heavy metals from waste water of various origins	69
CS-SDBS-g-PBA	NMP (*grafting from*)	GMA, CH$_3$COOH, SDBS, DMSO, DMF, BA, UA, BlocBuilder$^{\#}$	• Considered as potential precursors of new bio-hybrid materials • Used in the recovery of heavy metals from various waste water of various origins	69
CS-g-GMA-R	NMP (*grafting to*)	GMA, acetic acid, SDBS, BlocBuilder®, 4-(diethoxyphosphinyl)-2,2,5,5-tetramethyl-3-azahexane-N-oxyl, Sty, BA, AA	• Used in biomedicine, water and wastewater treatment, bio-pharmaceuticals and agriculture	69
CS-g-GMA-PDEAEMA	NMP (*grafting to*)	DEAEMA, NHS-BB, GMA, acetic acid	• Absorbs metal from wastewater streams	70
CS-g-poly(PEGMA-co-Sty)	NMP (*grafting to/from*)	GMA, acetic acid, PEGMA, Sty, 2,2′-azobis[2-(2-imidazolin-2-yl) propane] Dihydrochloride, BlocBuilder®, [4-(diethoxyphosphinyl)-2,2,5,5-tetramethyl-3-azahexane-N-oxyl], NHS-BB	• Widely used in biomedicine and bio-pharmaceuticals, water and wastewater treatment and agriculture	71
N-Phthaloylchitosan-g-(PEO-PLLA-PEO)	Click chemistry and SET-NRC	L-Lactic, ethyl acetate, 3-bromo-1-propyne, BIBB, PMDETA, phthalic anhydride, sodium azide, nanosized Cu powder, TEMPO	• Useful for designing novel CS materials • Shows gelation behaviour	72

4. Conclusion and outlook

Chitosan is the only cationic polysaccharide found in nature among all the other naturally occurring polymers. It has unique structural, physicochemical and biological properties which make it suitable for pharmaceutical, biomedical and several other applications. However, its area of application is limited since it is insoluble in common neutral and basic aqueous solvents. To enhance its applicability, attempts have been made to modify chitosan *via* different RDRP techniques. Among various RDRP methods, ATRP and RAFT are found to be more versatile than NMP[28,29] because the latter needs slightly elevated temperature to activate alkoxyamines. In RAFT and NMP, transition metals are not used as catalysts, whereas in ATRP, transition metal catalysts are used to activate the alkyl halide initiator. ATRP is a very versatile technique.

However, in ATRP, there is a need to perform an extra purification step to remove the catalyst from the polymer, which is very important if the polymer is designed for biomedical applications. The RAFT technique is a very facile and versatile process which can be used in solution, emulsion and aqueous systems. The color and odor issues can be controlled by using suitable RAFT reagents and by adjusting their concentration. However, since the RAFT technique does not use any metal catalysts, the extra purification steps are not necessary to purify the polymer. This is one of the major advantages of using the RAFT process over ATRP. Recently, Destarac *et al.* reviewed the industrial perspectives of different RDRP methods.[30] In this review, we have mostly emphasized on numerous chemical modifications of CS by various functional groups to form derivatives which enhanced its solubility in both neutral and basic pH media. Furthermore, various attachments of functional groups to CS improve its hydrophobic, cationic and anionic properties which make it more efficient for diverse applications. Progress in this area of research is quite rapid and worthwhile. Thus, the derivatives of CS make it more versatile in diverse applications.

Abbreviations

AA	Acrylic acid
ACVA	4,4′-Azobis(4-cyanopentanoic acid)
AN	Acrylonitrile
AGET	Activator generated by electron transfer
AIBN	2,2-Azobisisobutyronitrile
AM	Acrylamide
APB	Allyltriphenylphosphonium bromide
ATRP	Atom transfer radical polymerization
AEMs	Anion exchange membranes
BA	Butyl acrylate
BDACT	S,S'-Bis(R,R'-dimethyl-R''-acetic acid)-trithiocarbonate
BIBB	2-Bromoisobutyryl bromide
BlocBuilder$^{@}$	2-Methyl-2-(N-*tert*-butyl-N-(1-diethoxyphosphoryl-2,2-dimethylpropyl)aminoxy)-propionic acid alkoxyamine
BlocBuilder$^{\#}$	N-(2-Methylpropyl)-N-(1-diethyl-phosphono-2,2-dimethylpropyl)-O-(2-carboxylprop-2-yl)hydroxylamine
BMPA	2-Bromo-2-methylpropionic acid
BPATT	3-Benzylsulfanyl thiocarbonylsulfanyl propionic acid
CCS	Cross-linked chitosan
CHI	Chitosan derivative
CSNS	Chitosan nanosphere
^{13}C-NMR	Carbon-13 nuclear magnetic resonance
CS	Chitosan
CTA	Chain transfer agent
DCC	1,3-Dicyclohexylcarbodiimide
DCM	Dichloromethane
DDACT	S-1-Dodecyl-S'-(α,α′-dimethyl-α″-acetic acid) trithiocarbonate
DMAEMA	(2-Dimethylamino) ethyl methacrylate

DMAP	4-(N,N-Dimethylamino) pyridine
DMF	N,N-Dimethylformamide
DMSO	Dimethyl sulfoxide
DSC	Differential scanning calorimetry
EBIB	Ethyl 2-bromoisobutyrate
EDC	1-Ethyl-3-(3-dimethyllaminopropyl) carbodiimide
EDCH	N-(3-(Dimethylamino)propyl)-N'-ethylcarbodiimide hydrochloride
EDGE	Ethylene glycol diglycidyl ether
Et$_3$N	Triethylamine
FT-IR	Fourier-transform infrared spectroscopy
GMA	Glycidyl methacrylate
GO	Graphene oxide
GPC	Gel permeation chromatography
GSH	L-Glutathione
HEPE	N-(2-Hydroxyethyl) prop-2-enamide
HMTETA	1,1,4,7,10,10-Hexamethyltriethylenetetramine
^{1}H-NMR	Proton nuclear magnetic resonance
MAA	Methacrylic acid
MAAS	Sodium methacrylate
MEO$_2$MA	2–2(Methoxyethoxy)ethyl methacrylate
MeO(PEG350)MA	Methoxy-poly(ethylene glycol) methacrylate
Me$_6$TREN	Tris[2-(dimethylamino)ethyl]amine
MES	2-(N-Morpholino)ethanesulfonic acid
MEMA MS	Trimethyloxyethylmethacryloyl ammonium methyl sulfate
MMA	Methylmethacrylate
NHS	N-Hydroxysuccinimide
NHS-BB	2-Methyl-2-[N-*tert*-butyl-N-(1-diethoxyphosphoryl-2,2-dimethylpropyl)aminoxy]-N-propionyloxysuccinimide
NIPAM	N-Isopropylacrylamide
NMP	Nitroxide mediated polymerization
NMRP	Nitroxide-mediated radical polymerization
OEGMA	Oligo-(ethylene glycol) methacrylate
4-OHTEMPO	4-Hydroxy-2,2,6,6-tetramethyl piperidine-1-oxyl
PCL	Poly(ε-caprolactone)
pDNA	Plasmid DNA
PEG	Polyethylene glycol
PEGMA	Poly(ethylene glycol)methyl ether methacrylate
PHCS	N-Phthaloyl chitosan
PMDTEA	N,N,N,N,N-Pentamethyldiethylenetriamine
PMPEG	Poly[poly(ethylene glycol)methacrylate]
PPh$_3$	Triphenylphosphine
QPGO	Quaternary phosphonium graphene oxide
RA	4-Cyano-4-[(phenylcarbithiol)sulfanyl] pentanoic acid
RAFT	Reversible addition–fragmentation chain transfer
RDRP	Reversible-deactivation radical polymerization
ROP	Ring opening polymerization
scCO$_2$	Supercritical carbon dioxide

SDBS	Sodium dodecylbenzenesulfonate
SEM	Scanning electron microscopy
SMA	Styrene-maleic anhydride
SS	Sodium 4-styrenesulfonate
Sty	Styrene
TEM	Transmission electron microscopy
TGA	Thermo gravimetric analysis
THF	Tetrahydrofuran
TIPNO	2,2,5-Trimethyl-3-(1-phenylethoxy)-4-phenyl-3-azahexane
UA	Universal alkoxyamine
UV-Vis	Ultraviolet–visible
XRD	X-Ray diffraction

Conflicts of interest

There are no conflicts to declare.

References

1 V. M. Correlo, L. Bhattacharya, J. F. Mano, N. M. Neves and R. L. Reis, Properties of melt processed chitosan and aliphatic polyester blends, *Mater. Sci. Eng., A*, 2005, **403**, 57–68.

2 P. K. Dutta, J. Dutta and V. S. Tripathi, Chitin and chitosan: Chemistry, properties and applications, *J. Sci. Ind. Res.*, 2004, **63**, 20–31.

3 D. Elieh-Ali-Komi and M. R. Hamblin, Chitin and chitosan: Production and application of versatile biomedical nanomaterials, *Int. J. Adv. Res.*, 2016, **4**, 411–427.

4 H. Moller, S. Grelier, P. Pardon and V. Coma, Antimicrobial and physicochemical properties of chitosan-HPMC-based films, *J. Agric. Food Chem.*, 2004, **52**, 6585–6591.

5 N. Sayari, A. Sila, B. E. Abdelmalek, R. B. Abdallah, S. Ellouz-Chaabouni, A. Bougatef and R. Balti, Chitin and chitosan from the Norway lobster by-products: Antimicrobial and anti-proliferative activities, *Int. J. Biol. Macromol.*, 2016, **87**, 163–171.

6 M. E. I. Badawy, A new rapid and sensitive spectrophotometric method for determination of a biopolymer chitosan, *Int. J. Carbohydr. Chem.*, 2012, 139328.

7 D. Kafetzopoulos, A. Martinou and V. Bouriotis, Bioconversion of chitin to chitosan: Purification and characterization of chitin deacetylase from *Mucor rouxii*, *Proc. Natl. Acad. Sci. U. S. A.*, 1993, **90**, 2564–2568.

8 I. Younes and M. Rinaudo, Chitin and chitosan preparation from marine sources. Structure, properties and applications, *Mar. Drugs*, 2015, **13**, 1133–1174.

9 H. Struszczyk, D. Wawro and A. Niekraszewicz, Biodegradability of chitosan fibres, in *Advances in chitin and chitosan*, ed. C.J Brine, P.A Sandford and J.P Zikakis, Elsevier Applied Science, London, 1991, pp. 580–585.

10 J. Ji, L. Wang, H. Yu, Y. Chen, Y. Zhao, H. Zhang, W. A. Amer, Y. Sun, L. Huang and M. Saleem, Chemical modification of chitosan and its applications, *Polym.-Plast. Technol. Eng.*, 2014, **53**, 1494–1505.

11 S. L. Banerjee, M. Khamrai, K. Sarkar, N. K. Singha and P. P. Kundu, Modified chitosan encapsulated core-shell Ag Nps for superior antimicrobial and anticancer activity, *Int. J. Biol. Macromol.*, 2016, **85**, 157–167.

12 T. Zhao and T. Feng, Application of modified chitosan microspheres for nitrate and phosphate adsorption from aqueous solution, *RSC Adv.*, 2016, **6**, 90878–90886.

13 H. Sashiwa, N. Yamamori, Y. Ichinose, J. Sunamoto and S. Aiba, Chemical modification of chitosan, Michael reaction of chitosan with acrylic acid in water, *Macromol. Biosci.*, 2003, **3**, 231–233.

14 M. E. Fray, A. Niemczyk and B. Pabin-Szafko, Chemical modification of chitosan with fatty acids, *Prog. Chem. Appl. Chitin Its Deriv.*, 2012, **17**, 29–36.

15 V. K. Mourya and N. N. Inamdar, Chitosan-modifications and applications: Opportunities galore, *React. Funct. Polym.*, 2008, **68**, 1013–1051.

16 T. R. A. Sobahi, M. Y. Abdelaal and M. S. I. Makki, Chemical modification of chitosan for metal ion removal, *Arabian J. Chem.*, 2014, **7**, 741–746.

17 M. Rinaudo, Chitin and chitosan: Properties and applications, *Prog. Polym. Sci.*, 2006, **31**, 603–632.

18 R. Dongre, M. Thakur, D. Ghugal and J. Meshram, Bromine pretreated chitosan for adsorption of lead(II) from water, *Bull. Mater. Sci.*, 2012, **35**, 875–884.

19 A. Domard, M. Rinaudo and C. Terrassin, New method for the quaternization of chitosan, *Int. J. Biol. Macromol.*, 1986, **8**, 105–107.

20 Y. Kurita and A. Isogai, Reductive N-alkylation of chitosan with acetone and levulinic acid in aqueous media, *Int. J. Biol. Macromol.*, 2010, **47**, 184–189.

21 H. Sashiwa, N. Kawasaki, A. Nakayama, E. Muraki, N. Yamamoto and S. Aiba, Chemical modification of chitosan. 14:1 Synthesis of water-soluble chitosan derivatives by simple acetylation, *Biomacromolecules*, 2002, **3**, 1126–1128.

22 R. Jayakumar, M. Prabaharan, R. L. Reis and J. F. Mano, Graft copolymerized chitosan-present status and applications, *Carbohydr. Polym.*, 2005, **62**, 142–158.

23 D. Hua, J. Tang, J. Cheng, W. Deng and X. Zhu, A novel method of controlled grafting modification of chitosan via RAFT polymerization using chitosan-RAFT agent, *Carbohydr. Polym.*, 2008, **73**, 98–104.

24 I. F. Amaral, P. L. Granja and M. A. Barbosa, Chemical modification of chitosan by phosphorylation: An XPS, FT-IR and SEM study, *J. Biomater. Sci., Polym. Ed.*, 2005, **16**, 1575–1593.

25 J. Glasing, P. Champagne and M. F. Cunningham, Graft modification of chitosan, cellulose and alginate using reversible deactivation radical polymerization (RDRP), *Curr. Opin. Green Sustain. Chem.*, 2016, **2**, 15–21.

26 D. J. Haloi and N. K. Singha, Synthesis of Poly(2-ethylhexyl acrylate)/Clay nanocomposite by in situ living radical polymerization, *J. Polym. Sci., Part A: Polym. Chem.*, 2011, **49**, 1564–1571.

27 A. Dhar, B. P. Koiry and D. J. Haloi, Synthesis of poly (methyl methacrylate) via ARGET ATRP and study of the effect of solvents and temperatures on its polymerization kinetics, *Int. J. Chem. Kinet.*, 2018, **50**, 1–7.

28 K. Matyjaszewski, *Controlled/Living radical polymerization progress in ATRP, NMP and RAFT*, ACS Publications, Washington, DC, 2000.

29 *Reversible deactivation radical polymerization; synthesis and applications of functional polymers*, ed. N.K Singha and J. Mays, De Gruyter, 2020.

30 M. Destarac, Industrial development of reversible-deactivation radical polymerization: is the induction period over?, *Polym. Chem.*, 2018, **9**, 4947–4967.

31 K. Matyjaszewski, Atom transfer radical polymerization: From mechanisms to applications, *Isr. J. Chem.*, 2012, **52**, 206–220.

32 D. J. Haloi, S. Ata, N. K. Singha, D. Jehnichen and B. Voit, Acrylic AB and ABA block copolymers based on Poly(2-ethylhexylacrylate) (PEHA) and Poly(methyl methacrylate) (PMMA) via ATRP, *ACS Appl. Mater. Interfaces*, 2012, **4**, 4200–4207.

33 N. K. Singha, B. Ruiter and U. Schubert, Atom Transfer Radical Polymerization of an Acrylate Monomer bearing an Oxetane Group, *Macromolecules*, 2005, **38**, 3596–3600.

34 S. Perrier, 50th anniversary perspective: RAFT polymerization-A user guide, *Macromolecules*, 2017, **50**, 7433–7447.

35 C. Barner-Kowollik and S. Perrier, The future of reversible addition fragmentation chain transfer polymerization, *J. Polym. Sci., Part A: Polym. Chem.*, 2008, **46**, 5715–5723.

36 R. K. O'Reilly and C. Hansell, Mild and facile synthesis of multi-functional RAFT chain transfer agents, *Polymer*, 2009, **1**, 3–15.

37 J. F. Quinn, L. Barner, C. Barner-Kowollik, E. Rizzardo and T. P. Davis, Reversible addition-fragmentation chain transfer polymerization initiated with ultraviolet radiation, *Macromolecules*, 2002, **35**, 7620–7627.

38 N. B. Pramanik, D. S. Bag, S. Alam, G. B. Nando and N. K. Singha, Thermally amendable tailor-made functional polymer by RAFT polymerization and "Click Reaction", *J. Polym. Sci., Part A: Polym. Chem.*, 2013, **51**, 3365–3374.

39 C. Boyer, V. Bulmus, T. P. Davis, V. Ladmiral, J. Liu and S. Perrier, Bio applications of RAFT polymerization, *Chem. Rev.*, 2009, **109**, 5402–5436.

40 F. Chauvin, P. E. Dufils, D. Gigmes, Y. Guillaneuf, S. R. A. Marque, P. Tordo and D. Bertin, Nitroxide-mediated polymerization: The pivotal role of the k_d value of the initiating alkoxyamine and the importance of the experimental conditions, *Macromolecules*, 2006, **39**, 5238–5250.

41 P. M. Kazmaier, K. Daimon, M. K. Georges, G. K. Hamer and R. P. N. Veregin, Nitroxide-mediated "Living" free radical polymerization: A rapid polymerization of (chloromethyl)styrene for the preparation of random, block, and segmental arborescent polymers, *Macromolecules*, 1997, **30**, 2228–2231.

42 L. Petton, A. E. Ciolino, B. Dervaux and F. E. D. Prez, From one-pot stabilisation to in situ functionalisation in nitrox-

ide mediated polymerisation: An efficient extension towards atom transfer radical polymerization, *Polym. Chem.*, 2012, **3**, 1867–1878.

43 C. J. Hawker, A. W. Bosman and E. Harth, New polymer synthesis by nitroxide mediated living radical polymerizations, *Chem. Rev.*, 2001, **101**, 3661–3688.

44 W. Huang, Y. Wang, S. Zhang, L. Huang, D. Hua and X. Zhu, A facile approach for controlled modification of chitosan under γ-Ray irradiation for drug delivery, *Macromolecules*, 2013, **46**, 814–818.

45 H. Bao, J. Hu, L. H. Gan and L. Li, Stepped association of comb-like and stimuli-responsive graft chitosan copolymer synthesized using ATRP and active ester conjugation methods, *J. Polym. Sci., Part A: Polym. Chem.*, 2009, **47**, 6682–6692.

46 H. Bao, L. Li, L. H. Gan, Y. Ping, J. Li and P. Ravi, Thermo- and pH-responsive association behavior of dual hydrophilic graft chitosan terpolymer synthesized via ATRP and click chemistry, *Macromolecules*, 2010, **43**, 5679–5687.

47 W. Yuan, X. Li, S. Gu, A. Cao and J. Ren, Amphiphilic chitosan graft copolymer via combination of ROP, ATRP and click chemistry: Synthesis, self-assembly, thermosensitivity, fluorescence, and controlled drug release, *Polymer*, 2011, **52**, 658–666.

48 L. Liu and G. Sun, Promoting the OH^- ion conductivity of chitosan membrane using quaternary phosphonium polymer brush functionalized graphene oxide, *Int. J. Electrochem. Sci.*, 2017, **12**, 9262–9278.

49 K. E. Tahlawy and S. M. Hudson, Synthesis of a well-defined chitosan graft Poly(methoxy polyethyleneglycol methacrylate) by atom transfer radical polymerization, *J. Appl. Polym. Sci.*, 2003, **89**, 901–912.

50 C. Chen, M. Liu, C. Gao, S. Lu, J. Chen, X. Yu, E. Ding, C. Yu, J. Guo and G. Cui, A convenient way to synthesize comb-shaped chitosan-graft-poly(N-isopropylacrylamide) copolymer, *Carbohydr. Polym.*, 2013, **92**, 621–628.

51 N. Li, R. Bai and C. Liu, Enhanced and selective adsorption of mercury ions on chitosan beads grafted with polyacrylamide via surface-initiated atom transfer radical polymerization, *Langmuir*, 2005, **21**, 11780–11787.

52 P. Liu and Z. Su, Surface-initiated atom transfer radical polymerization (SI-ATRP) of styrene from chitosan particles, *Mater. Lett.*, 2006, **60**, 1137–1139.

53 S. S. Dryabina, K. M. Fotina, Y. V. Shulevich, V. V. Klimov, E. V. Bryuzgin, A. V. Navrotskii and I. A. Novakov, Synthesis of water–soluble grafted chitosan copolymers by atom transfer radical polymerization, *Polym. Bull.*, 2020, **77**, 1541–1554.

54 L. Huang, S. Yuan, L. Lv, G. Tan, B. Liang and S. O. Pehkonen, Poly(methacrylic acid)-grafted chitosan microspheres via surface-initiated ATRP for enhanced removal of Cd(II) ions from aqueous solution, *J. Colloid Interface Sci.*, 2013, **405**, 171–182.

55 F. Tang, L. Zhang, J. Zhu, Z. Cheng and X. Zhu, Surface functionalization of chitosan nanospheres via surface-initiated AGET ATRP mediated by iron catalyst in the pres-

ence of limited amounts of air, *Ind. Eng. Chem. Res.*, 2009, **48**, 6216–6223.

56 B. Y. Ping, C. D. Liu, G. P. Tang, J. S. Li, J. Li, W. T. Yang and F. J. Xu, Functionalization of chitosan via atom transfer radical polymerization for gene delivery, *Adv. Funct. Mater.*, 2010, **20**, 3106–3116.

57 M. Abbasian and F. Mahmoodzadeh, Synthesis of antibacterial silver–chitosan-modified bionanocomposites by RAFT polymerization and chemical reduction methods, *J. Elastomers Plast.*, 2017, **49**, 173–193.

58 J. Tang, D. Hua, J. Cheng, J. Jiang and X. Zhu, Synthesis and properties of temperature-responsive chitosan by controlled free radical polymerization with chitosan-RAFT agent, *Int. J. Biol. Macromol.*, 2008, **43**, 383–389.

59 K. Zhang, Z. Wang, Y. Li, Z. Jiang, Q. Hua, M. Liu and Q. Zhao, Dual stimuli-responsive N-phthaloylchitosan-graft-(poly(N-isopropylacrylamide)-block-poly(acrylicacid)) copolymer prepared via RAFT polymerization, *Carbohydr. Polym.*, 2013, **92**, 662–667.

60 L. Cheng-bin, W. Xiao-jian, L. Rong-hua, W. Yu-lin and L. Sheng-lian, A new multifunctional polymer: Synthesis and characterization of mPEG-b-PAA-grafted chitosan copolymer, *J. Cent. South Univ. Technol.*, 2010, **17**, 936–942.

61 C. Li, T. Guo, D. Zhou, Y. Hu, H. Zhou, S. Wang, J. Chen and Z. Zhang, A novel glutathione modified chitosan conjugate for efficient gene delivery, *J. Controlled Release*, 2011, **154**, 177–188.

62 S. Hosseinzadeh, H. Hosseinzadeh, S. Pashaei and Z. Khodaparast, Synthesis of stimuli-responsive chitosan nanocomposites via RAFT copolymerization for doxorubicin delivery, *Int. J. Biol. Macromol.*, 2019, **121**, 677–685.

63 D. Hua, W. Deng, J. Tang, J. Cheng and X. Zhu, A new method of controlled grafting modification of chitosan via nitroxide-mediated polymerization using chitosan-TEMPO macroinitiator, *Int. J. Biol. Macromol.*, 2008, **43**, 43–47.

64 J. Jiang, D. Hua, J. Jiang, J. Tang and X. Zhu, Synthesis and property of poly(sodium 4-styrenesulfonate) grafted chitosan by nitroxide-mediated polymerization with chitosan-TEMPO macroinitiator, *Carbohydr. Polym.*, 2010, **81**, 358–364.

65 O. García-Valdez, D. G. Ramírez-Wong, E. Saldívar-Guerra and G. Luna-Bárcenas, Grafting of chitosan with styrene and maleic anhydride via nitroxide-mediated radical polymerization in supercritical carbon dioxide, *Macromol. Chem. Phys.*, 2013, **214**, 1396–1404.

66 C. Lefay, Y. Guillaneuf, G. Moreira, J. J. Thevarajah, P. Castignolles, F. Ziarelli, E. Bloch, M. Major, L. Charles, M. Gaborieau, D. Bertin and D. Gigmes, Heterogeneous modification of chitosan via nitroxide-mediated polymerization, *Polym. Chem.*, 2013, **4**, 322–328.

67 S. Kwan and M. Mari, Thermoresponsive polymers with tunable cloud point temperatures grafted from chitosan via nitroxide mediated polymerization, *Polymer*, 2016, **86**, 69–82.

68 O. García-Valdez, R. Champagne-Hartley, E. Saldívar-Guerra, P. Champagne and M. F. Cunningham, Modification of chitosan with polystyrene and poly(n-butyl acrylate) via nitroxide-mediated polymerization and grafting from approach in homogeneous media, *Polym. Chem.*, 2015, **6**, 2827–2836.

69 O. García-Valdez, S. George, R. Champagne-Hartley, E. Saldívar-Guerra, P. Champagne and M. F. Cunningham, Chitosan modification via nitroxide-mediated polymerization and grafting to approach in homogeneous media, *Polymer*, 2015, **67**, 139–147.

70 E. A. W. Madill, O. Garcia-Valdez, P. Champagne and M. F. Cunningham, CO_2-responsive graft modified chitosan for heavy metal (nickel) recovery, *Polymer*, 2017, **9**, 394–406.

71 A. Darabi, O. Garcia-Valdez, P. Champagne and M. F. Cunningham, PEGylation of chitosan via nitroxide-mediated polymerization in aqueous media, *Macromol. React. Eng.*, 2016, **10**, 82–89.

72 K. Zhang, P. Zhuang, Z. Wang, Y. Li, Z. Jiang, Q. Hu, M. Liu and Q. Zhao, One-pot synthesis of chitosan-g-(PEO-PLLA-PEO) via "click" chemistry and "SET-NRC" reaction, *Carbohydr. Polym.*, 2012, **90**, 1515–1521.

Preparation, Characterization, and Antimicrobial Activity of Chitosan/Kaolin Clay Biocomposite Films

Madhabi Bhattacharjee, Shyam Goswami, Pranab Borah, Mousmi Saikia, Jayanta Barman, Nabendu B. Pramanik, and Dhruba J. Haloi*

Chitosan (CS) is a polycation found in nature that exhibits many good properties. Kaolin (KAO) clay is a natural inorganic filler and is being used in medicine, ceramic, food additives, etc. Therefore, the mixing of two such biomaterials, a natural polycation (CS) and natural filler (KAO clay) may lead to a biocomposite, chitosan/kaolin (CS/KAO) clay, with many interesting properties. In this study, the composites of CS and KAO clay are prepared by mixing the solution of CS (in dilute acetic acid) with KAO clay at various weight ratios. FT-IR, UV/Vis, X-Ray diffraction, SEM, UTM, TGA, and DSC analyses are used to investigate these biocomposites thoroughly. Agar well diffusion method has been used to determine the antibacterial activities of different concentrations of the CS- KAO clay against gram -positive (*Bacillus subtilis*) and gram- negative (*Escherichia coli*) bacteria. The biocomposites exhibited antibacterial activities against tested microrganisms. In addition, swelling tests of the biocomposites are also carried out. The CS/KAO clay biocomposite films show better tensile strength than CS film. It is observed that dispersed KAO clay improves the thermal stability and enhances the hardness of the matrix systematically with the increase of its loading.

1. Introduction

One of the major possibilities to eradicate the global environmental contamination is extensive applicability and availability of biodegradable plastics. In this contrast biodegradable polymers are found to be an excellent candidate. It has been observed that biodegradable plastics playing a great role in enhancing the quality of living standards, and industrial development throughout the globe.[1] By implementation of biodegradable films can enable us the final replacement of plastic packaging bags which are basically environment hazard and not recyclable. The prime goal of this current research is to create biodegradable, environmentally friendly materials with improvised characteristic which can mitigate the issue.[2]

In the present scenario, various composites made from synthetic polymers derived from petroleum have a negative impact on the ecosystem of the planet as they are non-biodegradable. Moreover, hazardous or toxic properties of these polymers make them a worse contender. In this contrast an urgent eco-friendly green composite material of natural origin must be come into effect.[3] As it is known that biopolymer films are eco-friendly substitutes for synthetic, non-biodegradable films, hence researchers taking a great interest in developing such materials.[4] Generally, the syntheses of bio-composites are an interdisciplinary field that composed of basic science, material science, and engineering which adds new dimensions to the properties of biopolymers.[5]

Several industrial applications of bio-composites are basically made from various waste and naturally occurring materials.[6] In this regard, biodegradable polymer chitosan (CS) (**Figure 1**) is a wonderful option due to its unique qualities, such as its low cost, wide availability, biocompatibility, biodegradability, hydrophilicity, lack of toxicity, ease of chemical modification, good adhesion, ion-exchange and adsorption properties, etc.[7–9] CS, a polysaccharide deacetylated from chitin, is primarily composed of poly-(1,4)-2-deoxy-2-amino-D-glucose.[10] It is made from chitin, which is the second most prevalent polymer in nature after cellulose.[11] The exoskeletons of some insects and crustacean fungi can be used to extract CS.[12] Naturally occurring polysaccharides cellulose, dextran, pectin, alginic acid, agar, agarose, and carrageenans are examples of neutral or acidic

M. Bhattacharjee
Department of Chemistry
Bodoland University
Kokrajhar, Assam 783370, India

S. Goswami
Drugs and Narcotics Division, Directorate of Forensic Science
Guwahati, Assam 781019, India

P. Borah, M. Saikia
Department of Herbal Science & Technology
ADP College
Nagaon, Assam 782002, India

J. Barman
Department of Physics
ADP College
Nagaon, Assam 782002, India

N. B. Pramanik
Department of Chemistry
ICT Mumbai - IOC Bhubaneswar Campus
Bhubaneswar, Odisha 751013, India

D. J. Haloi
Department of Applied Sciences
Tezpur University
Tezpur, Assam 784028, India
E-mail: djhaloi@tezu.ernet.in

**ADVANCED
SCIENCE NEWS**

www.advancedsciencenews.com

[M] macro-molecular
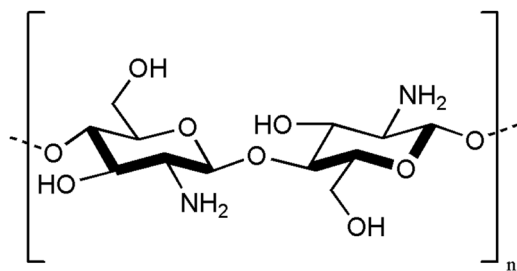Chemistry and Physics

www.mcp-journal.de

Figure 1. Structure of CS.

polysaccharides, in contrast to chitin and CS, which are examples of extremely basic polysaccharides. As a result of these exceptional properties, numerous CS-composite based products have been developed extensively[13] viz. in wastewater treatment,[14] tissue engineering,[15] agriculture,[16] biomedicine,[17] drug delivery[18] etc. The lone CS-based products are very few as it doesn't have such exceptional properties like CS-composite materials.[19]

To overcome these issues various kind of CS-based composites have been developed in the recent years.[20] In this purpose CS immobilization on clay minerals has received magnificent attention.[21] They have a higher selective gas permeability ratio CO_2/O_2 than traditional synthetic films and are also excellent fat and oil barriers.[22] However, they generally have poor water vapor barrier properties. Polymer/clay composites have drawn a lot of recognition in the recent years due to their extraordinary potential to enhance the barrier properties of thin films.[4] Due to their high aspect ratios and high surface area, these composites are a class of hybrid materials made of organic polymer matrices and micro/nanoscale organophilic clay fillers. If clay particles are properly dispersed in the polymer matrix at a loading level of 1% to 5% (w/w), unique combinations of physical and chemical properties will be obtained, making these composites appealing for making films and coatings for a variety of industrial applications.[4,23]

Clay minerals have been identified as natural inorganic substances with distinct structural adsorption, rheological, and thermal properties by recent research.[24] Due to the presence of their surface hydroxyl (–OH) groups, which may easily connect with water molecules, these materials naturally have a hydrophilic nature.[25] The use of clay minerals for metal binding,[24] dye removal,[26] and fruit packaging,[27] either alone or in combination with other natural or manufactured polymers, has a long and enchanted history. To improve clay's compatibility with other polymers, however, purification and modification may occasionally be required.[28] Because of their smaller particle size, larger surface area, favorable aspect ratio, and superior dispersion capabilities, clay minerals can greatly enhance the properties of CS.[29] The acidity of the $-NH_3^+$ group is primarily responsible for the CS's electrolytic nature and chelating properties. CS can be intercalated with KAO through cationic exchange and hydrogen bonding due to the polycationic character of this biopolymer in acidic conditions, and the resultant composites exhibit fascinating features.[30]

In addition, clay minerals have certain wonderful qualities including strong biocompatibility, non-toxicity, and excellent controlled release prospects, which support their use in food,

medicine, pharmacy, cosmetics, and other industries.[31] To the best of our knowledge, however, the KAO-based CS biocomposite has received minimal attention and has received fewer scholarly articles. W. Ma et al. synthesized a magnetically separable adsorbent (CS/KAO/Fe_3O_4) by emulsion cross-linking. The microspheres were used as an adsorbent for the removal of ciprofloxacin.[32] S. C. Dey et al. synthesized pH triggered bicomposites using different proportion of KAO and CS. This biocomposites have numerous industrial applications in leather, textile, food, pharmaceuticals etc.[3] S. Biswas et al. synthesized high-performance composites by using CS and modified KAO clay in various combinations.[33] H. Y. Zhu et al. synthesized CS/KAO/nanosized $\gamma - Fe_2O_3$ composites by a micro-emulsion process. The composites can be used as a low-cost alternative for anionic dyes removal from industrial wastewater.[34] I. P. Chen et al. prepared CS-coated KAO beads using hydrochloric acid without any cross-linking agent.[35] To the best our knowledge no report has been done on antibacterial activities for one gram positive and one gram negative bacteria using CS/KAO clay biocomposite films in different weight ratios so far. Moreover, swelling tests of the same are also never been reported. We think the novelty of our work lies in the biological application, swelling property as well as comparative study of different physico-chemical properties of CS/KAO clay biocomposite films of different weight ratios.

We were therefore highly interested in synthesizing some CS/KAO-based green bio-composite materials which must be environmentally benign. The purpose of the current study is to create CS/KAO biocomposite films in which KAO is combined with a CS solution in acetic acid. By using various characterizing techniques viz. FT-IR, UV/Vis, XRD, SEM, UTM, TGA, and DSC, the structure of the produced CS/KAO biocomposites films were successfully investigated. Moreover, the present work is designed to investigate the antibacterial effects of different CS/KAO clay ratio against two pathogenic bacteria- Bacillus subtilis (gram -positive) and Escherichia Coli (gram- negative bacteria). Also, the swelling tests of the biocomposites have been observed. From our literature survey analysis, it has been observed that CS/KAO clay biocomposite films of different weight ratios received minimal attention towards various physicochemical properties viz. mechanical, thermal, swelling tests etc. as compared to pure CS film. Furthermore, no antibacterial properties have been investigated and reported till now for the same. We thought there have been lots of scopes to study on this area and this is the basic reason why we are interested for the development of this work. Moreover, these biocomposites may find some applications in the field of analytical and environmental science.

2. Experimental Section

2.1. Materials

Chitosan (from Shrimp Shells) with 75% degree of deacetylation was bought from LOBA Chemie. Aluminium Silicate Hydrate (trade name Kaolin) was purchased from Oxford Lab Fine Chem LLP. Glacial acetic acid $\geq$ 99% from EMPLURA, India and distilled water were used as a solvent. Two tested bacterial species one gram-negative and gram-positive pathogen (MTCC-739-*Escherichia coli* and MTCC-441-*Bacillus subtilis respectively*)

**ADVANCED
SCIENCE NEWS**

www.advancedsciencenews.com

+[M] acro-
molecular
Chemistry and Physics

www.mcp-journal.de

Table 1. The details of the CS/KAO clay biocomposites.

Sample Name	% Of CS	% Of KAO	Thickness of the film [mm]
CS	100	0	0.11
CS/KAO-1	100	10	0.13
CS/KAO-2	100	20	0.14
CS/KAO-3	100	30	0.16
CS/KAO-4	100	40	0.18

CS indicates for chitosan and CS/KAO-1, CS/KAO-2, CS/KAO-3 and CS/KAO-4 for chitosan/kaolin clay biocomposites with 10%, 20%, 30%, 40% respectively.

were supplied by MTCC, Chandigarh, Punjab, India. All other chemicals used were of analytical grade and used as received.

2.2. Preparation of Chitosan Film

CS solution was prepared by dissolving 1 g of CS powder in 100 mL of aqueous acetic acid solution (2%, v/v), which was then stirred at 40 °C for 5 h followed by vacuum filtration to remove the insoluble residue. The solution thus formed were cast into Petri dishes and dried at 60 °C for 24 h to evaporate the solvent. The film thus formed was soaked with an aqueous solution of 0.05 M NaOH to remove residual acetic acid. Further film was neutralized by rinsing with distilled water and then dried at room temperature.

2.3. Preparation of Chitosan/Kaolin Films

First 2% CS solution was prepared by above mentioned procedure. After that, 0.1 g KAO clay was added to the CS solution and stirred at room temperature for 24 h with ≈700 rpm. The solution thus formed was cast into Petri dishes and dried at 60 °C for 24 h to evaporate the solvent and films were formed thereof. Following the same procedure applied for CS films, the dried films were soaked with an aqueous solution of 0.05 M NaOH to remove residual acetic acid and further film was neutralize by rinsing with distilled water and then dried at room temperature. In the similar manner, other films were obtained by varying the amount of the KAO clay (*viz.* 0.2 g, 0.3 g, and 0.4 g). **Table 1** summarizes the details of CS/KAO clay biocomposites.

The pictorial presentation of the CS and CS/KAO clay biocomposite films was shown below (**Figure 2**):

2.4. Preparation of Crude Sample for Antibacterial Activity

Different concentrations of dry CS and CS/KAO films were dissolved in 2% acetic solution at 10 mg mL^{-1} concentration. The dissolved mixtures were strewed at 40 °C at constant rotation for 5 h. Then, the samples were used for antibacterial activity.

2.5. Characterization Techniques Used

2.5.1. Instrumental Measurements of the Biocomposites

Fourier Transform Infrared (FT-IR) spectra of the samples were recorded by an Agilent Cary 630 FT-IR spectrometer in the range

of 4000–700 cm^{-1}. UV/Vis spectra of the samples were recorded on Agilent Cary 60 UV/Vis spectrophotometer in the region of 200–800 nm. X-Ray Diffraction (XRD) pattern of the samples were recorded by an X-ray diffractometer (Rigaku Ultima IV) at room temperature. Cu Kα radiation ($\lambda = 1.5418$ Å), from a broad focus Cu tube operated at 40 kV and 40 mA, was applied to the samples for measurement. Scanning Electron Microscopy (SEM) images of samples were recorded by an analytical scanning electron microscope (Zeiss SIGMA 300) operated at an accelerating voltage of 5.00 kV. Tensile properties of the samples were determined with a Zwick/Roell universal testing machine (UTM). The separation of the grip was set at 10 mm and also a cross head speed of 10 mm min^{-1}. The tensile strength and elongation measurements were done with three specimens cut from each sheet of film. Thus, the measurements were done on a total of three specimens per each film type with the mean values for tensile strength and elongation for a single sample. Thermogravimetric analyses (TGA) were completed using a Netzch instrument (Model: STA449F3A000). Samples were placed in the balance system and heated from 20 °C to 600 °C at a heating rate of 10 °C min^{-1} under argon atmosphere. Differential scanning calorimetry (DSC) of the samples was performed with a Netzch instrument (Model: STA449F3A000). The samples were heated from 20 °C to 600 °C at a heating rate of 10 °C min^{-1} under argon atmosphere.

2.6. Antibacterial Activity Study by Agar Well Diffusion Method

The agar well diffusion assay of the samples was performed according the Magladi et al. 2004 & Valgas et al. 2007 with minor modifications.[36,37] The assay method was carried out by preparation of 3 wells of 6 mm diameter for each extract using a sterile cork borer in agar plate aseptically. The agar cylinders were removed using a sterile loop. Then the test organism (bacterial species) was swabbed by sterile streak on prepared agar plate. After swabbing the test organism, the well filled with different volume (60, 100, and 140 µL mg^{-1}) of stock solutions of the test materials. Amoxycillin was used as standard with different volume (60, 100, and 140 µL mg^{-1}) of concentration of 1 mg mL^{-1}. The wells were kept for drying by passing the blower in laminar air flow (LAF). The plates were then taken out from the LAF aseptically when all plates became completely dry and incubated at 37 °C for 18 h. The inhibition zones were recorded in the test, for both standard as well as control.

2.7. Swelling Study

The swelling properties of CS and CS/KAO clay biocomposite films were examined after being soaked in distilled water having pH 7.0 at room temperature for 1, 3, 6, 9, and 12 h. The samples were first dried in an oven, their initial weight (w_i) were measured and then they were placed into bottles filled with distilled water. The initial time of immersing the samples was recorded as t = 0 and subsequent measurements were performed at certain time intervals until a stable value had been achieved, i.e., (w_f), then the samples were filtered with filter paper. The whole procedure was
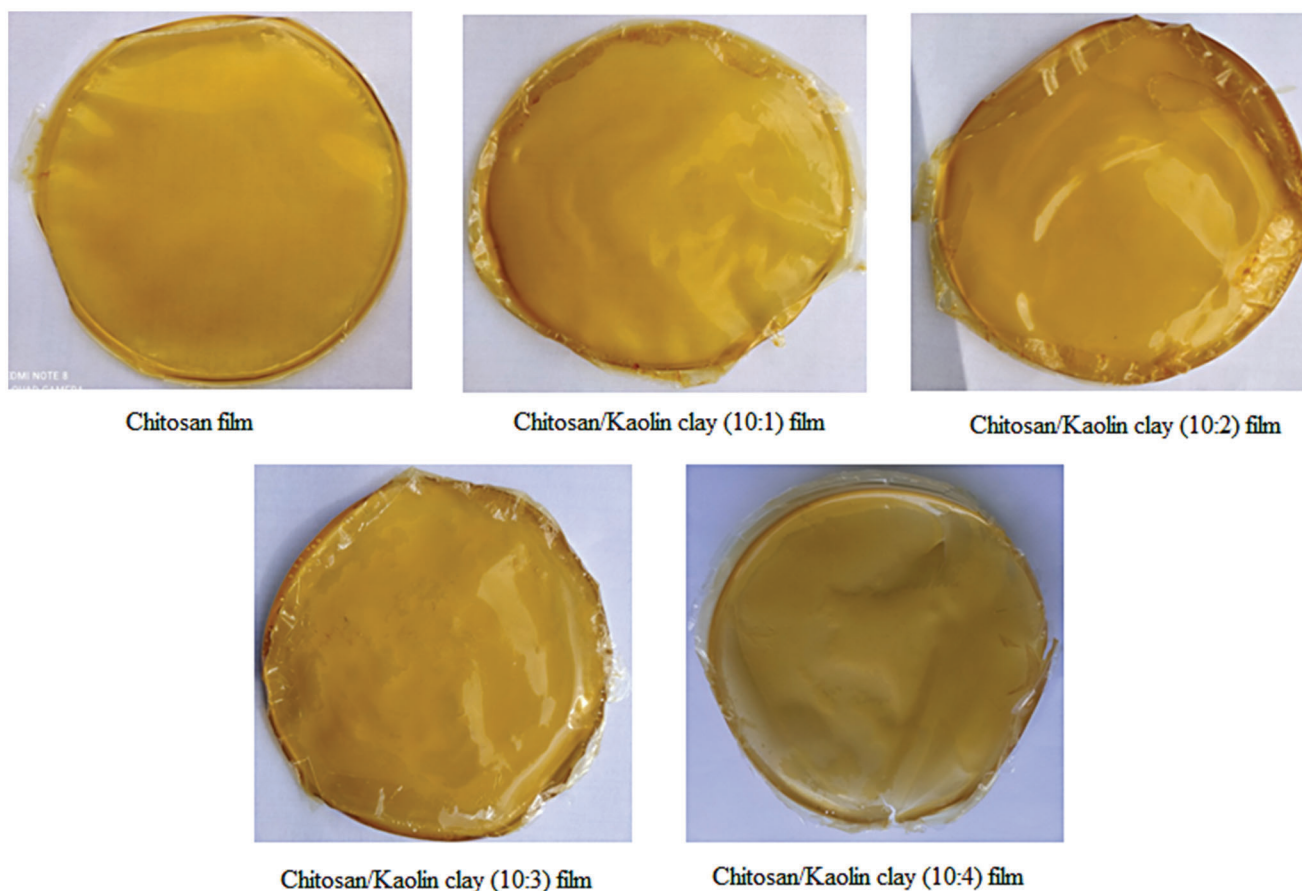
**ADVANCED
SCIENCE NEWS**

www.advancedsciencenews.com

[M]acro-
olecular
Chemistry and Physics

www.mcp-journal.de

Figure 2. Images of CS and CS/KAO clay biocomposite films.

repeated thrice to observe the results. The swelling percentage (S_w) of each sample was calculated by the following Equation:[38]

$$S_w = \frac{w_f - w_i}{w_i} \times 100 \tag{1}$$

3. Result and Discussion

3.1. Analysis via Fourier Transform Infrared (FT-IR) Spectroscopy

FT-IR spectra were recorded in the region 4000–700 cm^{-1} for the CS/KAO clay biocomposite films in the ratios of CS: KAO clay 10:01, 10:02, 10:03, and 10:04 as depicted in the **Figure 3**. The band at 3675 cm^{-1} corresponds to the stretching frequencies of the OH group of the KAO clay whereas the band at 3384 cm^{-1} was observed for the main functional group of CS, i.e., O–H stretching vibrations. The bands of the biocomposites (i.e., from a-d) at 2924 and 1068 cm^{-1} are consistent with bands those observed for the pure CS film. The bands at 2924 and 1068 cm^{-1} are corresponds to C–H symmetric stretching and C–O stretching respectively. The band at 796 cm^{-1} corresponding to the vibration bands of the silicate remain unaffected in the biocomposite. In the spectrum of CS, the absorption band at 1639 cm^{-1} corresponds to the in-plane N–H bending vibration. From the Figure it has been evident that the absorption band at 1639 cm^{-1} for CS
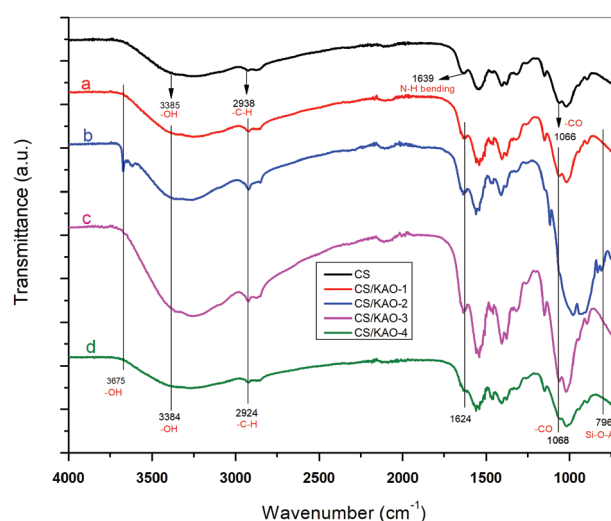

Figure 3. FT-IR Spectra of CS and CS/KAO clay biocomposite films (a–d).

film was shifted to 1624 cm^{-1} in the biocomposite films which shows close agreement with the results reported by S. C. Dey et al.[3] In their investigation they have confirmed that the bicomposites prepared was not a physical mixture for which absorption
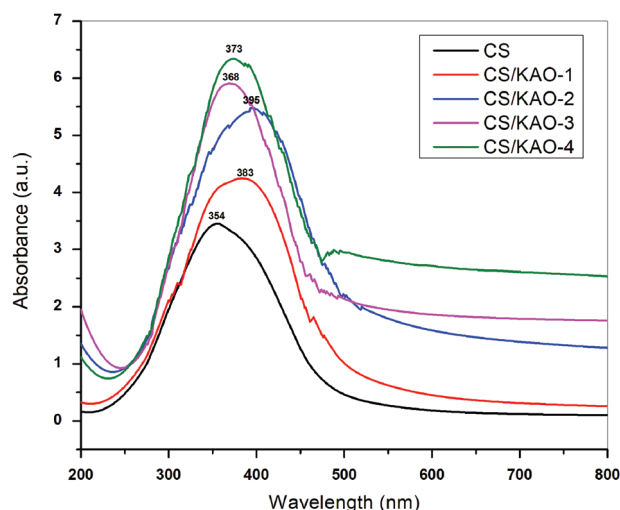
**ADVANCED
SCIENCE NEWS**

www.advancedsciencenews.com

acro-
{M} molecular
Chemistry and Physics

www.mcp-journal.de

Figure 4. UV/Vis Spectra of CS and CS/KAO clay biocomposite films.

band was observed at 1633 cm^{-1} but for biocomposite films it was at 1624 cm^{-1}. The electrostatic interaction between the protonated amine groups (NH_3^+) of CS and negatively charged sites of KAO clay might be the reason for this frequency shifting.[2,39]

3.2. Analysis via Ultraviolet/Visible (UV/Vis) Spectroscopy

The UV/Vis spectra of the CS and CS/KAO clay biocomposite films were taken at room temperature as shown in **Figure 4**. The absorption bands were observed in the range of 300–400 nm. The wavelength of CS film was found to be at 354 nm, while for the CS/KAO clay biocomposite films assigned as CS/KAO-1, CS/KAO-2, CS/KAO-3, and CS/KAO-4 were found to be at 383 nm, 395 nm, 368 nm, and 373 nm respectively. The absorption bands observed at 300–400 nm is due to the direct electronic transition from d-π^* orbital's which is also termed as the Soret band. The concentration of KAO clay on addition to the CS affects the position and shape of the UV absorption bands. The increases in concentration of the clay in the biocomposites are directly proportional to the intensity of light absorption, thus influencing the position and shape of the wavelength in the spectrum. At high concentration molecular interaction occurs, which alters the shape and position of the bands. As a result, the peak shift happens in the different CS/KAO clay biocomposite films. From the Figure, it has also been observed that the maximum absorption for CS/KAO-4 film signifies the highest concentration of the KAO clay presents in the film. From the UV/Vis analysis we are basically want to investigate the interaction of KAO clay on the pure CS matrix. Moreover, we also like to observe how does the different weight ratios of CS/KAO clay biocomposites influence on absorption band. Another evidence of this analysis is to obtain the Soret band at 300–400 nm which were observed in all the cases of our synthesized biocomposites as well as for the pure one. Furthermore, this analysis also provides a supporting structural information obtained from other spectroscopic methods, especially FT-IR analysis.
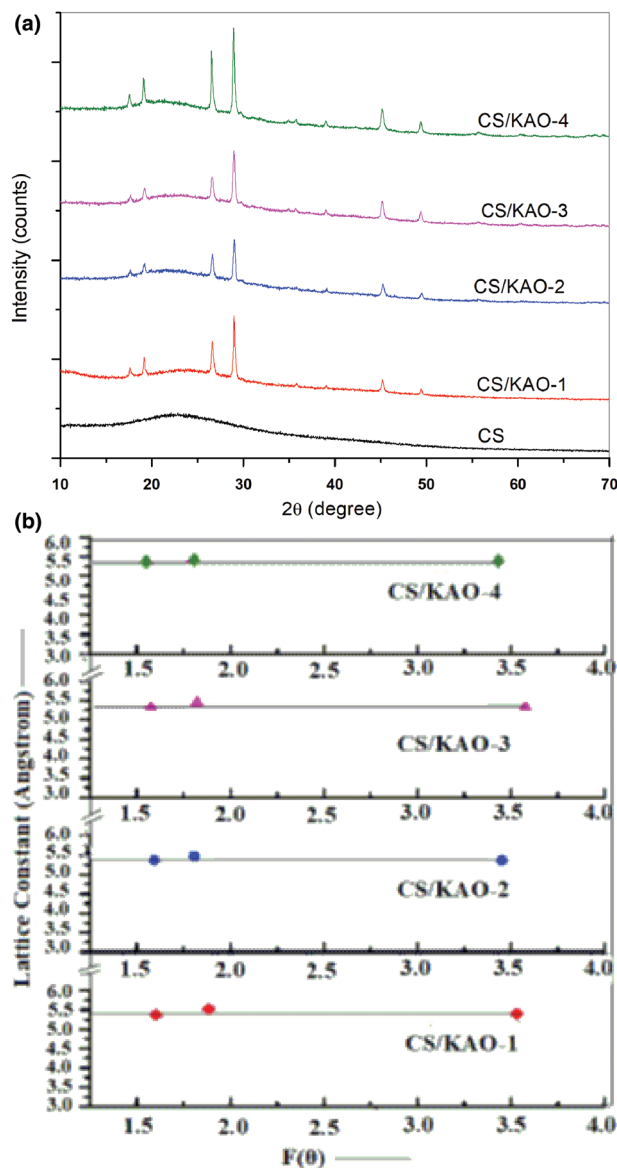

Figure 5. a) XRD patterns of CS and CS/KAO clay biocomposite films. b) Nelson and Rilay Plots of CS and CS/KAO clay biocomposite films.

3.3. X-Ray Diffraction (XRD) Analysis

XRD analysis of the CS and CS/KAO clay biocomposite films were investigated as shown in **Figure 5**a. Peaks thus obtained for CS film was compared with CS/KAO clay biocomposite films to know the preliminary information regarding the presence KAO clay in the biocomposites. It has been found that CS has a semi crystalline nature whereas KAO clay has crystalline nature. In the 2θ range of about 10°-70°, six characteristics peaks were obtained for CS/KAO clay biocomposite films. The XRD pattern of CS showed broad diffraction peaks at 2θ around 22.4° corresponding to the typical fingerprints of semicrystalline CS.[3] From the Figure 5a it is clear that the crystallinity of CS was disappeared in the CS/KAO clay biocomposite films as the peak of CS at 2θ = 22.4° is
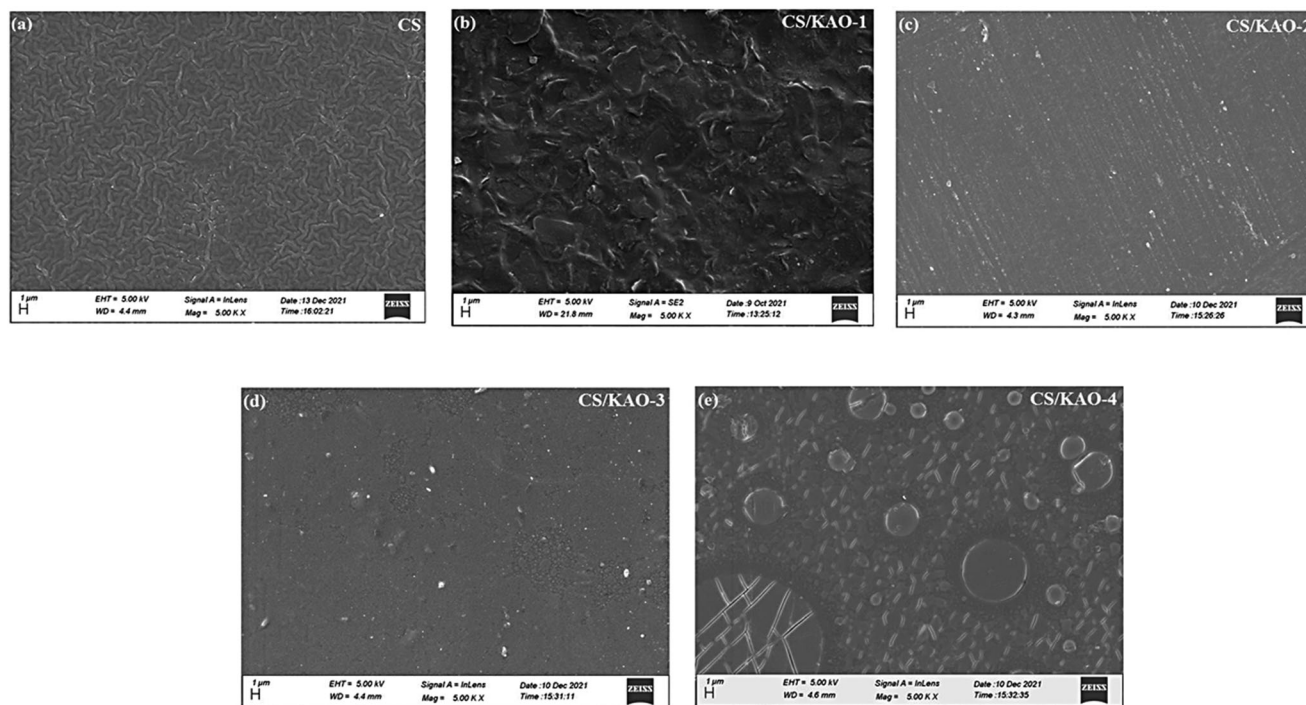
Figure 6. SEM images of a) CS b) CS/KAO-1 c) CS/KAO-2 d) CS/KAO-3 and e) CS/KAO-4.

absent in the CS/KAO clay biocomposite films. The investigation resembles the results obtained by S. Biswas et al. which indicate a pretty good dispersion of the CS and KAO clay on CS.[33] It has been observed that in the biocomposites CS/KAO-1 to CS/KAO-4 with increasing concentration of the clay particle the intensities of the peaks were also increases and small broadening takes place. Therefore, it can be assumed that the KAO clay with different concentration was successfully incorporated into the CS.

From the Figure 5a it is cleared that from CS/KAO-4 to CS/KAO-1 the peaks are slightly shifted to higher diffraction angle indicating the lattice contraction and suggested smaller crystalline size. A broad peak was observed in $2\theta = 26.60°$, $26.68°$, $27.10°$, and $27.30°$ in samples CS/KAO-1 to CS/KAO-4 and from this peak using Scherer formula crystallite size was calculated. The position of the peaks was calculated from Origin graphic software. The corresponding peaks are $2\theta = 26.60°$, $26.68°$, $27.10°$, and $27.30°$ in samples CS/KAO-1, $2\theta = 26.58°$, $26.48°$, $27.07°$, and $27.29°$ in samples CS/KAO-2, $2\theta = 26.28°$, $26.18°$, $26.70°$, and $27.16°$ in samples CS/KAO-3, $2\theta = 26.60°$, $26.68°$, $27.10°$, and $27.30°$ in samples CS/KAO-4. The average size of crystallite was determined using Scherer formula.[40]

$$D = \frac{kl}{Vw_{2q} \cos q_B} \tag{2}$$

Where, q_B is the Bragg angle in radian and K = 0.9 for spherical shape. It was found that particle size increases from sample CS/KAO-1 to CS/KAO-4 and ranges from 18 nm to 21 nm. For CS/KAO-1 particle size were 18.72 nm, for CS/KAO-2 particle size were 19.46 nm, for CS/KAO-3 particle size were 21.32 nm, for CS/KAO-4 particle size were 21.97 nm.

Since we used in thin film form within capping material so possibility of agglomeration can be neglected. Therefore, XRD peak broadening was considered only for size.

The lattice parameter "a" was determined from three prominent peak $2\theta = 26.60°$, $29.06°$, and $45.18°$ and systematic errors in 2θ were eliminated by Nelson and Riley plot from three peaks. The corrected value of lattice constant "a" is calculated by $F(\theta)$ to zero. The lattice constant was explained in Figure 5b.

3.4. Scanning Electron Microscope (SEM) Analysis

SEM images were obtained for the film of CS and CS/KAO clay biocomposites to know the morphologies of the same. For better resolution, images were taken at the 5.00 KX magnifications. The micrographs in **Figure 6** show the changes in the morphologies of CS and biocomposites CS/KAO-1 to CS/KAO-4. SEM micrographs of biocomposites show how the clay particles were dispersed in the CS matrix. The surface of CS was smooth and irregular, while in case of biocomposites the clay particles were dispersed in the polymer matrix. Figure 6a shows a fibrous network of CS matrix while in case of CS/KAO-1 biocomposite, the clay particles were exfoliated and intercalated in the CS matrix as shown in the Figure 6b. This also shows that the clay particles were dispersed throughout the CS matrix.[33] However, the micrographs of CS/KAO-2 and CS/KAO-3 as shown in the Figure 6c,d revealed that the homogeneous dispersion of KAO clay in the CS matrix. The micrographs also affirm that the CS/KAO-2 possessed a more uniform and smoother surface than CS/KAO-3.[38] The composite CS/KAO-4 shows a fibrous network with rough surface which may be due to the presence of higher amount of

**ADVANCED
SCIENCE NEWS**

www.advancedsciencenews.com

[M]acro-
olecular
Chemistry and Physics

www.mcp-journal.de

Table 2. Mechanical properties of the CS film and CS/KAO biocomposite films.

Film type	Tensile Strength (MPa)	Young's Modulus (MPa)	Elongation at Break (%)
CS	29.6	5.1	6.2
CS/KAO-1	26.1	6.1	5.8
CS/KAO-2	29.1	6.6	5.6
CS/KAO-3	31.4	6.7	5.5
CS/KAO-4	34.7	7.6	5.3

KAO clay in the CS matrix. From the analysis it can be understand that with the increase in the amount of clay in the biocomposite films the surface getting rougher which shows close agreement with the results reported by S. Biswas et al. in their investigation.[33]

3.5. Tensile Properties

From our literature analysis it was found that the tensile properties of CS/KAO clay biocomposite films gain minimal attention. Basically, the mechanical properties of polymers are one of the features that distinguish them from small molecules. For better understanding the physical behaviors of the CS and CS/KAO clay biocomposites film, mechanical properties viz. tensile strength, Young's modulus and elongation at break were taken into consideration. The properties were investigated listed in **Table 2**. Table 2 showed that tensile strength and Young's Modulus of the composites were increased whereas the elongation at break decreased as the amount of KAO clay in the biocomposite films increased. From the UTM analysis, it was observed that on increasing the amount of KAO clay in the biocomposites the values of tensile strength increase which indicates the increase in the rigidity of the biocomposite. A higher Young's modulus values for the biocomposites indicates the characteristics of lower toughness. Higher Young's modulus value also indicates the brittleness for the same. Thus, high value of Young's modulus for CS/KAO-4 biocomposite indicates lower toughness and more brittleness than the other synthesized biocomposites. Moreover, the lower elongation at break values indicates low ductility. As a result, it may be concluded that among all the biocomposites, CS/KAO-4 has low ductility and higher rigidity, which indicates the higher brittleness of the material. The enhanced tensile strength and modulus observed for the biocomposites reflect that there was better polymer-filler interaction. In an investigation reported by A. Laaraibi et al. observed some similar trends on addition of bentonite clay to the CS matrix.[1] As the biocomposites shows significant tensile strength which is considered as an interesting mechanical property therefore it can be used as a food packaging material. We are planning to explore this application in our upcoming project.

3.6. Thermogravimetric Analyses (TGA)

TGA analyses of the synthesized films of CS and CS/KAO clay biocomposites were carried out to investigate the thermal stabil-
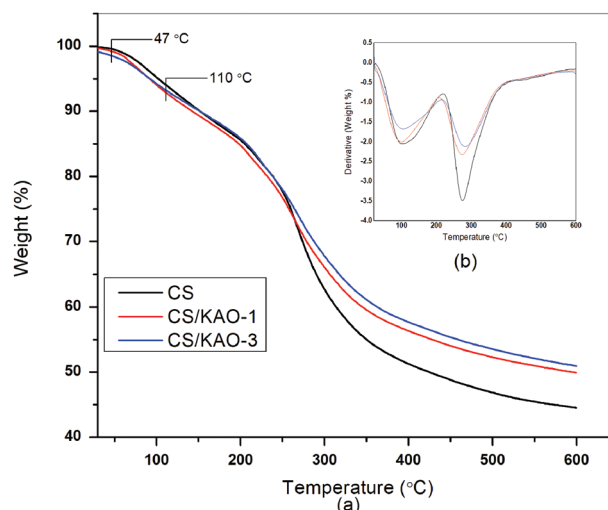

Figure 7. a) TGA and b) DTG plots of CS and CS/KAO clay biocomposite films.

Table 3. Thermal properties of CS and CS/KAO clay biocomposite films.

Sample	KAO Loading [% weight w.r.t. polymer weight]	First degradation		Second degradation	
		T_{onset}	T_{max}	T_{onset}	T_{max}
CS	Nil	47	107	245	457
CS/KAO-1	10	48	108	250	487
CS/KAO-3	30	48	110	258	506

ity of the materials. TGA and DTG (Derivative thermogravimetry) curves of the CS, CS/KAO-1 and CS/KAO-3 were depicted in the **Figure 7**a,b respectively. The degradation processes of the same were undergone through two steps. All biocomposites were degraded in the range of 47–110 °C. This is considered as the first range of degradation, which occurred due to loss of water molecules. Pure CS starts breakdown mostly at temperature about 245°C and degradation almost completed at about 457 °C. The oxidative break down of the carbonaceous residue occurred in the temperature range of between 457 and 550 °C which is considered to be the second stage of degradation.[1,41]

Table 3 summarizes the both degradation temperature ranges of CS and CS/KAO clay biocomposite films. From the data's it is observed that CS/KAO clay biocomposite films have superior thermal stability than the pure CS. It is also observed that on increasing the clay proportion in the biocomposites, there is an enhancement in the stability of CS/KAO clay biocomposite films which expected to be close agreement with the assumption we try to draw. In an investigation reported by S. Biswas et al. shows good resemblance with the results obtained in this work.[33] This observation is due to the chemical impregnation of the KAO clay particles to the matrix of the CS.

3.7. Differential Scanning Calorimetry (DSC)

DSC measurements were carried out to ascertain the glass transition temperature (T_g) of the CS and CS/KAO clay biocomposite
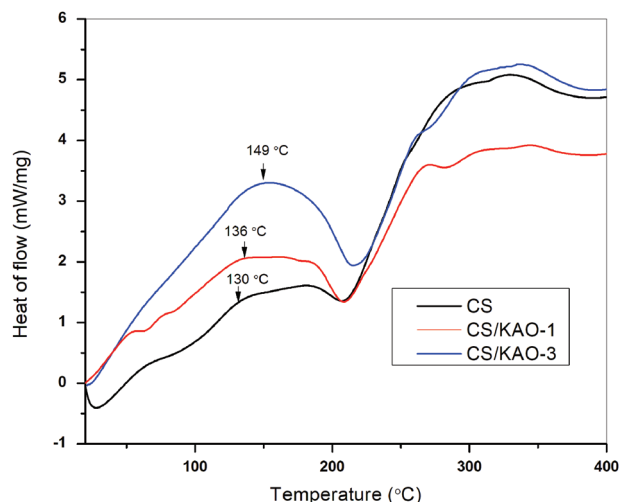
ADVANCED
SCIENCE NEWS
www.advancedsciencenews.com

[M] acro-
molecular
Chemistry and Physics
www.mcp-journal.de

Figure 8. DSC plots of CS and CS/KAO clay biocomposite films.

films. To the best our knowledge, T_g of CS/KAO clay biocomposites with different weight ratios have never been reported. During the investigation it was found that the T_g values for CS, CS/KAO-1, and CS/KAO-3 were found to be 130, 136, and 149 °C respectively. The T_g value increased with the increase of KAO clay content in the CS matrix. This indicates that there is increase in crystallinity of the biocomposite films. A notable difference in the DSC thermograms of the CS and CS/KAO clay biocomposite films were observed, as illustrated in the **Figure 8**. It was found that CS has an exothermic degradation peak between 328–329 °C, whereas biocomposites have a degradation peak between 340–343 °C. These results indicate that the degradation was getting slowed down in the composites due to its chemical interaction of the KAO clay with CS matrix. Hence it is observed that the CS/KAO clay biocomposites have improved the thermal stability than that of CS which shows close agreement with the results reported by S. C. Dey el al.[3]

3.8. Antibacterial Activity Study by Agar Well Diffusion Method

The agar well diffusion test[36,37] results for CS and CS/KAO clay biocomposite films are shown in **Figure 9**. The test samples, i.e., CS, CS/KAO-1, CS/KAO-2, CS/KAO-3, and CS/KAO-4 were evaluated for antibacterial assay against one gram-negative bacteria *Escherichia coli* (MTCC-739) and one gram-positive bacteria *Bacillus subtilis* (MTCC-441) in concentration of 10 mg mL⁻¹. Minimum inhibitory concentration (MIC) was tested against bacterial pathogens *Bacillus subtilis and Escherichia Coli* at different concentrations of the test samples (10, 5, 2.5, 1.25, 0.625, and 0.31 mg mL⁻¹). In vitro susceptibility tests showed that test samples had antibacterial effects against both the bacteria at MIC 10 mg ml⁻¹. Therefore 10 mg mL⁻¹ concentration was selected for antibacterial activity to determine the zone of inhibition using agar well diffusion method. The solution used for dissolving the test samples (2% acetic acid) also showed some inhibition properties. The highest zone of inhibition was seen up to 21 mm diameter by CS/KAO-2 followed by 18 mm in

both CS/KAO-1 and CS, 13 mm on CS/KAO-4 and lowest inhibition 10 mm diameter was seen on CS/KAO-3 against *Escherichia coli* at 140 µg mL⁻¹. In case of gram-positive bacteria, the highest zone of inhibition was seen up to 17 mm diameter on CS/KAO-3 followed by 15 mm on CS/KAO-1 and CS/KAO-2 each, 13 mm on CS and lowest inhibition 12 mm diameter was seen on CS/KAO-4 against *Bacillus subtilis* at 140 µg mL⁻¹. CS is the only test sample which showed antibacterial activity on all concentration against gram-negative bacteria but only one concentration against gram-positive bacteria. According to our literature analysis, the antibacterial study of CS/KAO clay biocomposite films for different weight ratios by agar well diffusion method has never been reported. The biocomposites shows significant inhibitory effect against gram-negative bacteria as well as gram positive bacteria. It was observed that this was somewhat more effective against gram-negative bacteria than gram positive bacteria. This is due to higher hydrophilicity in gram-negative bacteria than in gram-positive, CS is more sensitive to gram-negative bacteria which exhibits increased morphological changes on treatment when compared to gram-positive.[42] Gram-negative bacteria are surrounded by a thin peptidoglycan cell wall, whereas gram-positive bacteria are surrounded by layers of peptidoglycan many times thicker than is found in the gram-negatives. In the presence of a thin peptidoglycan layer in gram-negative bacteria than gram-positive, the low molecular weight CS can easily cross the cell wall of gram- negative bacteria, while high molecular weight CS acts as a barrier interfering with the proper absorption of nutrients by the microbial cell.[43] Moreover, CS is reported to be polycationic in nature, so it can easily interfere with negatively charged residues at the cell surfaces causing cell wall disruption and alteration of membrane permeability which results in the inhibition of DNA replication and subsequently cell death.[44] It is also reported that cationic analogous can easily bind the surface membrane of gram- negative bacteria due to the presence of anionic structures such as lipopolysaccharides and proteins.[45] N. Cankaya et al. reported the antibacterial properties for CS/Na⁺ Montmorillonite, CS/Nanoclay 1–135 and CS/Nanoclay 1–140 and observed good antimicrobial activities for those biocomposites.[38]

The zone of inhibition of crude extract against bacterial strain MTCC-739 and MTCC-441 are summarized in **Table 4**.

3.9. Swelling Test Analysis

To the best of our knowledge, the swelling test of the CS/KAO clay biocomposite with various weight ratio have never been reported. Swelling tests were performed for all the synthesized CS and CS/KAO clay biocomposite films. It has been observed that the highest swelling property was observed for CS/KAO-1 while the least was observed in case of CS/KAO-4 (**Table 5**).

The following hierarchy was obtained by comparing the swelling behavior of CS and CS/KAO biocomposite films (**Figure 10**):

CS > CS/KAO-1 > CS/KAO-2 > CS/KAO-3 > CS/KAO-4

Swelling experiment shows that the CS and CS/KAO clay biocomposite films have different levels of water absorption capacity.
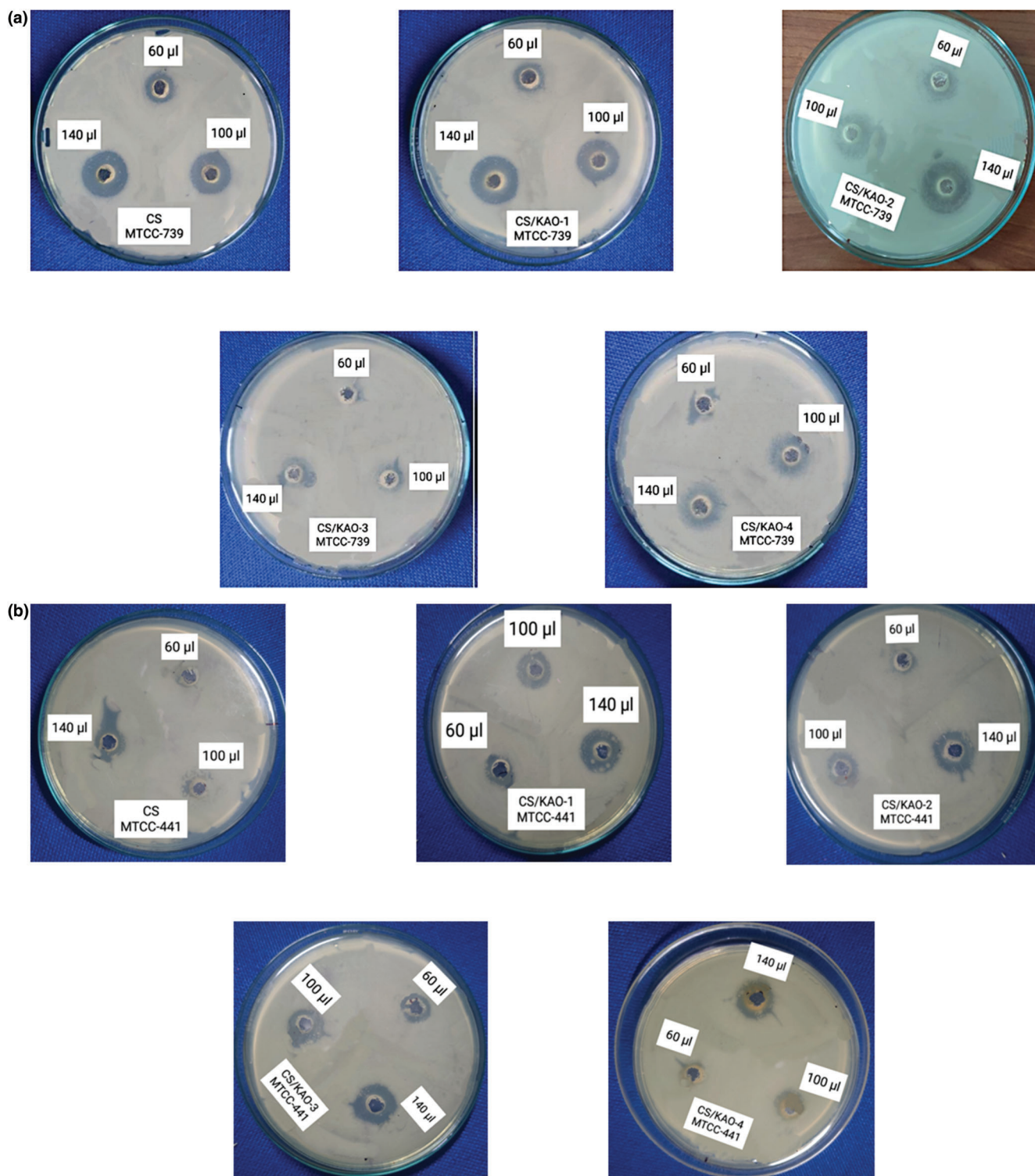
**ADVANCED
SCIENCE NEWS**

www.advancedsciencenews.com

**⟨M⟩ acro-
olecular
Chemistry and Physics**

www.mcp-journal.de

Figure 9. a) Antibacterial activities of CS and CS/KAO clay against gram-negative bacteria. b) Antibacterial activities of CS and CS/KAO clay against gram-positive bacteria.

**ADVANCED
SCIENCE NEWS**

www.advancedsciencenews.com

Macro-
molecular
Chemistry and Physics

www.mcp-journal.de

Table 4. Zone of inhibition (diameter in mm) in different concentration against MTCC-739 and MTCC-441 bacterial strain.

Sl. No.	Sample [Test & Standard]	Zone of inhibition (diameter) in 140 µl solution concentration	
		Gram negative bacteria (*E. coli*)	Gram positive bacteria (*B. subtilis*)
1.	CS	18 mm	13 mm
2.	CS/KAO-1	18 mm	15 mm
3.	CS/KAO-2	21 mm	15 mm
4.	CS/KAO-3	10 mm	17 mm
5.	CS/KAO-4	13 mm	12 mm
6.	Amoxycillin	23 mm	23 mm

Table 5. Percentage of swelling for all the biocomposite films.

Sample	Swelling %				
	1 h	3 h	6 h	9 h	12 h
CS	47.4	57.2	60.1	60.6	61
CS/KAO-1	46.8	56.3	56.7	57	57.2
CS/KAO-2	45.5	54.8	55.1	55.3	55.4
CS/KAO-3	44.3	52.2	52.4	52.5	52.5
CS/KAO-4	43.2	49.7	49.8	49.8	49.8

It was observed that on increase in the KAO clay amount to the CS matrix shows an inverse effect to the swelling of the films. The hydrophilic property provided by groups OH and NH_2 in the structure of CS matrix with the clay particles would be the reason of this behavior. The results agree well with the investigation reported by N. Cankayaet al. using CS/Na^+ Montmorillonite, CS/Nanoclay 1–135 and CS/Nanoclay 1–140.[38]

4. Conclusion

In this work, four films of CS/KAO clay biocomposite films were prepared using CS and KAO clay at different weight ratios in a 2% acetic acid solution. The ratios of the biocomposite films were maintained at about 10:01, 10:02, 10:03, and 10:04 respectively. All the biocomposite films were characterized by various

Figure 10. Swelling test plots of CS and CS/KAO clay biocomposite films.

physico-chemical methods viz. FT-IR, UV/Vis, XRD, SEM, UTM, TGA/DTA, and DSC. Two tested bacteria's viz. *Escherichia coli* and *Bacillus subtilis* were used to determine the antibacterial activities of the biocomposite films. The biocomposite films were also performed with swelling tests. FT-IR analysis reveals that absorption band at 1639 cm^{-1} for CS film was shifted to 1624 cm^{-1} in the biocomposites. CS/KAO clay biocomposite films showed a high UV/Vis absorption than pure CS matrix. XRD pattern confirmed that the KAO clay was effectively incorporated into the CS with four different concentrations. SEM micrographs showed that in case of CS/KAO-1 biocomposite, the clay particles were uniformly dispersed into the matrix and thus showed an exfoliated structure whereas in case of CS/KAO-2 and CS/KAO-3 the filler and matrix interaction was more prominent. The fibrous network and rough surface in CS/KAO-4 was due to the high concentration of KAO clay in the CS matrix. The gradual addition of filler is the reason of enhancement in the mechanical properties of biocomposites. The biocomposite films showed greater thermal stability than that of the CS matrix. The thermal stabilities improved with the increase of clay amount into the CS matrix. Further DSC suggests that the thermal stability of CS was improved due to composite formation. Antibacterial activity of biocomposite films was investigated in which the test materials had significant inhibitory impact against gram-negative bacteria, *Escherichia coli* than gram-positive bacteria, *Bacillus subtilis*. Swelling experiment shows that the CS and CS/KAO clay biocomposites have different levels of water absorption capacity and increase of the clay is inversely related to the swelling of the films. From our literature analysis it was observed that the CS/KAO clay biocomposites has several applications. As the synthesized biocomposites shows good tensile strength as well as significant antibacterial properties it may be used in the food packaging purposes. We can believe that all biocmposites have the ability to perform well as food packaging material but since CS/KAO-2 shows highest zone of inhibition against Escherichia coli, so that among all the biocomposites CS/KAO-2 may be the best material for food packaging applications. Also, it may be observed that among all the biocomposites, CS/KAO-2 possessed a more uniform and smoother surface which is desirable for its industrial applications. It was also observed that, as the biocomposites were rich in clay it may shows some good performance in the absorption for various cationic dye and heavy metals. On the basis of the literature investigation, we can say that CS/KAO-4 may have possibly better performance for cationic dye uptake because CS/KAO-4 biocomposite contain highest amount of KAO clay whereas CS/KAO-1 may adsorb heavy metals because lowest amount of KAO clay is present. The findings suggest that CS/KAO clay biocomposites have exceptional properties with wide applications, hence able to occupy a potential market across the globe.

Conflict of Interest

The authors declare no conflict of interest.

Data Availability Statement

The data that support the findings of this study are available from the corresponding author upon reasonable request.

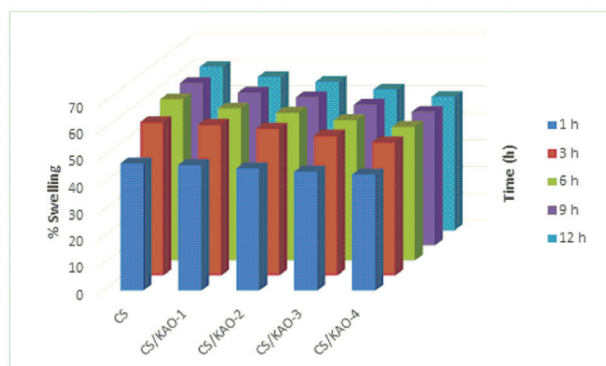[1] A. Laaraibi, F. Moughaoui, F. Damiri, A. Ouakit, I. Charhouf, S. Hamdouch, A. Jaafari, A. Abourriche, N. Knouzi, A. Bennamara, M. Berrada, in *Chitin-Chitosan-Myriad Functionalities in Science and Technology* (Eds: R. Dongre), IntechOpen **2018**, pp. 45–69.

[2] W. Tan, Y. Zhang, Y.-S. Szeto, L. Liao, *Compos. Sci. Technol.* **2008**, *68*, 2917.

[3] S. C. Dey, M. Al-Amin, T. U. Rashid, M. Ashaduzzaman, S. Md Shamsuddin, *Int. Lett. Chem., Phys. Astron.* **2016**, *68*, 1.

[4] A. Casariego, B. W. S. Souza, M. A. Cerqueira, J. A. Teixeira, L. Cruz, R. Díaz, A. A. Vicente, *Food Hydrocoll* **2009**, *23*, 1895.

[5] R. A. Hule, D. J. Pochan, *MRS Bull.* **2007**, *32*, 354.

[6] K. N. Bharath, S. Basavarajappa, *Sci. Eng. Compos. Mater.* **2016**, *23*, 123.

[7] M. N. V. Ravi Kumar, *React. Funct. Polym.* **2000**, *46*, 1.

[8] R. Tang, Y. Du, L. Fan, *J. Polym. Sci., Part B: Polym. Phys.* **2003**, *41*, 993.

[9] S. Trujillo, E. Pérez-Román, A. Kyritsis, J. L. Gómez Ribelles, C. Pandis, *J. Polym. Sci., Part B: Polym. Phys.* **2015**, *53*, 1391.

[10] M. Bhattacharjee, N. B. Pramanik, N. K. Singha, D. J. Haloi, *Polym. Chem.* **2020**, *11*, 6718.

[11] S. Biswas, T. U. Rashid, T. Debnath, P. Haque, M. M. Rahman, *J. Compos. Sci.* **2020**, *4*, 16.

[12] S. C. Dey, M. Al-Amin, T. U. Rashid, M. Z. Sultan, M. Ashaduzzaman, M. Sarker, S. M. Shamsuddin, *International Journal of Latest Research in Engineering and Technology* **2016**, *2*, 52.

[13] L. L. Hench, *Biomaterials* **1998**, *19*, 1419.

[14] J. Desbrières, E. Guibal, *Polym. Int.* **2018**, *67*, 7.

[15] K.-F. Lin, C.-Y. Hsu, T.-S. Huang, W.-Y. Chiu, Y.-H. Lee, T.-H. Young, *J. Appl. Polym. Sci.* **2005**, *98*, 2042.

[16] S. Qasim, M. Zafar, S. Najeeb, Z. Khurshid, A. Shah, S. Husain, I. Rehman, *Int. J. Mol. Sci.* **2018**, *19*, 407.

[17] B. Bayón, I. R. Berti, A. M. Gagneten, G. R. Castro, in *Waste to Wealth*, (Eds: R. Singhania, R. Agarwal, R. Kumar, R. Sukumaran), Springer, Singapore **2018**, pp. 1–44.

[18] M. S. Islam, P. Haque, T. U. Rashid, M. N. Khan, A. K. Mallik, M. N. I. Khan, M. Khan, M. M. Rahman, *J Mater Sci Mater Med* **2017**, *28*, 1.

[19] S. R. Popuri, Y. Vijaya, V. M. Boddu, K. Abburi, *Bioresour. Technol.* **2009**, *100*, 194.

[20] A. Madni, R. Kousar, N. Naeem, F. Wahid, *J. Bioresour. Bioprod.* **2021**, *6*, 11.

[21] W. S. Wan Ngah, L. C. Teong, M. A. K. M. Hanafiah, *Carbohydr. Polym.* **2011**, *83*, 1446.

[22] N. Gontard, R. Thibault, B. Cuq, S. Guilbert, *J. Agric. Food Chem.* **1996**, *44*, 1064.

[23] J.-W. Rhim, S.-I. Hong, H.-M. Park, P. K. W. Ng, *J. Agric. Food Chem.* **2006**, *54*, 5814.

[24] S. Gu, X. Kang, L. Wang, E. Lichtfouse, C. Wang, *Environ. Chem. Lett.* **2019**, *17*, 629.

[25] A. D. Karathanasis, in *Encyclopedia of Soil Science*, CRC Press, Boca Raton, FL, USA **2017**, pp. 430–434.

[26] A. Oun, N. Tahri, S. Mahouche-Chergui, B. Carbonnier, S. Majumdar, S. Sarkar, G. C. Sahoo, R. Ben Amar, *Sep. Purif. Technol.* **2017**, *188*, 126.

[27] H. Ebrahimi, B. Abedi, H. Bodaghi, G. Davarynejad, H. Haratizadeh, A. Conte, *J Food Process Preserv* **2018**, *42*, e13466.

[28] L. Martino, N. Guigo, J. G. Van Berkel, N. Sbirrazzuoli, *Compos B Eng* **2017**, *110*, 96.

[29] M. Okamoto, *J Ind Eng Chem* **2004**, *10*, 1156.

[30] M. Darder, M. Colilla, E. Ruiz-Hitzky, *Chem. Mater.* **2003**, *15*, 3774.

[31] C.-M. Hristodor, N. Vrinceanu, A. Pui, O. Novac, V.-E. Copcia, E. Popovici, *Environ. Eng. Manag. J.* **2012**, *11*, 573.

[32] W. Ma, J. Dai, X. Dai, Y. Yan, *Adsorp. Sci. Technol.* **2014**, *32*, 775.

[33] S. Biswas, T. U. Rashid, A. K. Mallik, M. Islam, M. N. Khan, P. Haque, M. Khan, M. M. Rahman, *Int J Polym Sci* **2017**, *2017*, 1.

[34] H. Y. Zhu, R. Jiang, L. Xiao, *Appl. Clay Sci.* **2010**, *48*, 522.

[35] I. P. Chen, C. C. Kan, C. M. Futalan, M. J. C. Calagui, S. S. Lin, W. C. Tsai, M. W. Wan, *Sustainable Environment Research* **2015**, *25*, 73.

[36] C. Valgas, S. M. D. Souza, E. F. A. Smânia, A. Smânia Jr., *Braz J Microbiol* **2007**, *38*, 369.

[37] S. Magaldi, S. Mata-Essayag, C. Hartung De Capriles, C. Perez, M. T. Colella, C. Olaizola, Y. Ontiveros, *Int J Infect Dis* **2004**, *8*, 39.

[38] N. Cankaya, R. Sahin, *Cellul. Chem. Technol.* **2019**, *53*, 537.

[39] V. Mohanasrinivasan, M. Mishra, J. S. Paliwal, S. K. Singh, E. Selvarajan, V. Suganthi, C. Subathra Devi, *3 Biotech* **2014**, *4*, 167.

[40] J. Barman, K. C. Sarma, M. Sarma, K. Sarma, *Indian J. Pure Appl. Phys.* **2008**, *46*, 339.

[41] S. Kumar, J. Koh, *Int. J. Mol. Sci.* **2012**, *13*, 6102.

[42] R. C. Goy, D. D. Britto, O. B. G. Assis, *Polímeros* **2009**, *19*, 241.

[43] A. Guarnieri, M. Triunfo, C. Scieuzo, D. Ianniciello, E. Tafi, T. Hahn, S. Zibek, R. Salvia, A. D. Bonis, P. Falabella, *Sci. Rep.* **2022**, *12*, 1.

[44] N. R. Sudarshan, D. G. Hoover, D. Knorr, *Food Biotechnol* **1992**, *6*, 257.

[45] K. Tiwari, M. Singh, P. Kumar, K. Mukhopadhyay, *Sci. Rep.* **2022**, *12*, 1987.

Chitosan/Clay biocomposite films with enhanced physico-chemical, mechanical and antimicrobial properties

Madhabi Bhattacharjee, Shyam Goswami, Nabendu B. Pramanik, Jayanta Barman, Mousmi Saikia, Nishant Rachayya Swami Hulle & Dhruba J. Haloi

Published online: 10 Jan 2024.

Submit your article to this journal ⬈

View related articles ⬈

View Crossmark data ⬈

Research Article

Chitosan/clay biocomposite films with enhanced physico-chemical, mechanical and antimicrobial properties

Madhabi Bhattacharjee[1], Shyam Goswami[2], Nabendu B. Pramanik[3], Jayanta Barman[4], Mousmi Saikia[5], Nishant Rachayya Swami Hulle[6], Dhruba J. Haloi[7]*

[1] Department of Chemistry, Bodoland University, Kokrajhar, Assam-783370, India

[2] Drugs and Narcotics Division, Directorate of Forensic Science, Guwahati, Assam-781019, India

[3] ICT-IOC Bhubaneswar Campus, Bhubaneswar, Odisha-751013, India

[4] Department of Physics, ADP College, Nagaon, Assam-782002, India

[5] Department of Herbal Science & Technology, ADP College, Nagaon, Assam-782002, India

[6] Department of Food Engineering & Technology, Tezpur University, Assam-784028, India

[7] Department of Applied Sciences, Tezpur University, Assam-784028, India

Corresponding Author
Dhruba J. Haloi
djhaloi@tezu.ernet.in

Abstract

Chitosan (CS) is a biopolymer known for its outstanding biocompatibility, biodegradability, and antibacterial properties. On the other hand, Clays are natural inorganic materials and have good rheological and thermal properties. Therefore, it is expected that the biocomposite prepared from both these materials may have numerous intriguing properties. In this work, we report the preparation of chitosan (CS)/bentonite (BNTN) and chitosan (CS)/silica (Si) biocomposite films and characterizations of those via various analytical techniques such as X-ray diffraction (XRD), Scanning Electron Microscope (SEM), Fourier Transform Infrared (FT-IR) Spectroscopy, Thermogravimetric Analysis (TGA), Differential Scanning Calorimetry (DSC), Ultraviolet/Visible (UV/Vis) Spectroscopy and Universal Testing Machine (UTM). Swelling tests of prepared biocomposite films were also carried out in distilled water to evaluate their property towards packaging applications. The synthesized biocomposite films exhibit appreciable antimicrobial activity against *Escherichia coli* and *Bacillus subtilis* bacteria using the agar well diffusion method. Additionally, it has been noted that compared to the films of the other two biocomposites, the CS/BNTN biocomposite films showed greater tensile strength, swelling capacity and antimicrobial activity.

Keywords

Chitosan, Bentonite, Silica, Biocomposite, Physicochemical Property, Antimicrobial Property, Swelling Property

Introduction

In recent decades, biodegradable polymers have been greatly emphasized for their excellent applications in several industries due to their fascinating properties[1,2]. Among those, chitosan (CS) is one of the most promising biodegradable polymers[3]. From the structural point of view, it is a linear polysaccharide and a deacetylated derivative of chitin, which is the most prevalent natural polymer found in bacterial and fungal cell walls as well as in the exoskeleton of crustaceans[4,5]. CS is composed of units of glucosamine and N-acetylglucosamine linked by 1-4 glycosidic linkages[6]. CS doesn't dissolve in organic solvents or in water under a neutral or basic environment which is due to the protonation of free amino groups but dissolves in acidic medium (about pH< 6) such as acetic acid, formic acids, *etc*.[7]. It is observed that in the last two decades, CS has been explored greatly due to its exceptional properties viz. biocompatibility, biodegradability, anti-bacterial action, non-toxicity, cellular compatibility, *etc*.[8]. The chemical modifications of the CS framework drastically enhance the physicochemical properties. Various biocomposites of CS

are synthesized using different chemical functionality. This methodology escalates to creating some novel materials of the same with exciting characteristics. Basically, CS-based biocomposites are prepared by using different types of inorganic substances such as layered silicates. Only CS-based products are rare as they don't have characteristics similar to that of CS-biocomposite materials. In the last few years, many CS-based biocomposites were developed to help with environmental challenges. For this reason, CS immobilization on clay minerals has gained serious attention for various applications[9].

Various studies revealed that clay minerals as naturally occurring inorganic compounds with unique structural adsorption, rheological, and thermal characteristics[10]. These materials are inherently hydrophilic in nature due to the presence of hydroxyl (-OH) groups on their surface, which may readily form bonds with water molecules[11]. On very few occasions purification and modification are required to increase the clay's compatibility with other polymers [12]. Clay minerals significantly improve the characteristics of CS which are due to their smaller particle size, high surface area, favourable aspect ratio, and better dispersion ability. The implementations of clay minerals in the industries of food, pharmaceutical, cosmetic, and other areas can be a result of various properties of clay viz. biocompatibility, non-toxicity, and outstanding controlled release ability[13]. The most incorporated silicate in polymer composites is bentonite (BNTN) clay. It is an aluminosilicate of 2:1 type and is made up of recurring triple-layer sheets with a thickness of about 1 nm and a length between hundred to several hundred nanometers that is shared by two tetrahedral silica sheets and an octahedral sheet of alumina[14]. When layers are stacked over one other, a space between them is created which is referred to as the interlayer. Weak electrostatic forces hold these parallel layers together to make the entire structure. The cations inside the interlayer can be easily transferred by other cations as it holds weak interaction between the stacking layers[15]. Another clay with a characteristic porous inorganic morphology with significant pore

volume, varied pore structure and high surface area is silica (Si). It is also used as support and in some modification techniques of other materials. Moreover, Si is very much applicable to various industries like rubber, pesticides, papermaking, plastic processing, *etc.*[16,17].

The electrolytic and chelating nature of CS is characterized by the presence of the acidity of the -NH_3^+ group. Moreover, due to its polycationic nature in acidic environments, CS may be intercalated in the different clays through the cationic exchange mechanism and hydrogen bonding interactions. Thus, the biocomposite form demonstrates intriguing structural and functional traits[15,18]. Recent literature reveals detailed the several characteristics and applications of these hybrid materials of clay and CS. In a report, Lin *et al.* proposed a novel method to synthesize CS/montmorillonite nanocomposites and investigated the mechanical properties and biodegradable characteristics. They reported that the tensile properties can be enhanced through the preparation of nanocomposites of CS, which can prevent degradation in the vitro test[1]. In some other studies, Tan *et al.* prepared CS/montmorillonite nanocomposites in the presence of hydroxy-aluminium oligomeric cations and nanocomposite. These nanocomposites were used in the absorption of organic and metal ions from dyes and finishing effluent[15]. Darder *et al.* investigated the intercalation of the cationic biopolymer CS in Na^{+-} montmorillonite and provided compact and robust 3-D nanocomposites with some interesting functional properties[18]. Laaraibi *et al.* also designed CS/montmorillonite nanocomposite films that showed potential utility in the food and the environmental field[19]. Cankaya *et al.* prepared some CS/montmorillonite nanocomposites from three major types of montmorillonites and their organo-clay and investigated the thermal, antimicrobial, and swelling properties of the biocomposites[20]. Another report investigated by Salama *et al.* prepared a new adsorbent material from CS and anionic silica clay through ionic interaction followed by a sol-gel process and showed that CS/Si nanocomposite was found to be an appropriate material for the adsorption of

organic pollutants in wastewater[21]. Mohammed *et al.* also synthesized CS/Si nanocomposite materials for the removal of methyl orange dye from water[22]. The report investigated by Sagheer *et al.* fabricated some CS/Si hybrid films by sol-gel process using tetraethoxysilane as a precursor material[23]. Zhong *et al.* used triblock co-polymer as the structure-directing agent, ethyl orthosilicate as the silicon source and CS as a carrier to prepare unique CS/Si composite with various mass ratios. Thus, the prepared composites showed quality application in removing dyes from the wastewater and the material has excellent reusability for up to six cycles[17]. Blachino *et al.* also prepared a CS/Si hybrid composite by physical adsorption and the sol-gel method and applied these materials for the removal of sulfonated azo dyes from an aqueous solution[24]. Cacciotti *et al.* assessed the possible uses of the CS/Montmorillonite systems as innovative carriers for enzyme covalent immobilization[25]. Benucci *et al.* prepared biopolymeric nanocomposite films by using CS and nanoclay to be used as carriers in the covalent immobilization of a proteolytic enzyme via glutaraldehyde crosslinking, with the intention of applying them in the winemaking process[26]. Moreover, in a different experiment, they incorporated two nanoclays into the CS-based nanocomposite films, the films exhibited enhanced mechanical properties, making them suitable for use in both synthetic and real white wine applications[27].

The main goal of our current investigation is to prepare CS/clay biocomposite films by combining BNTN and Si clay with an acidified aqueous solution of CS. A few biocomposite films using two different kinds of clay viz. BNTN and Si are prepared by the method explained in an earlier report[28] and the results are also compared with that report of chitosan(CS)/kaolin(KAO) biocomposite films. Various physicochemical methods, including XRD, SEM, FT-IR, TGA, DSC, UV/Vis and UTM are used to characterize these synthesized CS/clay biocomposite films. Swelling tests are performed for these biocomposite films. Notable antimicrobial activity of these biocomposite films was observed against two bacteria-*Escherichia coli* and *Bacillus subtilis*. To the extent that we are aware, there has not been comparative research done for different CS/clay biocomposite films. Moreover, there has been no investigation carried out on the swelling tests of CS/Si biocomposite films. Aside from that, the antimicrobial activity of those materials for *Escherichia Coli* and *Bacillus subtilis* bacteria has never been reported. We strongly believe that swelling property investigation, biological applicability and comparative analysis of various physicochemical characteristics of CS/clay biocomposite films make our work a novel and applicable one for diversified areas. We are thus very much interested in synthesizing these green bio-composite materials based on CS and clay material which are bio-friendly and non-hazardous to the environment. We believe that there are several aspects yet to be explored in this area, and our investigation is just a breakthrough in this domain.

Experimental
Chemical ingredients and Bacterial strain
Chitosan (from shrimp shells) with a deacetylation level of 75% is the key component of this research work and was purchased from LOBA Chemie Pvt Ltd. Bentonite also known as Montmorillonite and Aluminium Silicate Hydrate, was bought from Sisco Research Laboratories Pvt. Ltd. Silica Gel (SiO_2) was obtained from Thermo Fisher Scientific India Pvt. Ltd. Glacial acetic acid, which has a purity of >99% was purchased from EMPLURA in India, and distilled water was employed as solvent as required. The MTCC, Chandigarh, Punjab, India provided two bacterial species for antimicrobial activity - one gram negative (MTCC-739-*Escherichia coli*) and one gram positive (MTCC-441-*Bacillus subtilis*).

All additional reagents and chemicals were of analytical grade and used exactly as they were supplied.

Synthesis of CS/Clay Biocomposite Films
First 100 mL of 2% aqueous acetic acid solution were used to dissolve 1 g of CS powder.

This mixture was subsequently agitated at a temperature of 40 °C for a duration of 5 h. The resulting CS solution was then combined with 0.1 g of BNTN clay while being agitated at room temperature for 24 h at a speed of roughly 700 rpm. Subsequently, the resultant solution was poured into a petri dish and subjected to a 24 h drying period at 60 °C to facilitate the evaporation of the solvent, ultimately yielded the biocomposite films. To eliminate any remaining acetic acid residue, the film was immersed in an aqueous solution containing 0.05 M NaOH. Following this, the film underwent neutralization by rinsing it with distilled water and was then allowed to air dry at room temperature. The similar procedure was applied for the synthesis of CS/Si clay biocomposite films. The details of preparative data of CS/clay biocomposite films are shown in Table 1. CS/BNTN clay biocomposite films with 10% and 30% of BNTN clay are denoted as CS/BNTN-1 and CS/BNTN-3 respectively, whereas CS/Si biocomposite films with 10% and 30% of Si clay are denoted as CS/Si-1 and CS/Si-3 respectively.

The prepared CS/clay biocomposite films with different physical parameters are shown in **T**able 1 and Fig. 1.

Synthesis of crude sample for analysis of antimicrobial activity
In order to assess the antibacterial properties, the CS/clay biocomposite films were dried and then dissolved in a 2% acetic acid solution at a concentration of 10 mg/mL. To facilitate the dissolution of these films, the solutions were stirred with continuous rotation for approximately 5 h at a temperature of 40 °C. The resulting solutions were subsequently employed to evaluate their antibacterial effectiveness.

Instrumental techniques for the characterization of biocomposite films
The XRD patterns of the biocomposite films were examined using a Bruker AXS X-Ray Diffractometer (model D8 Focus, Germany) with Cu-Kα radiation (wavelength λ = 0.154 nm). The instrument was operated at 30 kV and 30 mA, and the scanning rate was set at 0.05 degrees per second, covering a 2θ range from 10° to 70° with step size of 0.1 (2θ) for the investigation. Using Debye Scherrer equation, [29] the average crystallite size is determined by taking into account the full-width at half-maximum (FWHM) of the first intense peak.

$$D_{hkl} = F \lambda / M \cos\theta \qquad (1)$$

In equation 1, D represents the average crystallite size, θ is the Braggs angle and M is FWHM. The value of F is 0.89 for a spherical shape. SEM images of the samples were captured using an analytical scanning electron microscope (JSM-7610F), with an operating accelerating voltage of 5.00 kV. Samples were were cut into small pieces and then mounted with the SEM holder using the double glue tape. After that, the mixture of Pd and Au plasma sputted over the surface of the samples. The FT-IR analyses of the samples were conducted using an Agilent Cary 630 FT-IR spectrometer, within the spectral range of 4000-700 cm^{-1} with a resolution of 4 cm^{-1}. Each spectrum was obtained by accumulating 8 scans. The TGA results were acquired using a Netzsch instrument (Model: STA2500A-0297-N). The samples (~3 mg) were introduced into the balance system of the machine and subjected to heating within a temperature range spanning from 20°C to 600°C. The heating rate employed was 10 °C/min and the analysis was conducted under a nitrogen atmosphere with a constant flow rate of 30 mL/min. Then,

Table 1. The preparative data of CS/clay biocomposite films

Sample	Film thickness (mm)	Amount of CS (g)	Clay used	Clay % w. r. t. the amount of CS
CS/BNTN-1	0.15	1	BNTN	10
CS/BNTN-3	0.18	1	BNTN	30
CS/Si-1	0.14	1	Si	10
CS/Si-3	0.18	1	Si	30

Chitosan/Bentonite Clay (10:1) Film

Chitosan/Bentonite Clay (10:3) Film

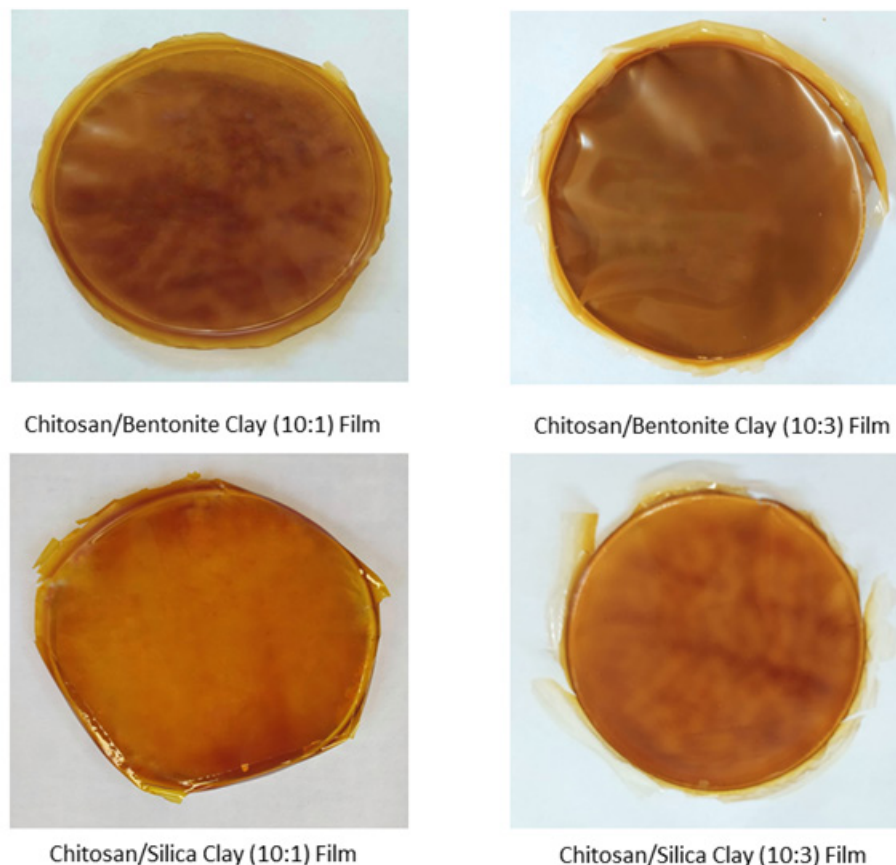Chitosan/Silica Clay (10:1) Film

Chitosan/Silica Clay (10:3) Film

Fig. 1. Biocomposite films made of CS and clay

the samples were cooled under air flow and the analysis was conducted with a dwelling time of 58 min. The DSC for all the samples (~6 mg) were carried out using a NETZSCH DSC 214 Polyma DSC21400A-0438-L. The samples were subjected to heating, starting from 30°C and reaching 400°C, at a controlled heating rate of 10 °C/min. This DSC analysis was conducted under a nitrogen atmosphere with a constant flow rate 20 mL/min. The UV/Vis analyses of the samples were conducted using an Agilent Cary 60 UV/Vis spectrophotometer, covering the spectral range from 200 to 800 nm with a resolution of 1 nm. The tensile properties of the samples were determined using a Texture Analyzer (TA-HDPlus, Stable Microsystems, UK). Thin strips were cut in 10 mm from each biocomposite film to assess their textural characteristics. The strips were placed in grips of testing machine and an initial gap was 20 mm between the grips. The tests were conducted with the following

parameters: a pre-test speed of 2 mm/s, a test speed of 3 mm/s, a post-test speed of 10 mm/s, a distance of 75 mm, and a trigger force of 10 g. The probe used for testing was attached to a 5 kg load cell. All the measurements were done in triplicates and average values were reported.

Analysis of Swelling capacity
The swelling characteristics of all the CS/clay biocomposite films that were synthesized were examined by immersing them in distilled water with a pH of 7.0 at room temperature for various time intervals, namely 1, 3, 6, 9, and 12 h. To initiate the process, the samples were first dried in an oven and their initial weights were measured. Subsequently, the samples were placed into containers filled with distilled water, with the first immersion occurring at t= 0. Measurements were then taken at specified intervals until a consistent weight was attained. The samples were later filtered using filter paper. This entire procedure

was repeated three times to ensure reliable and consistent results. The swelling percentage (S_w) of each sample was calculated using the formula

$$S_w = \frac{w_f - w_i}{w_i},\qquad(2)$$

In equation (2), w_i is the initial weight of the dried sample and w_f is the final weight of the prepared sample at time t.

Antimicrobial Study

The agar well diffusion assay for the samples was carried out with a few minor modifications in the method proposed by Valgas *et.al.*[30]. In order to carry out the investigation, 4 (four) wells with a diameter of 6 mm each had to be generated aseptically in the nutrient agar plates with a cork borer. A sterile loop was employed to carefully extract the agar cylinders. Subsequently, the test organism, a bacterial species, was swabbed onto sterile agar plates. Following the swabbing process, each well was loaded with 140 μL of the previously prepared test samples. To ensure the samples dried properly, the wells were placed under a blower in the laminar airflow (LAF). Once the plates were completely dry, they were aseptically removed from the LAF and incubated at a temperature of 37 °C for 18 h. The inhibition zones were then measured as part of the investigation.

Results and discussion
Analysis via XRD technique
Fig. 2(a) depicts the results of an investigation of the XRD study of the CS/clay biocomposite films. The intense peaks obtained for CS/BNTN and CS/Si biocomposite films were compared with CS/KAO biocomposite films reported by Bhattacharjee *et al.*[28] to know the preliminary information about the incorporation of BNTN and Si clay in the CS. CS has been shown to have semi-crystalline character whereas BNTN clay is crystalline and Si clay is amorphous. All the outcomes were noted in the 2θ range, which is around 10°-70°. For CS/BNTN clay biocomposite films, several intense peaks were observed; however, no such peaks were seen for CS/Si biocomposite films, which was mostly due to the amorphous nature of the Si clay. The XRD

pattern of CS revealed a large diffraction peak at about 22.4° reported by Bhattacharjee *et al.*, which corresponds to the usual fingerprints of the semicrystalline nature of CS. The absence of the peak at 22.4° in the CS/clay biocomposite films, as can be seen in Fig. 2(a), indicates that the CS in those biocomposite films has lost its crystallinity. It was found that the intensities of the peaks increased as well as a slight broadening in the biocomposite films from CS/BNTN-1 to CS/BNTN-3 with increasing concentrations of BNTN clay particles. On the other hand, the diffraction peak at 2θ around 22.4° weakened with an increase in the Si clay percentage in the XRD patterns of CS/Si-1 and CS/Si-3. This might be due to the addition of Si clay which destroyed the hydrogen bond between the CS molecules and thus affected the crystalline structure of CS[17]. Therefore, it can be assumed that all the clays were successfully incorporated into the CS. It was observed that more characteristic peaks were observed in CS/BNTN clay than in CS/KAO biocomposite films and no such distinguish characteristic peaks were observed in the case of CS/Si clay biocomposite film. This finding indicates that the crystallinity of biocomposite films is arranged as follows: CS/BNTN > CS/KAO > CS/Si

Using the Debye-Scherrer equation, the average crystallite size was determined. For all of the samples, the average value shifts from 18.08 to 19.83 nm. The particle sizes decrease and peaks are slightly shifted to a greater diffraction angle as the clay particle concentration rises.

For the purpose of removing the strain caused by the integration of CS, the lattice constant was computed from three significant peaks by the Nelson and Riley plot, and an average value of 5.3912 Å was found. Fig. 2(b) shows the Nelson Riley plot.

Analysis via SEM
To understand and visualize the morphologies of the synthesised CS/clay biocomposite films, SEM images were recorded. Fig. 3 shows the micrographs which illustrate the morphological changes of the biocomposite films. SEM micrograph of the biocomposites shows in which
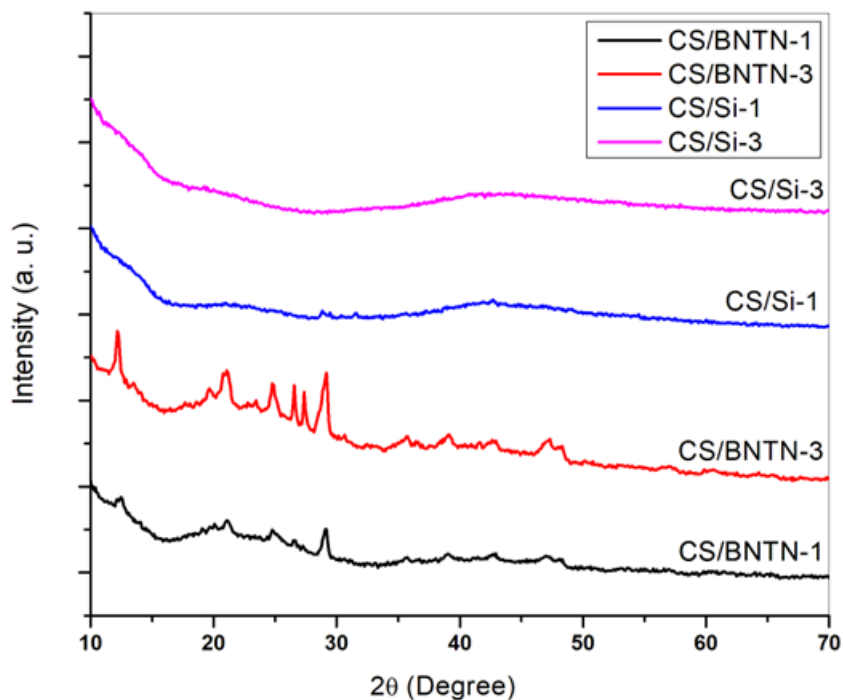
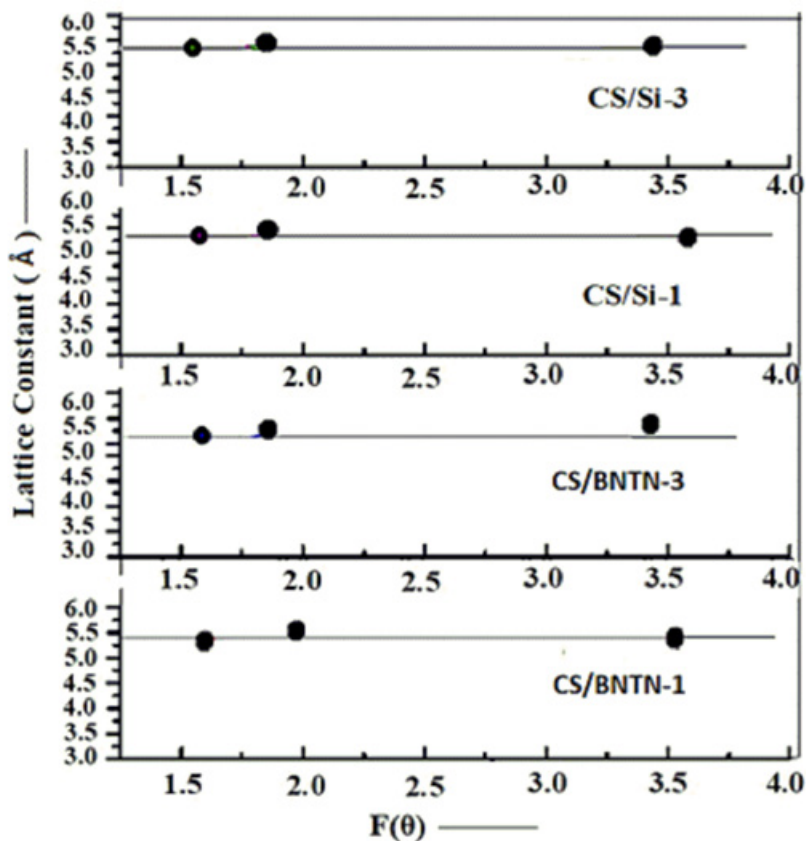**Fig. 2(a).** XRD patterns of different biocomposite films comprising CS and Clay

Fig. 2(b). Nelson and Riley graphs for biocomposite films containing CS and Clay

manner the clay particles are incorporated into the CS molecules. Additionally, the distribution of the clay particles throughout the CS molecule is observed. For CS/BNTN biocomposite films, an increase in the clay amount results in a more rugged structure. The homogeneous dispersion of the clay particles proves the presence of an exfoliated structure[20]. Analysis of Fig. 3(a) and 3(b) reveals that the CS/BNTN biocomposite films have a uniform appearance with small irregularities and bumps. In the case of CS/Si biocomposite films, the SEM images are shown in Fig. 3(c) and 3(d) which shows that the biocomposite films have a rough and irregular surface[31] and a flocculated fraction of Si is observed. It is observed that the biocomposite films exhibit considerable flocculation and intercalated morphology. The hydroxylated edge-edge interaction of the silicate layers causes the formation of a flocculated structure in the biocomposite films[15]. An article reported by Bhattacharjee *et al.* discussed the SEM micrographs of CS and CS/KAO biocomposite films where it was observed that with an increase in the amount of KAO clay in the biocomposite, the surface becomes more rough[28]. By analysing the SEM images of all the biocomposite films, the surface of the CS/KAO biocomposite films was found to be smoother and more uniform than those of the CS/BNTN and CS/Si biocomposite films. According to the structure of CS, it possesses one amino group and two hydroxyl functional groups. The silicate layers and matrix are thought to interact strongly because it is expected that the hydroxylated silicate edge groups and the functional groups of CS can form hydrogen bonds. The results indicate that CS is intercalated over the clay particles[13].

FT-IR spectral analysis

The FT-IR spectra were recorded for the synthesized biocomposites films i.e., CS/BNTN and CS/Si in the ratios of 10:01 and 10:03 at the region of 4000-700 cm^{-1} (Fig. 4). The bands at 3630, 3433, 1638, 994, and 797 cm^{-1} in Fig. 4(a) and Fig. 4(b) correspond to the vibrational
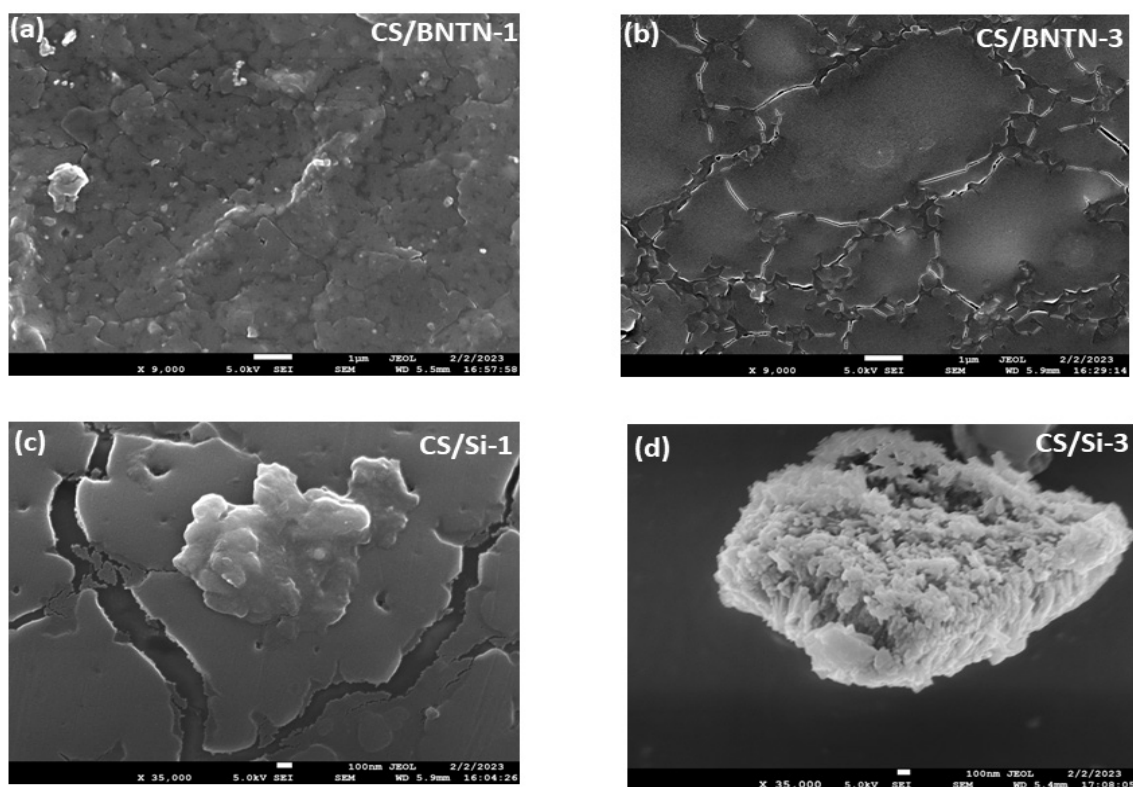

Fig. 3. SEM micrographs of (a) CS/BNTN-1 (b) CS/BNTN-3 (c) CS/Si-1 and (d) CS/Si-3
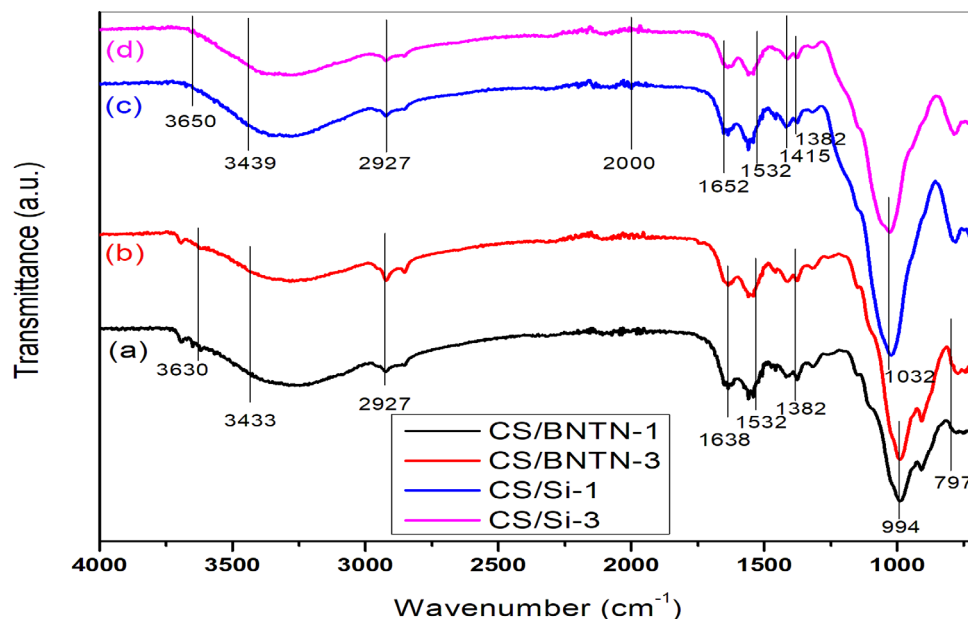
Fig. 4. FT-IR Spectra of different biocomposite films composed of CS and Clay

bands of the silicate which stay unaffected in the biocomposite films. The additional bands in the biocomposites at 2927 and 1382 cm^{-1}, are consistent with those observed in the pure CS film[15]. The band at 3439 cm^{-1} in Fig. 4(c) and Fig. 4(d) is the result of stretching vibrations of -OH groups attached to the carbon atom. C-H stretching vibrations arise with intense absorption bands at 2927 cm^{-1} and bending vibrations arise with intense bands at 1415 and 1382 (cm^{-1})[31]. The vibration bands at 1532 cm^{-1} in all of the biocomposite films show the electrostatic interaction between the NH_3^+ group of CS and the negatively charged sites in the added clay. The obtained results are in close agreement with the CS-based hybrid materials[15,24]. We have thoroughly discussed the FT-IR results of CS and CS/KAO biocomposite films in one of our earlier reports[28]. When all the biocomposite films are compared with different clay materials (viz. KAO, BNTN, and Si), it is observed that the vibration band that corresponds to the deformation vibration of the charged amine group in the CS film is found to be shifted towards more low-frequency values in the biocomposite films. This evidence confirmed that the films thus synthesized are not a physical mixture of CS and clay particles; in fact, these are biocomposite films[32].

Thermal Analyses

To investigate the thermal stability of the material, TGA of the CS/clay biocomposite films is performed. Fig. 5 shows the TGA plots for the CS/clay biocomposite films. The plots show that the degradation processes for the biocomposite films took place in two steps. In the case of CS/BNTN biocomposite films, the first degradation range (50-200 °C) is related to the loss of water, while the second breakdown occurs at about 280 °C for CS/BNTN-1 and about 287 °C for CS/BNTN-3 which represents the deacetylation and degradation of CS and the final stage which occurs in the vicinity of 450–550 °C can be assumed to be related to the oxidative breakdown of the carbon-based residue produced during the preceding stage. The results thus obtained are well agreed with the TGA data obtained by Laaraibi *et al.* in their investigation[19]. For CS/Si biocomposite films, the first stage of degradation is observed at a temperature below 120 °C, which can be considered as evaporation of water. The second stage observed at 200-350 °C indicates the breakdown of the organic components of the CS/Si biocomposite films and the third stage at the range of about 370-590 °C. These showed the high stability exhibited by the biocomposite films, composed of CS and Si clay. The results
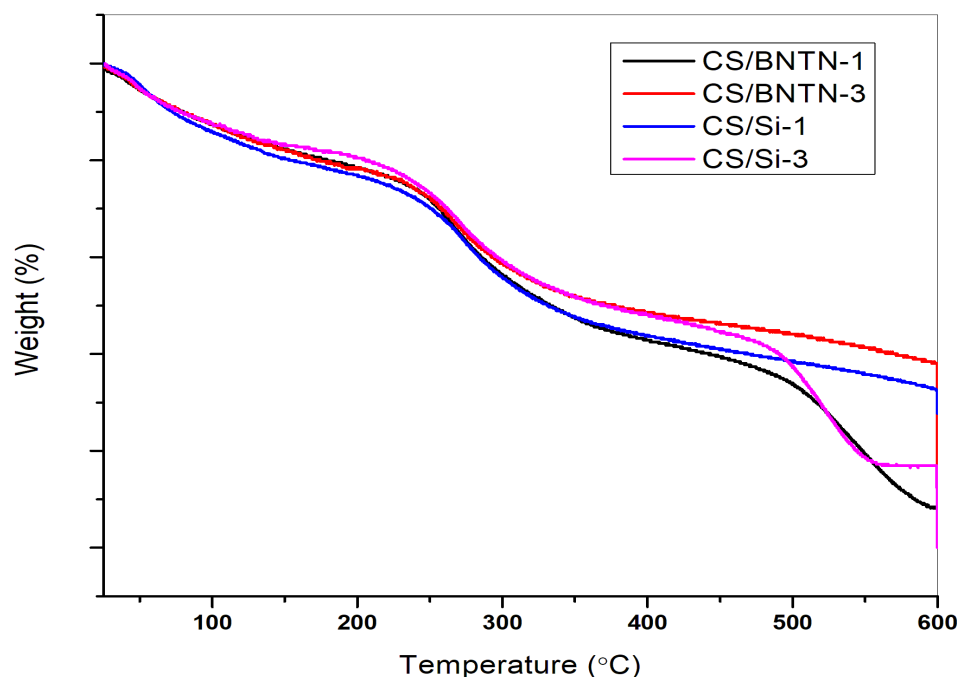
Fig. 5. TGA graphs for different biocomposite films comprising CS and clay

show close agreement with the results obtained by the Salama *et al.* in their report[21]. One of our previous reports revealed the thermal stability of CS and CS/KAO biocomposite films where we explored that the CS/KAO biocomposites have superior thermal stability than the pure CS and also on increasing the clay proportion in the biocomposite, there was a clear enhancement in the stability of CS/KAO biocomposites films[28]. Herein, we have explored that the thermal stability of the biocomposite films progressively rises as the clay percentage increases and that the decomposition temperature of CS/BNTN and CS/Si biocomposite films display greater thermal stability than the pure CS. The temperature ranges at which synthesized CS/clay biocomposite films degrade are listed in Table 2. On comparing the outcomes with Bhattacharjee *et al.*[28] which is based on the CS/KAO biocomposite films, it has been noticed that the CS/Si biocomposite films exhibited a slightly higher thermal stability than the CS/BNTN biocomposite films and the CS/BNTN biocomposite films exhibited slightly greater than those of CS/KAO biocomposite films. The high melting point of Si clay, which has the ability to withstand very high temperatures

without suffering substantial degradation, and BNTN clay, which can sustain moderately high temperatures without suffering vital degradation, are thought to be causes of this order. The KAO clay, on the other hand, undergoes a phase transformation as the temperature rises.

Table 2. Thermal properties of
CS/clay biocomposite films

Sample	1st breakdown		2nd breakdown	
	T_{onset} (ºC)	T_{max} (ºC)	T_{onset} (ºC)	T_{max} (ºC)
CS/BNTN-1	219	280	450	545
CS/BNTN-3	227	287	460	550
CS/Si-1	200	343	370	565
CS/Si-3	216	350	378	570

DSC investigation

As shown in Fig. 6, thermograms obtained from DSC for the CS/BNTN and CS/Si biocomposite films provided some substantial results. Bhattacharjee *et al.* reported that the CS degrades exothermically in the temperature range between
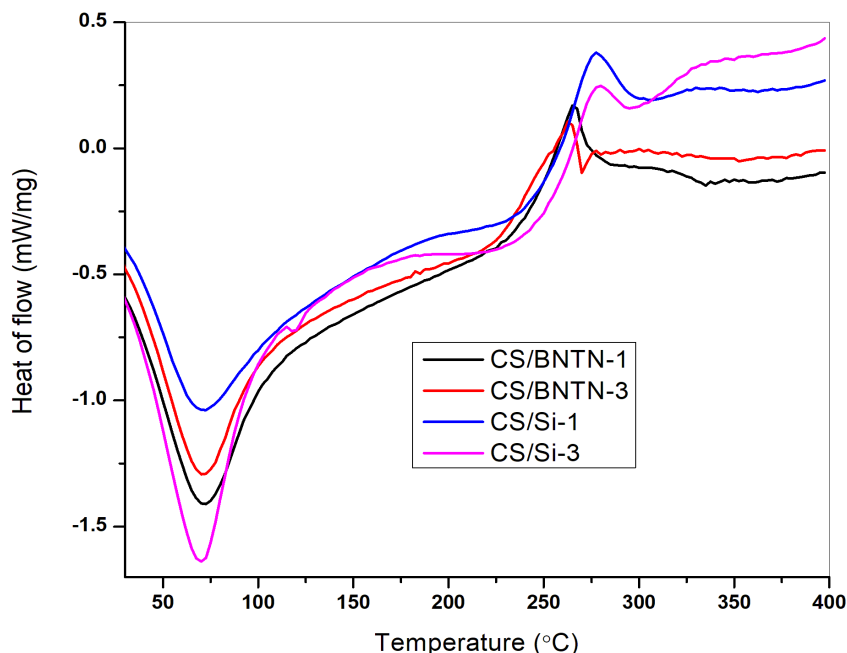
Fig. 6. DSC thermograms of different CS/clay biocomposite films

328-329 °C, whereas CS/KAO biocomposite films degrade between 340-343 °C[28]. Herein, the degradation peak was obtained for CS/BNTN biocomposite films in the temperature range between 347-349 °C, whereas the peak for CS/Si biocomposite films was obtained between 350-353 °C. The result indicates that the degradation of biocomposite films was delayed because of their interaction with the particles of clay. As a consequence, the thermal stability of CS/clay biocomposite films was enhanced distinctly. The thermal stability order of all three types of biocomposite films is as follows:
CS/Si > CS/BNTN > CS/KAO

Spectral analysis via UV-Vis spectroscopy
Fig. 7 displays the UV-Vis Spectra of CS/clay biocomposite films that were recorded at ambient temperature. The absorption bands for synthesized biocomposite films were visible between 200-800 nm. Maximum wavelengths for films viz. CS/BNTN-1, CS/BNTN-3, CS/Si-1, and CS/Si-3 are obtained at 388 nm, 374 nm, 358 nm and 380 nm, respectively. The absorption bands observed at the range of 300-400 nm are mostly responsible for the direct electronic transition from d-π^* orbital which is also termed

the Soret band[33]. The position and shape of the UV absorption band were affected by the amount of clay introduced to CS. The variations in the intensity of the absorbed light were closely associated with the increase in the amount of clay in the biocomposite films. When clay particles get concentrated, the molecular interaction occurs as a result the alteration in the shape and position of the bands takes place. Therefore, the peak shifting was observed in various CS/clay biocomposite films. Absorption parameter includes the maximum absorption wavelength (λ_{max}), absorption intensity and peak shape in the absorption spectrum. Maximum absorption indicates the wavelength where the biocomposite absorbs light most strongly. Shifts in λ_{max} can signal changes in the interaction between CS and clay. In our previous report[28] we reported that CS shows λ_{max} value at 354 nm and in the case of all the other CS/clay biocomposite films, the λ_{max} value shifts towards longer wavelengths which may be corroborated with the enhanced interaction in the biocomposites' electronic structure. Moreover, absorption intensity changes with concentration or the extent of interaction between components. An increase in intensity also indicates enhanced interaction. By comparing CS/BNTN clay
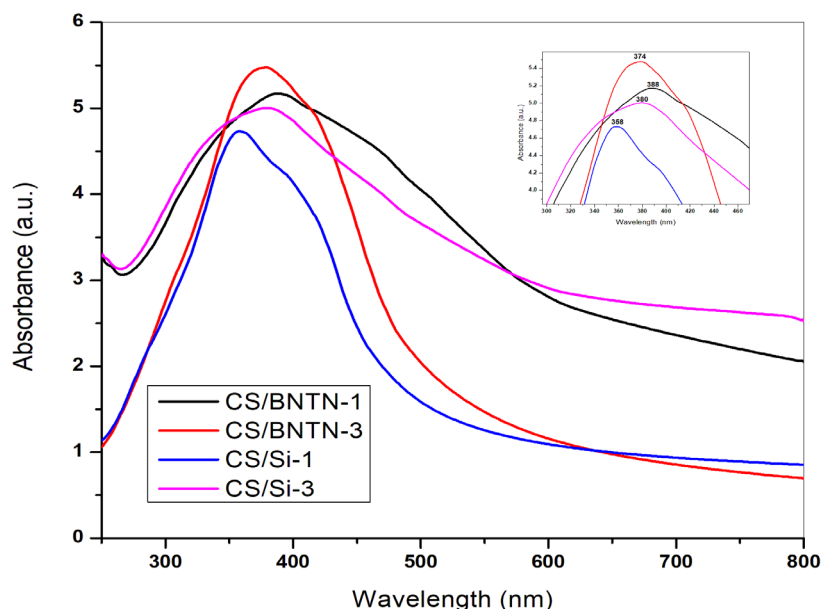
Fig. 7. UV-Vis Spectra of different biocomposite films composed of CS and clay

and CS/Si clay biocomposite films with CS/ KAO clay biocomposite films reported by Bhattacharjee *et al.*[28], it was observed that in all the cases maximum absorption was shown by the biocomposite films which contained the highest concentration of clay. Among all the biocomposite films CS/KAO-3 and CS/ BNTN-3 showed maximum absorption (both the values are almost similar). The fact behind the observation may be due to the amount of clay particles in the biocomposite films and the path length it travels. We primarily want to investigate the interaction of various clays with the pure CS molecule from the UV/Vis study. In addition, we were interested in examining how various biocomposite films influence the shape and position of the absorption band. The Soret band at 300-400 nm, which was clearly visible for all the synthesized films, is another goal of this investigation. Therefore, in addition to FT-IR analysis, this analysis also provided strong supporting structural information.

Analysis of tensile properties

The literature survey prevails that researchers have given much importance to the development of CS/Clay biocomposites intending to use them for some specific kind of applications where good mechanical properties are not a requirement. However, one of the key qualities that can separate polymers from tiny molecules is often found to be their mechanical properties. The mechanical properties such as elongation at break and tensile strength are examined to gain more knowledge of the physical properties of CS/clay biocomposite films. In Table 3 both characteristics are listed. It has been shown that when the number of clay particles in biocomposite film rises, the elongation at break reduces but the tensile strength improves. Lin *et al.*[1] and Laaraibi *et al.*[19] also observed similar trends in the addition of BNTN clay to the CS matrix. In comparison to CS/KAO and CS/Si biocomposite films, it is noted that CS/BNTN biocomposite films possess the highest tensile strength. A high tensile strength value indicates an increase in the stiffness of the biocomposite film whereas low elongation at break result shows that decrease in ductility. The finding indicates that CS/BNTN-3 possesses the highest stiffness and lowest ductile properties among all synthetic biocomposite films. These properties indicate that CS/BNTN-3 has higher brittleness characteristics. Thus, the fragility order of the synthesized biocomposite films is as follows:

CS/BNTN-3 > CS/BNTN-1 > CS/KAO-3 > CS/ KAO-1 > CS/Si-3 > CS/Si-1

The higher tensile strength of CS/clay

Table 3. Tensile properties of various CS/clay biocomposite films

Biocomposite Films	Elongation at break (%)	Tensile Strength (in N)
CS/KAO-1	5.8 ± 0.1	55.1 ± 2.2
CS/KAO-3	5.5 ± 0.1	58.5 ± 2.4
CS/BNTN-1	5.2 ± 0.2	94.3 ± 3.1
CS/BNTN-3	4.3 ± 0.1	96.2 ± 3.3
CS/Si-1	5.5 ± 0.2	37.9 ± 1.2
CS/Si-3	5.2 ± 0.2	40.2 ± 1.3

biocomposite films indicates an improved polymer-filler interaction. The high tensile strength of CS/clay biocomposite films, an intriguing mechanical characteristic, makes them attractive options for use as a food packaging material.

Analysis of Swelling Capacity

All the synthesized CS/clay biocomposite films underwent swelling test analyses, and key findings are shown in Fig. 8. All the findings thus obtained were compared with the investigation on CS and CS/KAO biocomposite films reported by Bhattacharjee *et al.*[28]. The literature review reveals that no swelling test analysis for CS/Si biocomposite films has been reported. Herein, it is found that the swelling capacity of CS/BNTN biocomposite films increases with time

along with an increase in BNTN clay content. In comparison to pure CS film, these biocomposite films exhibit enhanced swelling characteristics. The reason for this change may be assumed to be the structural correlation between CS and BNTN clay. The water absorption capacity of CS rises with an increase in the concentration of BNTN clay, which provides additional sites for water to interact, as a result, the biocomposite films swell more[34]. Abdelkrim *et al.* reported similar results with BNTN clay[35]. On the other hand, CS/Si biocomposite films exhibit some interesting results that are quite similar to those of CS/KAO clay biocomposite films. The analysis reveals that the swelling property of the biocomposite films has an inverse relationship to the addition of Si clay to the CS matrix. The hydrophilic properties offered by the $-NH_2$ and$-$OH groups present within the CS, which provide some interactions with the clay particles, can be used to explain this property. The percentages of swelling for synthesized CS/clay biocomposite films are summarized in Table 4. From the analysis, it is clear that CS/BNTN-3 exhibited the highest swelling characteristics.

Antimicrobial study

The agar well diffusion procedure for antimicrobial analysis[30] of the CS/clay biocomposite films is shown in Fig. 9. At a concentration of 10 mg/mL, the antimicrobial activity of the test samples i.e., CS/BNTN-1, CS/BNTN-3, CS/Si-1, and
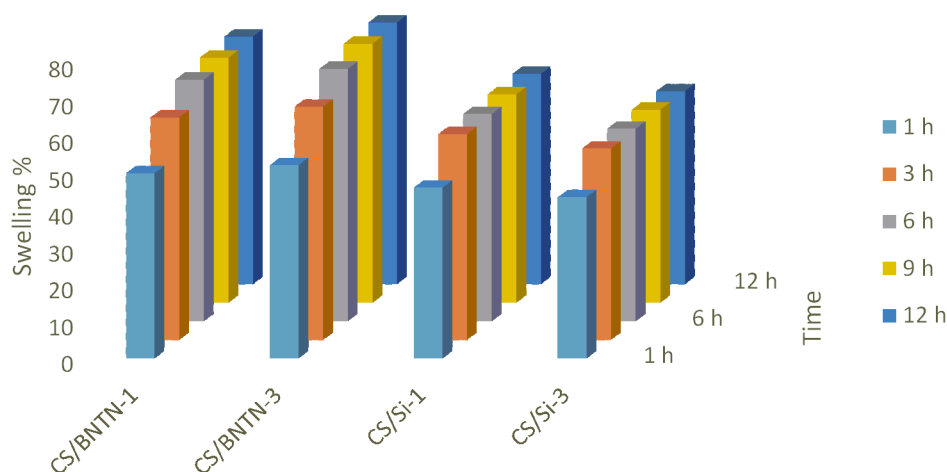

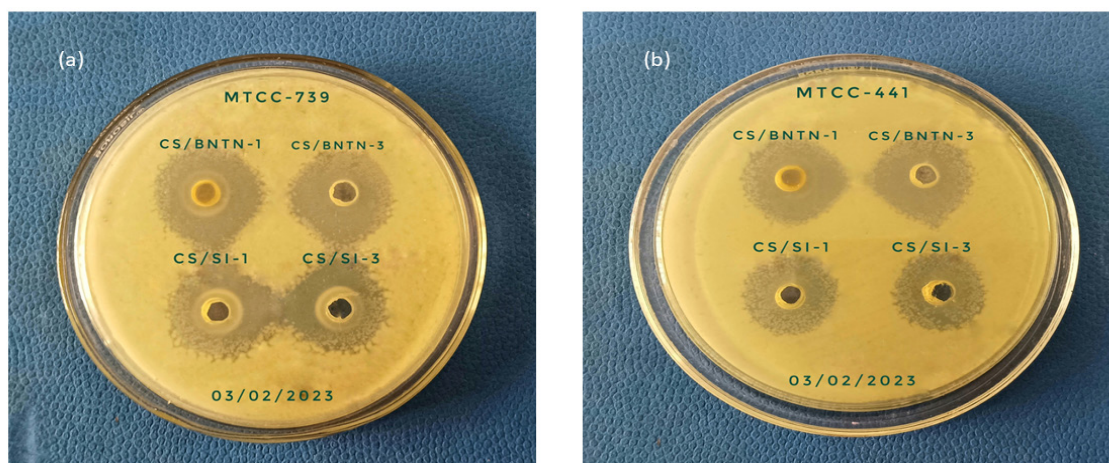**Fig. 8.** Plots of swelling test of various CS/clay biocomposite films

Fig. 9. Antimicrobial activities showing zone of inhibition by CS/clay biocomposite films against (a) *Escherichia coli* and (b) *Bacillus subtilis*

Table 4. Swelling % of various CS/clay biocomposite films

Sample Type	% of Swelling				
	1 h	3 h	6 h	9 h	12 h
CS/BNTN-1	50.2	60.3	65.5	66.4	67.1
CS/BNTN-3	52.4	63.2	68.4	70.2	70.9
CS/Si-1	46.3	55.8	56.2	56.5	57
CS/Si-3	43.7	51.9	52.2	52.3	52.3

CS/Si-3, were assessed against *Escherichia* and *Bacillus subtilis*. With respect to *Escherichia coli,* CS/BNTN-3 showed the largest zone of inhibition, measuring up to 26 mm in diameter, followed by CS/BNTN-1 with 25 mm, CS/Si-3 with 24 mm and CS/Si-1 with 23 mm. In case of *Bacillus subtilis*, CS/BNTN-3 showed the maximum zone of inhibition, measuring up to 23 mm, followed by CS/BNTN-1 and CS/Si-3 with 22 mm and CS/Si-1 with 21 mm. The obtained antimicrobial results were compared with the published article of CS/KAO biocomposite films reported by Bhattacharjee *et al.*[28]. It is observed that a significant zone of inhibition in millimetres (mm) among the three combinations of CS/clay biocomposite films is as follows:
CS/BNTN > CS/Si > CS/KAO

Our literature review revealed that the agar well diffusion method has never been used to evaluate the antimicrobial effects of CS/Si biocomposite films. In the current investigation, all of the biocomposite films demonstrate measurable inhibitory effects against both gram negative and gram-positive bacteria. Cankaya *et al.* have reported the antibacterial characteristics of CS/Na$^+$ Montmorillonite and CS/Nanoclay, highlighting their significant antimicrobial efficacy in these biocomposite materials[20]. Vijayalekshmi *et al*. also investigated the antibacterial activity of Chitosan-Montmorillonite Clay/TiO$_2$ nanocomposites using gram negative and gram positive bacteria and observed all the nanocomposite shows high antibacterial activity[33].

Table 5 summarizes the zone of inhibition of crude extract against bacterial strains MTCC-739 and MTCC-441.

Conclusion

The prepared CS/clay biocomposite films were characterized via XRD, SEM, FT-IR, TGA, DSC, UV/Vis and UTM analyses. XRD and SEM analyses provide the necessary information about the distribution of clay particles in the CS molecule. CS/BNTN biocomposite films show a bit more complicated crystalline structure than the CS/Si biocomposite films. SEM micrographs indicate an intercalated kind of morphology exhibited by both types of biocomposite films. FT-IR and UV-Vis analyses show the interactions between CS and clay particles in the prepared

Table 5. Zone of inhibition in a test against bacterial strains MTCC-739 and MTCC-441

S. No.	Test Sample	Zone of inhibition (diameter) mm	
		Escherichia coli bacteria (MTCC-739)	*Bacillus subtilis* bacteria (MTCC-441)
1.	CS/BNTN-1	25 ± 0.02	22 ± 0.02
2.	CS/BNTN-3	26 ± 0.01	23 ± 0.01
3.	CS/Si-1	23 ± 0.02	21 ± 0.02
4.	CS/Si-3	24 ± 0.01	22 ± 0.01

biocomposite revealing the successful preparation of biocomposite rather than a physical mixture. The thermal stability of all the biocomposite films was remarkable. The CS/Si biocomposite films were found to have better thermal stability than CS/BNTN and CS/Si biocomposite films. For all the biocomposite films, an improvement in mechanical properties has been observed. Compared to CS/Si and CS/KAO biocomposite films, CS/BNTN biocomposite films have a higher tensile strength. Antimicrobial activity results reveal that both gram-negative and gram-positive bacterial growth are strongly inhibited by all of the biocomposite films. Additionally, CS/BNTN biocomposite film exhibits the highest zone of inhibition against both types of bacteria. Among the synthesized biocomposite films, CS/BNTN-3 exhibits good mechanical and significant antimicrobial properties than the other two. Therefore, it is assumed that CS/BNTN-3 would be an excellent candidate for food packaging material.

References

1. **Lin, K.F., Hsu, C.Y., Huang, T.S., Chiu, W.Y., Lee, Y.H., Young, T.H. (2005).** A novel method to prepare chitosan/montmorillonite nanocomposites. J. Appl. Polym. Sci. 98: 2042-2047.

2. **Ahari, H., Golestan, L., Anvar, S.A.A., Cacciotti, I., Garavand, F., Rezaei, A., Sani, M.A., Jafari, S.M. (2022).** Bio-nanocomposites as food packaging materials; the main production techniques and analytical parameters. Adv. Colloid Interface Sci. 310: 102806.

3. **Garavand, Y., Taheri-Garavand, A.**

Garavand F., Shahbazi, F., Khodaei, D., Cacciotti, I. (2022).** Starch-polyvinyl alcohol-based films reinforced with chitosan nanoparticles: physical, mechanical, structural, thermal and antimicrobial properties. Appl. Sci. 12: 1111.

4. **Bhattacharjee, M., Pramanik, N.B., Singha, N.K., Haloi, D.J. (2020).** Recent advances in RDRP-modified chitosan: a review of its synthesis, properties and applications. Polym. Chem. 11: 6718- 6738.

5. **Vijayasri, K., Tiwari A. (2019).** Radiation degraded chitosan: Efficiency and investigation of adsorption of arsenic (V) from aqueous solution. Anal. Chem. Lett. 9: 182-195.

6. **Vijayasri, K., Tiwari, A., Chaudhari C.V. (2019).** Fixed-bed column studies on removal of As (V) by radiation grafted polymer "Chitosan-g-MAETC". Anal. Chem. Lett. 9: 486-503.

7. **Pandis, C., Madeira, S., Matos, J., Kyritsis, A., Mano, J. F. (2014).** Chitosan-silica hybrid porous membranes. Mater. Sci. Eng. 42: 553-561.

8. **Kean, T., Thanou, M. (2010).** Biodegradation, biodistribution and toxicity of chitosan. Adv. Drug Deliv. Rev. 62: 3-11.

9. **Madni, A., Kousar, R., Naeem, N., Wahid, F. (2021).** Recent advancements in applications of chitosan-based biomaterials for skin tissue engineering. J. Bioresour. Bioprod. 6: 11-25.

10. **Gu, S., Kang, X., Wang, L., Lichtfouse, E., Wang, C. (2019).** Clay mineral adsorbents for heavy metal removal from wastewater: a review. Environ. Chem. Lett. 17: 629-654.

11. **Karathanasis, A.D. (2017).** Clay Minerals: Weathering and Alteration of Encyclopedia of Soil Science. CRC Press: Boca Raton, FL, USA 430–434.

12. **Martino, L., Guigo, N. van Berkel, J.G., Sbirrazzuoli, N. (2017).** Influence of organically modified montmorillonite and sepiolite clays on the physical properties of bio-based poly (ethylene 2, 5-furandicarboxylate). Compos. B. Eng. 110: 96-105.

13. **Hristodor, C.M., Vrinceanu, N., Pui, A., Novac, O., Copcia, V.E., Popovici, E. (2012).** Textural and morphological characterization of chitosan/bentonite nano-composite. Environ. Eng. Manag. J. 11: 573-578.

14. **Grim, R. E., Guven, N. (2011).** Bentonites: geology, mineralogy, properties and uses. Elsevier, Amsterdam, Oxford, New York.

15. **Tan, W., Zhang, Y., Szeto, Y.S., Liao, L. (2008).** A novel method to prepare chitosan/montmorillonite nanocomposites in the presence of hydroxy-aluminum oligomeric cations. Compos. Sci. Technol. 68: 2917-2921.

16. **Arruebo, M. (2012).** Drug delivery from structured porous inorganic materials. Wiley Interdiscip. Rev. Nanomed. Nanobiotechnol. 4: 16-30.

17. **Zhong, T., Xia, M., Yao, Z., Han, C. (2022).** Chitosan/Silica nanocomposite preparation from shrimp shell and its adsorption performance for methylene blue. Sustainability 15: 47.

18. **Darder, M., Colilla, M., Ruiz-Hitzky, E. (2003).** Biopolymer-clay nanocomposites based on chitosan intercalated in montmorillonite. Chem. Mater. 15: 3774-3780.

19. **Laaraibi, A., Moughaoui, F., Damiri, F., Ouakit, A., Charhouf, I., Hamdouch, S., Jaafari, A., Abourriche, A., Knouzi, N., Bennamara, A., Berrada, M. (2018).** Chitosan-clay based (CS-NaBNT) biodegradable nanocomposite films for potential utility in food and environment. Chitin-Chitosan-Myriad Functionalities in Science and Technology, IntechOpen 46-69.

20. **Cankaya, N., Sahin, R. (2019).** Chitosan/clay bionanocomposites: structural, antibacterial, thermal and swelling properties. Cellul. Chem. Technol. 53: 537-549.

21. **Salama, A., Abou-Zeid, R.E. (2021).** Ionic chitosan/silica nanocomposite as efficient adsorbent for organic dyes. Int. J. Biol. Macromol. 188: 404-410.

22. **Mohammed, M.I., Ismael, M.K., Gonen, M. (2020).** Synthesis of chitosan-silica nanocomposite for removal of methyl orange from water: composite characterization and adsorption performance. In IOP Conference Series: Materials Science and Engineering 745: 012084.

23. **Al-Sagheer, F., Muslim, S. (2010).** Thermal and mechanical properties of chitosan/SiO$_2$ hybrid Composites. J. Nanomater. 2010: 1-7.

24. **Blachnio, M., Budnyak, T.M., Derylo-Marczewska, A., Marczewski, A.W., Tertykh, V.A. (2018).** Chitosan-silica hybrid composites for removal of sulfonated azo dyes from aqueous solutions. Langmuir 34: 2258-2273.

25. **Cacciotti, I., Lombardelli, C., Benucci, I., Esti, M. (2019).** Clay/chitosan biocomposite systems as novel green carriers for covalent immobilization of food enzymes. J. Mater. Res. Technol. 8: 3644-3652.

26. **Benucci, I., Liburdi, K., Cacciotti, I., Lombardelli, C., Zappino, M., Nanni, F., Esti, M. (2018).** Chitosan/clay nano-composite films as supports for enzyme immobilization: An innovative green approach for winemaking applications. Food Hydrocoll. 74: 124-131.

27. **Benucci, I., Lombardelli, C., Cacciotti, I., Esti, M. (2020).** Papain covalently immobilized on chitosan–clay nanocomposite films: Application in synthetic and real white wine. Nanomater. 10: 1622.

28. **Bhattacharjee, M., Goswami, S., Borah, P., *et al.* (2023).** Preparation, characterization, and antimicrobial activity of chitosan/kaolin Clay biocomposite Films. Macromol. Chem. Phys. 2300008.

29. **Barman, J., Sarma, K.C., Sarma, M., Sarma, K. (2008).** Structural and optical

studies of chemically prepared CdS nano-crystalline thin films. Indian Journal of Pure and Applied Physics 46: 339-343.

30. **Valgas, C., Souza, S.M.D., Smania, E.F., Smania Jr., A. (2007).** Screening methods to determine antibacterial activity of natural products. Braz. J. Microbiol. 38: 369-380.

31. **Budnyak, T.M., Pylypchuk, I.V., Tertykh, V.A., Yanovska, E.S., Kolodynska, D. (2015).** Synthesis and adsorption properties of chitosan-silica nanocomposite prepared by sol-gel method. Nanoscale Res. Lett. 10: 1-10.

32. **Dey, S.C., Al-Amin, M., Rashid, T.U., Ashaduzzaman, M., Shamsuddin, S.M. (2016).** pH induced fabrication of kaolinite-chitosan biocomposite. Int. Lett. Chem. Phys. Astron. 68: 1-9.

33. **Vijayalekshmi, V. (2015).** UV-Visible, mechanical and anti-microbial studies of chitosan-montmorillonite clay/TiO_2 nano-composites. Res. J. Recent Sci. 131-135.

34. **Devi, N., Dutta, J. (2017).** Preparation and characterization of chitosan-bentonite nanocomposite films for wound healing application. Int. J. Biol. Macromol. 104: 1897-1904.

35. **Abdelkrim, S., Mokhtar, A., Djelad, A., Bennabi, F., Souna, A., Bengueddach, A., Sassi, M. (2020).** Chitosan/Ag-bentonite nanocomposites: preparation, characteri-zation, swelling biological properties. J. Inorg. Organomet. Polym. Mater. 30: 831-840.